

The Configuration and Demonstration of a
Rapid Scan Correlation Fourier Transform
Nuclear Magnetic Resonance Spectrometer

Geoffrey John Nesbitt

A Thesis
in
The Department
of
Chemistry

Presented in Partial Fulfilment of the Requirements
for the degree of Master of Science at
Concordia University
Montreal, Quebec, Canada

September 1983

© Geoffrey John Nesbitt, 1983

ABSTRACT

THE CONFIGURATION AND DEMONSTRATION OF A RAPID SCAN CORRELATION FOURIER TRANSFORM NUCLEAR MAGNETIC RESONANCE SPECTROMETER

Geoffrey John Nesbitt

A nuclear magnetic resonance correlation spectrometer has been constructed, and shown to be a useful complement to the magnetic resonance facilities already present in this Department. This thesis first describes the theory behind the principles of the spectrometer operation, which then support the decisions necessary to configure the complete instrumental hardware and software systems. The spectrometer capabilities are demonstrated, under a variety of conditions, culminating in its application to a problem whose solution would be very difficult, if not unobtainable, by any other method. Finally, future applications are suggested, and conclusions drawn upon the text.

I know who John Galt is.

ACKNOWLEDGEMENTS

The multifaceted nature of this thesis dictates a rather lengthy compendium, in order to place credit and thanks where they belong. My standard reply to all the people who have contributed efforts, through-out the course of this project has been: ".... get in line! ". Brevity shall be exercised, hopefully without offence. First, I would like to offer my most humble thanks to Dr. L. D. Colebrook, who has honored me with his attention as my very learned research supervisor.

Further demonstrations of thanks to:

- Dr.(Mrs.) Colebrook for her efforts in consultation.
- the staff of the Concordia Electrical and Machine Shop, Christie, Jacques, Rolf, Claude, and Robert, for their advice and assistance with "wires 'n stuff".
- Dr. O.S.Tee et al, for the thiazole ring compound.
- Paul Cahill for invaluable glassblowing.
- Wayne Wood for administrative assistance.
- fellow graduate students and staff.
- Walter Chazin, un mentor extraordinaire.
- Carolynne and Terry for their support.
- Bou-Bear for perspective.
- lastly, Trudie, without whom I would have been finished months in advance, but not nearly so happily.

To all of you, thank-you.

TABLE OF CONTENTS

Chapter 1	INTRODUCTION.....	1
Chapter 2	THEORY.....	5
2.1	Nuclei in Magnetic Field.....	5
2.2	Boltzmann and the Resonance Phenomenon...	10
2.3	Excitation and Measurement Technique.....	16
2.4	The Fourier Transform.....	23
2.5	Correlation.....	28
Chapter 3	HARDWARE.....	34
3.1	The Magnet.....	38
3.2	Transmitter, Receiver, Probe.....	43
3.3	Computer Interface.....	45
Chapter 4	SOFTWARE.....	51
4.1	NMRUN.....	53
4.2	NMRAN.....	59
4.3	NMPLT.....	77
Chapter 5	EXPERIMENTAL.....	79
5.1	Sweep Rate Aberrations.....	80
5.2	Organic Molecules.....	86
5.3	Aqueous Environments.....	98
5.4	Study of a Thiazole.....	105
Chapter 6	Future Considerations and Conclusions...	111
References	114
Appendix	A1

LIST OF FIGURES

Chapter 2	5
2.1	The Magnetic Moment.....	6
2.2	Classical and Quantum Mechanical Description of Energy Levels.....	8
2.3	Nuclear Spin Environments.....	11
2.4	Illustration of T_1 and T_2	12
2.5	Resonance Phenomenon.....	14
2.6	Vectorial Representation of Relaxation....	18
2.7	Fast Passage Ringing.....	20
2.8	The Fourier Transform.....	24
2.9	Euler's Theorem.....	25
2.10	Correlation FT Relationship.....	29
2.11	Linear System Response.....	30
Chapter 3	34
3.1	Basic NMR Spectrometer.....	35
3.2	HA-100 Configuration.....	37
3.3	Signal Lock.....	40
3.4	Spectrometer Channel Configuration.....	40
3.5	AIM-65 Assembler Program.....	47
3.6	RS-232 Communication Interface.....	49
Chapter 4	51
4.1	NMRUN Flowchart.....	54, 55
4.2	SWEEP Flowchart.....	56, 57
4.3	Data Processing Illustration.....	60, 61
4.4	NMRAN Flowchart.....	63, 64
4.5	Signal Flow Graph of FFT.....	69

4.6	FFT Equations.....	70
4.7	SHUFFL Action Flow Graph.....	71
4.8	NMPLT Flowchart.....	78
Chapter 5	79
5.1	Sweep Rate Aberrations.....	81
5.2	"	82
5.3	"	83
5.4	"	84
5.5	"	85
5.6	Ethylbenzene.....	88
5.7	"	89
5.8	Crotonaldehyde (trans).....	90
5.9	"	91
5.10	Ethyltoluene.....	93
5.11	"	94
5.12	Orthodichlorobenzene.....	95
5.13	"	96
5.14	Chloroform.....	97
5.15	Ethanol.....	100
5.16	Proline in D ₂ O.....	101
5.17	Proline in H ₂ O.....	102
5.18	Imidazole in H ₂ O.....	103
5.19	Thiazole Ring in H ₂ O.....	106
5.20	Thiazole Ring in D ₂ O.....	107
5.21	Base Opened Thiazole, in H ₂ O.....	108
5.22	Thiamin Cleavage.....	105
5.23	Thiazole Base Opening.....	109

Chapter 1

INTRODUCTION

The field of Nuclear Magnetic Resonance (NMR) has seen phenomenally fast growth from conception to the state at which technology now stands.

When Bloch¹ and Purcell² first demonstrated NMR in bulk samples, the experiment was simply the observation of a nuclear resonance and the determination of its magnetic moment. The observation of the chemical shift³ ushered the technique into the role of an analytical tool, finding employment in structure elucidation. At this time, the standard method to obtain high-resolution spectra was the continuous wave (CW) experiment. This procedure requires the continuous excitation to be slowly swept through the resonance condition in order to approximate the steady state solutions to the Bloch equations.⁴ Under these circumstances the sweep rate is of the order

$$\frac{1}{2 \pi T_2} \text{ Hz/sec (often } < 1 \text{ Hz/sec).}$$

where T_2 = spin-spin relaxation time

Very little power is introduced to the sample, hence the system is perturbed only slightly and a weak signal procured as a result.

In 1966, Ernst and Anderson⁵ capitalized on ground work laid previously by Torrey⁶, Hahn⁷, and Fourier⁸, to establish that the Fourier transformation (FT) of the free induction

decay observed upon irradiation, with a short intense radio frequency (RF) pulse, could yield high resolution NMR spectra also. Further, the entire spectrum can be obtained with a single pulse, on a time order of $3 \cdot T_2$ (after which the FID is reduced to 45%), and the magnetization vector is tipped from the equilibrium value (for a 90° pulse) yielding an increase in sensitivity (relative to the CW experiment).

To a large degree the quickly developing computer industry and the elucidation of the "fast Fourier transform" by Cooley and Tukey⁹ have been responsible for the Pulse FT method becoming the most popular and convenient mode to obtain high resolution NMR spectra.

One significant difference between the CW and pulse FT methods lies in the execution of the experiment. The pulse technique requires the entire spectrum to be excited during each scan, while the CW mode allows selection of any specific part of the spectrum. This becomes important when there is a particularly large solvent peak in the sample, which would cause dynamic range problems in the pulse experiment but could be skirted in the CW mode by not scanning that portion of the spectrum.

An alternative approach to the above techniques is found in the rapid passage (RP) experiment¹⁰. Similar to the CW method the spectrometer is simply swept through the resonance under fast passage conditions. This results in magnetization being left in the x-y plane (see later), which produces a

ringing wiggle beat pattern that persists a time $3 \cdot T_2$ after resonance.

This is useful only if the ringing artifact can be removed in order to obtain the high resolution spectrum wished. It has been shown that the cross-correlation of this distorted fast passage response with a function representing either a reference line recorded under fast passage conditions¹¹ or a theoretical calculated lineshape¹² will result in an artifact-free spectrum. The method necessitates the use of Fourier transformations and has thus been coined Rapid Scan FT Spectroscopy. This offers a mode of operation comparable to pulse techniques in many ways:

- approximately equivalent signal to noise (S/N) ratio.
- comparable resolution depending on the T_2 of sample.
- approximately the same time required for a single scan.
- control of the sweep rate allows regulation of the power input and hence the tip angle of the bulk magnetization vector, which in turn affects the sensitivity.
- dynamic range problems can be skirted by simply not exciting that portion of the spectrum containing the unwanted (problem) line.

This technique has seen further enhancement with the addition of solvent suppression methods¹³, wing processing¹⁴, and has been demonstrated measuring spin-lattice relaxation times,^{15,16} and applications in biological systems^{16,17}.

8

The purpose of this thesis is to demonstrate the resurrection of an aging CW instrument in the form of a Rapid Passage Correlation NMR spectrometer, and the successful application of its unique capabilities to a chemical problem.

This will be accomplished within the text by first presenting a discourse on the theoretical background of the experiment and the computational methods critical to the project. The hardware arrangement will then be discussed and explained as a consequence of the theoretical requirements of the experiment. The software configuration follows in detail with an operational flowchart demonstrating the step by step processing of the data. The experimental chapter will substantiate the previous performance claims and illustrate the functional application of the spectrometer over a range of operating conditions. Finally, conclusions will be drawn from the text and possible future development/evolution of the instrument suggested.

Chapter 2
Section 1

THEORY OF NUCLEI IN A MAGNETIC FIELD

Nuclear magnetic resonance is possible because some nuclei act as though they possess the properties of spin and angular momentum. The property of spin confers upon the nuclei a magnetic moment which is proportional to the magnitude of the spin and may be described as shown in equation 2.1.

$$(2.1) \quad U_n = g_n * B_n * I_n \quad \text{where}$$

g_n = nuclear g-factor

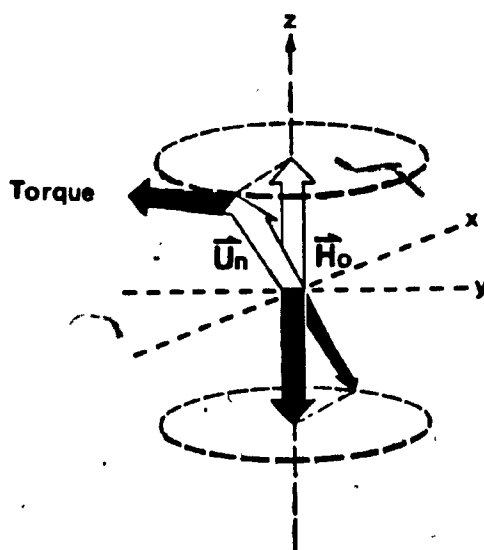
B_n = Nuclear magneton $\frac{e h}{2 M C}$

I_n = Nuclear spin quantum number

The properties of the nuclear magneton do not change, e and M are the charge and mass of the proton respectively, C , the speed of light and h Planck's constant over 2π . g_n is a dimensionless constant whose contribution depends upon the nuclei under observation. Hence, only g_n and I_n change to modify the equation to fit the characteristics of any nuclei. Quantum mechanics predicts the value of I , being a characteristic of the isotope in question and a consequence of its atomic mass and number.

If the nuclei are placed in a magnetic field, the interaction between the magnetic moment and the field produces a torque which may be described classically as the vector product of the two, and pictured in Figure 2.1.

FIGURE 2.1



$$\tau = \vec{U}_n \times \vec{H}_0$$

such that the energy of the interaction is the Hamiltonian

$$\mathcal{H} = -\vec{U}_n \times \vec{H}_0 \quad (2.2)$$

By substituting equations 2.1 into 2.2 we generate a Hamiltonian equation which models the coupling of the moment with the field, which will provide an explicit solution enabling the measurement of the nuclei energy.

$$(2.3) \quad \mathcal{H} = -g_n B_n H_0 I_z$$

Quantum mechanics predicts multiple spin states through the variable I_z in equation 2.3, each with peculiar energy levels. Classically, Newton's law dictates that this coupling is also equal to the rate of change of the angular momentum (U_n). U_n has only one degree of freedom within the constraints imposed by equation 2.3, the rate of precession about H_0 . The result is that the magnetic moment vector precesses about the field direction with a characteristic frequency, known as the Larmor frequency, ω_0 where

$$(2.4) \quad |\omega_0| = 2 \pi \nu_0$$

where ν_0 (Hz) is the frequency of precession of the magnetic moment about H_0 .

Bringing equation 2.3 under closer scrutiny it should be obvious that for any nuclei with $I \neq 0$, the application of the static field through H_0 will effect a separation of the spin states observable in the Hamiltonian. In order to detect the presence of these energy levels, a tool is needed to perturb the system to enable transitions between the levels, which may then be measured. This materializes in the form of a circularly polarized radio frequency energy, usually applied along the x axis of the classical picture, illustrated in Figure 2.2a. The two possible states for U_n defined by I_z are shown in line with H_1 , the perturbing field. If H_1 is varied through ω_0 the resonance is observed. The equivalent quantum mechanical picture is portrayed in Figure 2.2b.

Examining equation 2.5, it is apparent that in a given magnetic field, the resonance condition requires a unique precession frequency for each distinct nucleus. If the magnetic moment is thought of as a top, then in a spin $I = 1/2$ system the top may have two orientations when placed in the field, anti or parallel to the field direction.

This is realized quantum mechanically in the form of the two energy levels shown in Figure 2.2b. A transition can occur at the resonance condition if the top receives

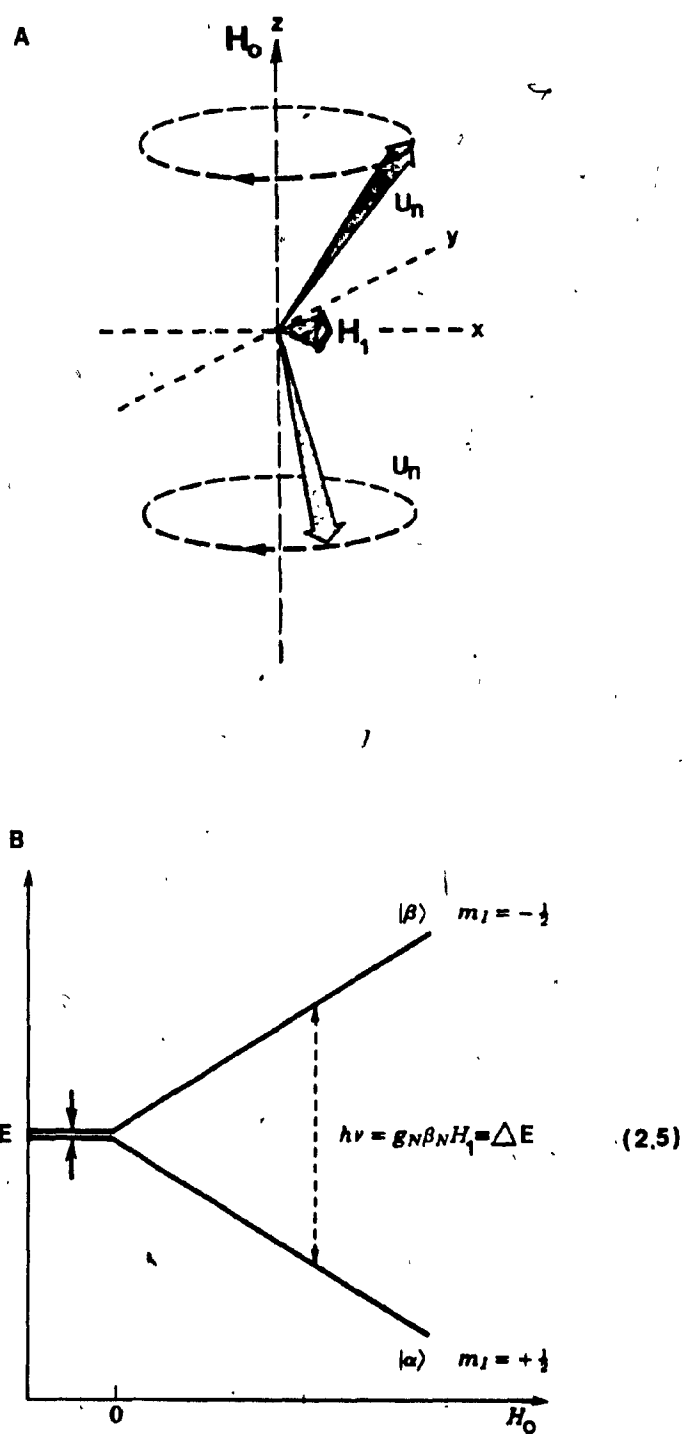


Figure 2.2

the unique amount of energy $h\nu$ dictated by Planck's law.

The transition will happen only when this condition is met exactly; this provides the exclusive nature of the magnetic resonance experiment. By varying either V or H_1 in equation 2.5, a transition can be caused peculiar to a particular nucleus, as an exact solution to equation 2.5.

Section 2

BOLTZMANN AND THE RESONANCE PHENOMENON

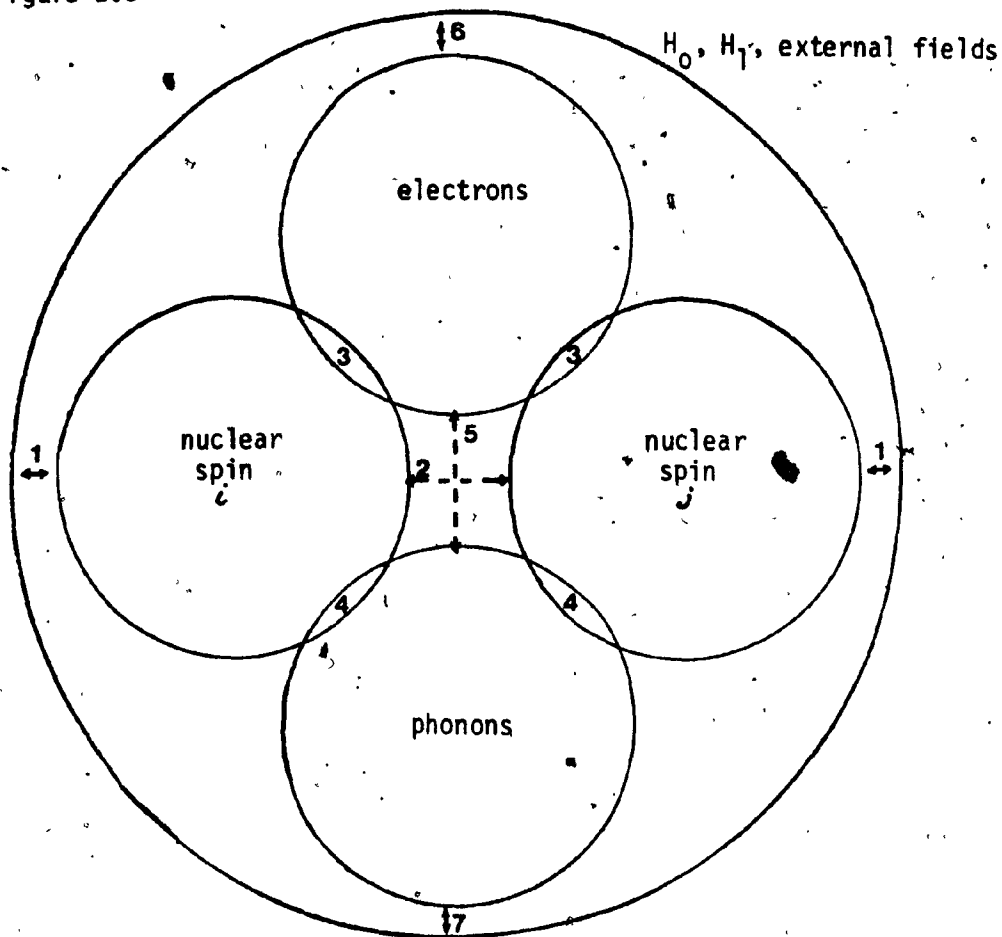
Until this point the discussion has considered only the behavior of a single isolated nucleus, while in practice the N.M.R experiment measures the mean behavior of a bulk sample in a very complicated magnetic environment. Boltzmann theory predicts that, left to its own devices, the populations of each energy level will approach an equilibrium derived from all the forces which affect the magnetic environment of the sample, shown in Figure 2.3. Given a two spin system, the Boltzmann equation (2.6) can be used to describe the population distribution at equilibrium.

$$(2.6) \quad \frac{n_+}{n_-} \text{ equilibrium} = \exp \frac{\Delta E}{KT} = \exp \frac{-U_n H_0}{KT}$$

The transitional probability from each state is equal in both directions. Upon irradiation with H_1 , the applied field, a forced equilibrium can be reached which results in saturation of the population levels. No detection of transitions would occur at this point if it were not for the presence of natural relaxation mechanisms which allow the system to dissipate the energy.

These processes can be characterized in the form of two measurable relaxation rates which represent the two most important pathways, shown in Figure 2.4.

Figure 2.3



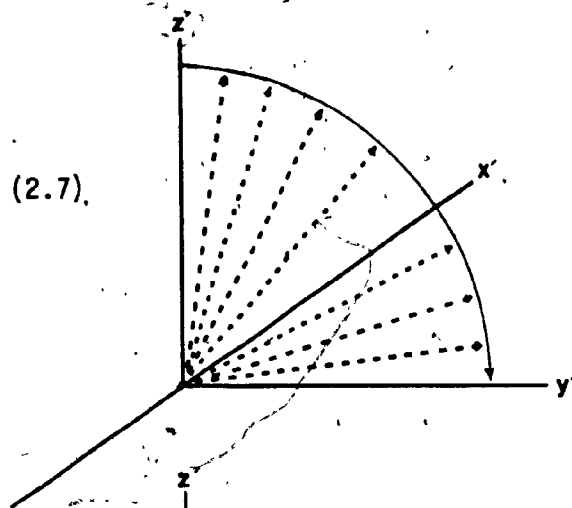
Two spin system

- 1. = Zeeman interaction
- 2. = Direct spin-spin interaction
- 3. = Nuclear spin-electron interaction
- 4. = Direct spin-lattice coupling
- 3.-5. = Indirect spin-lattice via electrons
- 3.-6. = Shielding and polarization via electrons
- 4.-7. = Coupling of nuclear spins to sound fields

Figure 2.4

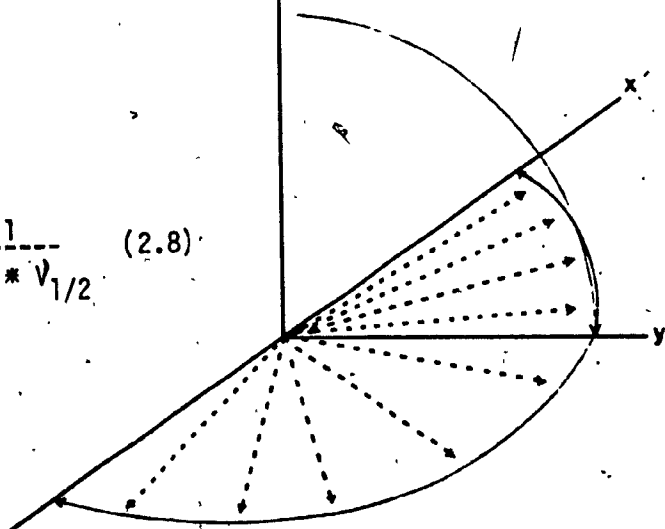
A

$$T_1 = \frac{1}{W_+ + W_-} \quad (2.7)$$



B

$$T_2 = \frac{1}{\pi * V_{1/2}} \quad (2.8)$$



The isochromats above illustrate a classical picture of the effect of the two dominant relaxation pathways T_1 and T_2 , on the vectors of the magnetic moments.

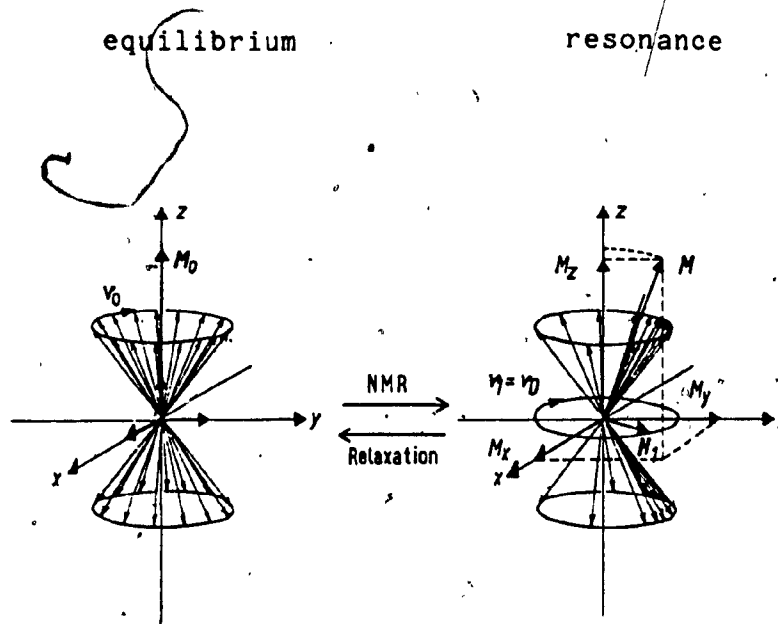
- A. T_1 causes the distribution of the nuclear moments along the z axis.
- B. T_2 causes a dephasing of the spins in the x-y plane.

When describing the bulk sample it is necessary to introduce a bulk magnetization vector M which represents the mean of the individual nuclear vectors. In Figure 2.4 equations 2.7 and 2.8 model the two dominant relaxation pathways. T_1 is derived in terms of probability since the rate of return to equilibrium via the spin lattice is directly related to the original population condition under the experiment and the transitional probability of these populations changing. T_2 can be thought of most easily as a dephasing of the nuclear vectors via spin-spin interactions and field inhomogeneities. The NMR experiment works because when the R.F. energy that is used to perturb the system forces the population levels from their natural equilibrium, these pathways act as a lever to restore the Boltzmann distribution. At room temperature the distribution is weighted such that a greater number of vectors (actually nuclei) reside in the lower energy level.

THE BLOCH EQUATIONS

The relaxation times, T_1 and T_2 are predicted by a set of equations postulated by Bloch which describe the behavior of the bulk magnetization vector, M , in the presence of an applied R.F. field. The approach used was to first model the effect of the applied field upon the bulk magnetic moment.

Figure 2.5



The Figure above illustrates the states possible for the spin vectors representing the nuclei in the bulk sample.

The terms used in equations 2.10, 2.11, 2.12, can be visualized clearly, showing example contributions.

$$(2.9) \quad \frac{dM}{dt} = \gamma M \times H$$

This may be expanded to account for each separate component of M , M_z, M_x, M_y , where the field components H_z, H_x, H_y , would by convention be the fixed ($H_z = H_0$) and rotating fields respectively. In order to account for relaxation mechanisms the following assumptions were made:

1. M_z would decay to M_0 (equilibrium) by entirely first order processes with a time constant T_1 .
2. M_x, M_y would decay to zero by the first order time constant T_2 .

The result is the equations presented below:

$$(2.10) \quad \frac{dM_x}{dt} = \gamma (M_y H_0 + M_z H_1 \sin \omega t) - \frac{M_x}{T_2}$$

$$(2.11) \quad \frac{dM_y}{dt} = \gamma (M_z H_1 \cos \omega t - M_x H_0) - \frac{M_y}{T_2}$$

$$(2.12) \quad \frac{dM_z}{dt} = -\gamma (M_x H_1 \sin \omega t + M_y H_1 \cos \omega t) - \frac{(M_z - M_0)}{T_1}$$

Chapter 2
Section 3

EXCITATION AND MEASURING TECHNIQUE

In the classic CW experiment, the field or frequency is swept slowly through the spectrum such that the stationary solution of the Bloch equations yields analytical solutions, under certain limiting conditions. The criteria are that the applied field H_1 is small, and the sweep rate is slow enough to establish a steady state where the time derivatives of the equations are zero. Accordingly, we get equation 2.13 as a result.

$$(2.13) \quad \frac{dM_x}{dt} = \frac{dM_y}{dt} = \frac{dM_z}{dt} = 0$$

Since the spectrometer measures the frequency component of the magnetization, the magnetic flux through the receiver coil induces an alternating potential which it can be shown yields two signals in the x, y plane.¹⁸

1. Absorption signal, 90° out of phase with H_1 ,
proportional to the V component of M_{xy} .
2. Dispersion signal, in phase with H_1 ,
proportional to the U component of M_{xy} .

The signal components, U and V represent the electromagnetic radiation as two rotating vectors out of phase with each other, this will be covered in more detail in Chapter 3.

Both the phase and magnitude are important, and each signal can be obtained separately by means of an radio-

frequency phase-sensitive detector as the spectrometer is swept through the resonance condition. This affords us a measuring technique and is illustrated vectorally by the isochromats in Figure 2.6.¹⁹

If the experimental arrangement is such that a receiver coil is placed along the x axis then the detected signal will be

$$(2.14) \quad S = A \frac{dM_x}{dt}$$

and the absorbance maximum will be

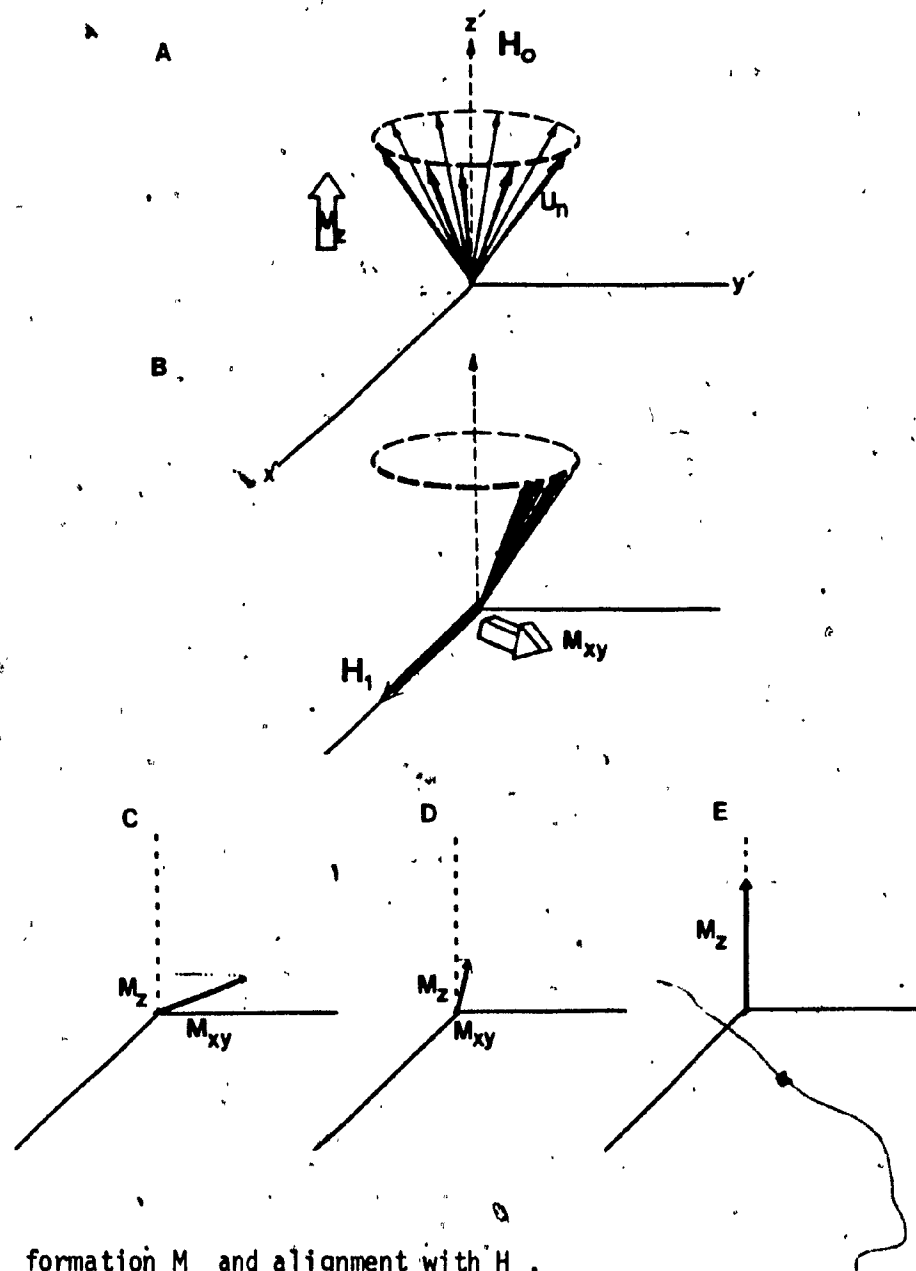
$$(2.15) \quad S \propto \frac{H_1}{1 + \gamma^2 H_1^2 T_1 T_2}$$

Some important conclusions can be drawn from this:

1. Under adiabatic slow passage conditions (eqn. 2.16), as the perturbing excitation reaches resonance the system at that point must absorb all the energy introduced by the excitation.
2. In order to avoid saturation the power level of the excitation must be carefully balanced.
3. The bulk magnetization vector is pushed only slightly from equilibrium and a weak signal results.

From the adiabatic theorem we know that equation 2.16 must be satisfied in order for the spectrometer passage to be considered adiabatic.²⁰

Figure 2.6



A. formation M_z and alignment with H_0 .

B. tipping of M by H_1 causes M_{xy} formation.

C.D. and E. relaxation to equilibrium.

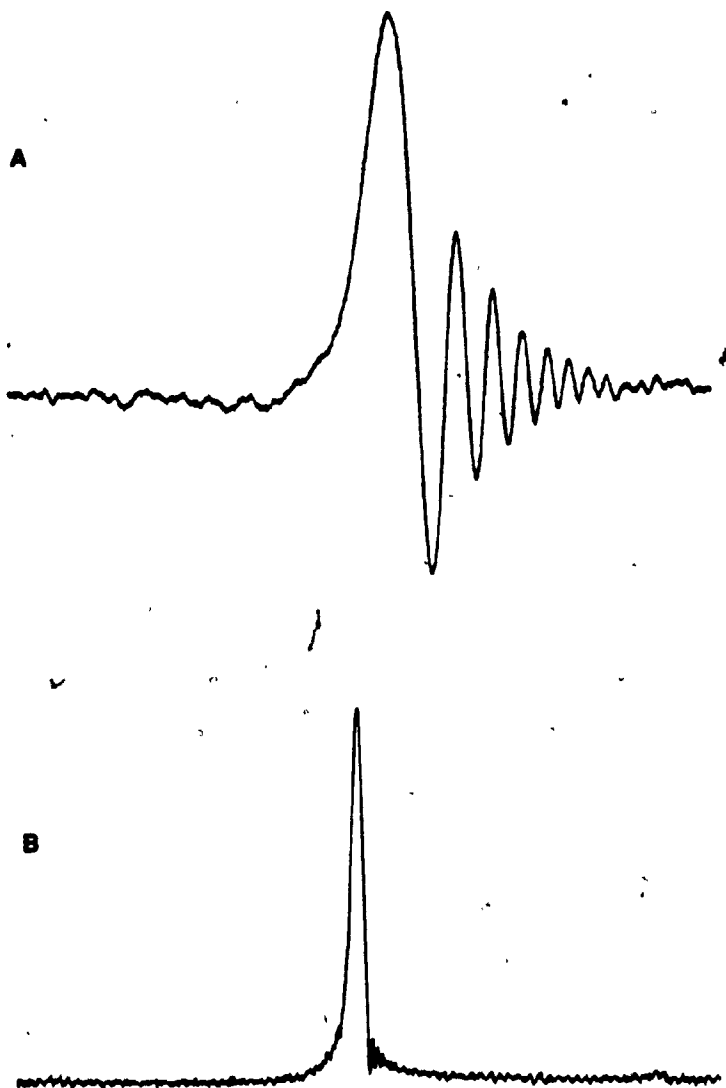
$$(2.16) \quad \frac{dH_0}{dt} \ll \gamma H_1^2$$

In liquids, the ratio of the spectrum width to the line width is very large, meaning the relative time spent searching a line is short with respect to the total scan time. The result is that in an unpopulated sample the entire spectrum must be scanned, and at a power level which will not saturate the populated parts of the spectrum.

When this requisite is ignored the Bloch equations no longer accurately describe the system. In practice, this results in a non-Lorentzian line shape with spurious ringing caused by excess magnetization left in the x-y plane after resonance.⁸³ Figure 2.7 illustrates the artifact, but the explanation is best delivered using Figure 2.6.

As the resonance condition in 2.6b is reached, H_1 is rotating in the x-y plane at the Larmor frequency ω_0 . Immediately after resonance the Larmor frequency has changed as a result of the sweeping excitation and H_1 now finds itself beating against M_{xy} , as shown in Figure 2.6c. This is the cause of the wiggle observed after the peak.

From the Bloch equations we know that M_{xy} decays with the characteristic time T_2 . In principle the envelope should contain information with respect to this decay.⁸² Unfortunately, field inhomogeneities cause nuclei in the bulk sample to experience slightly different values of H_0 and their vectors quickly dephase causing relaxation. In fact, this envelope is a better estimate of field homogeneity than

Figure 2.7**Figure 2.7**

- A. Fast passage scan of a formyl proton showing residual ringing. ~ 50 Hz/sec
- B. Slow passage run of same. ~ 2 Hz/sec

anything else, and it is common procedure to shim up the field against a single line wiggle beat pattern.

In order to drive the system into the fast passage region, equation 2.17 must be satisfied experimentally.

$$(2.17) \quad b' \gg \frac{1}{2 \pi T_2^2} \quad \text{where } b' = \text{sweep rate (Hz sec)} \\ T_2 = \text{natural decay time}$$

Concurrently, to minimize the system saturation, which should then yield the greatest peak height for the given sweep rate, equation 2.18 must be optimized.¹⁰

$$(2.18) \quad S_{op} = (\gamma H_1)^2 T_1 T_2 = 1 + 3.01 * b' * T_1 T_2$$

At its upper limit $S_{op} = 3.01 * b' * T_1 * T_2$
for an infinite power input.

The sweep rate, b' , must be optimized in accordance with the last two equations. This is difficult unless the operator has a priori intuition concerning the relaxation values for the system under investigation, but certainly these values can be guessed at. If the expectations are that a natural line width of 1 Hz is desirable, then the minimum value for b would be only 20 Hz by equation 2.17 while equation 2.18 would only be limited by the available transmitter power.

In general, it can be stated that the pulse method usually yields a better S/N ratio, with the difference closing as the sweep rate in the rapid scan experiment increases,² but the sensitivities are comparable. If equation 2.19 describes the time between scans⁶³, then

$$(2.19) \quad T = \frac{V_t}{V'} + 3T_2 \quad \text{where } V' = \text{sweep rate}$$

$$V_t = \text{sweep width}$$

therefore the time given by V_t/V' , is necessary to sweep the entire spectrum while $3T_2$ accounts for the time required for the last line scanned to decay. From this it is possible to conclude that at low T_1 values the $3T_2$ term lowers the sensitivity, while at high T_1 's the contribution would be negligible and the rapid scan has approximately equal sensitivity to pulse methods.

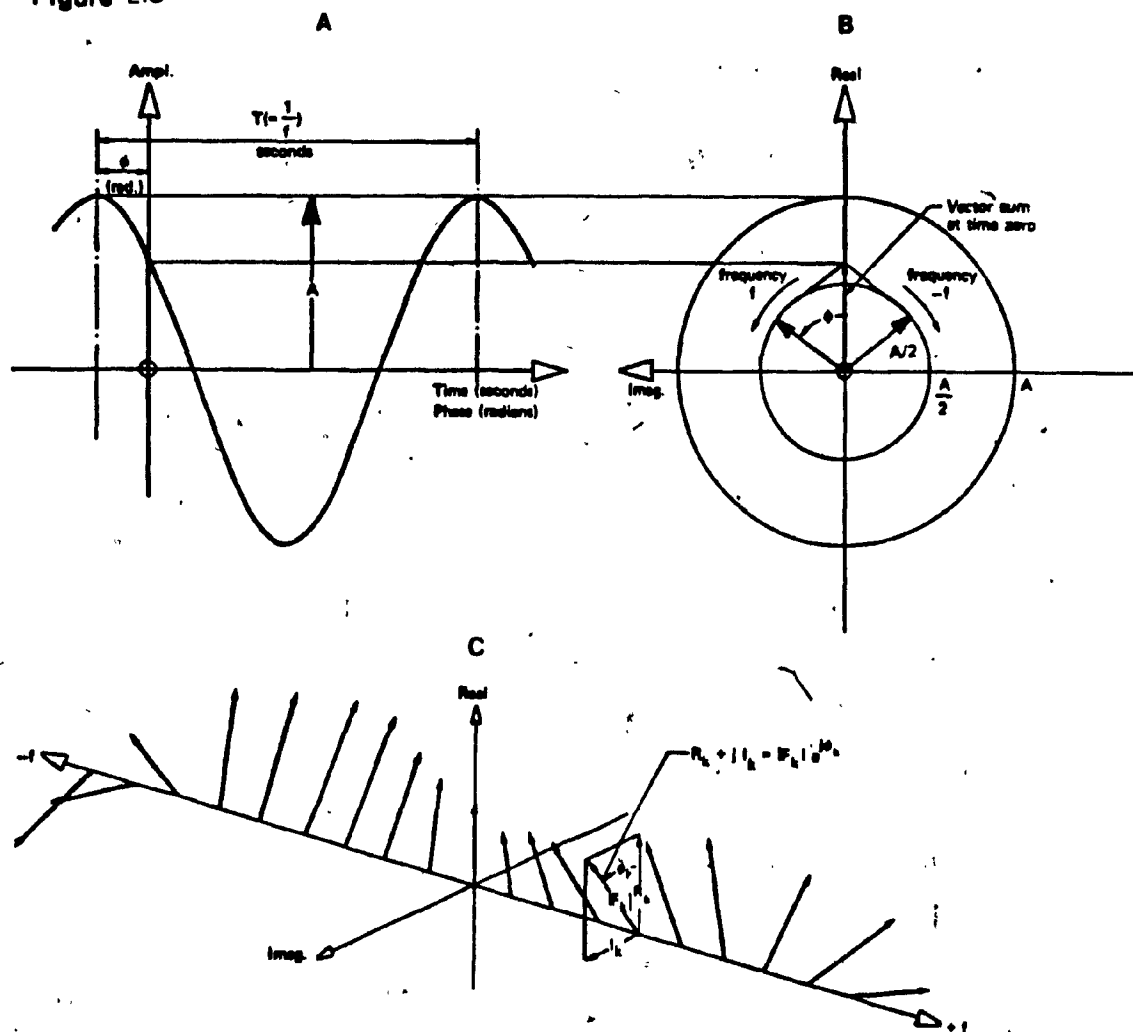
Chapter 2
Section 4

THE FOURIER TRANSFORM

The Fourier transform (FT) finds wide application among problems involving vibrations or oscillations. In order to describe a harmonic process it is necessary to employ a mathematical series which can precisely represent all the components present in the system. The Fourier series is particularly well suited to this case since, simply stated, it is a series whose terms are composed of periodic functions. By definition, at the limit of the sum the Fourier series may be replaced by an integral of the same name.

This integral may undergo transformation between two domains where the function is preserved coherently and exactly in both domains, but defined in different units, related directly through the transform. The transform may take different forms depending upon the nature of the system, but will be composed of a number (perhaps infinite) of (co-)sinusoidal components at various frequencies, each with a given amplitude and initial phase, as illustrated in Figure 2.8. The purpose of Figure 2.8 is to show an example component and the relationship possible between the two domains. By inspection, in Figure 2.8C, the real and imaginary vectors are 90° out of phase with each other, leading to the observation that a combination of sin and cos terms can describe the whole function.

Figure 2.8



- A. Example sinusoidal component $A \cos(2\pi ft + \phi)$ -both period and phase shift along x axis.
- B. Function in A. decomposed as sum of two contra-rotating vectors. Only real component of vectors add, by inspection imaginary parts always cancel.
- C. Three dimensional spectrum of part of function.

The time for one rotation of a vector equals one period, all at the same frequency. Equivalence of representation is obvious: $A \cos\phi = \frac{A}{2}(e^{j\phi} + e^{-j\phi})$

Both Fourier sine and cosine transforms are symmetrical about $t=0$, the cosine being an even function, the sine odd. These transforms alone allow the description of systems with either purely even or odd symmetry, a serious limiting condition.

The linear combination of the two transforms generates a new transform which will model all functions of arbitrary symmetry. This equation may be expressed by a Taylor expansion in exponential notation, as shown in Figure 2.9.

FIGURE 2.9

$$\sin(x) = x - \frac{x^3}{3!} + \frac{x^5}{5!} + \dots$$

$$\cos(x) = 1 - \frac{x^2}{2!} + \frac{x^4}{4!} + \dots$$

$$\exp(x) = 1 + x + \frac{x^2}{2!} + \frac{x^3}{3!} + \dots$$

$$\text{by Euler } \dots \exp(i\phi) = \cos(\phi) + i\sin(\phi).^{21}$$

The special properties of i accommodate the symmetry and preserve the orthogonality of the sine and cosine functions. Finally a notation can be ventured which represents the Fourier transform.²²

$$(2.20) \quad \int_{-\infty}^{\infty} h(t) \exp(-i2\pi ft) dt = \int_{-\infty}^{\infty} h(t) (\cos 2\pi ft - i\sin 2\pi ft) dt$$

The transform pair may now be presented, depicting the relationship between the two domains.

$$(2.21) \quad \begin{aligned} H(f) &= \int_{-\infty}^{\infty} h(t) \exp(-i2\pi ft) dt \\ h(t) &= \frac{1}{2\pi} \int_{-\infty}^{\infty} H(f) \exp(i2\pi ft) df \end{aligned}$$

The practical advantages of the Fourier transform are realized in the algorithm of the fast Fourier transform.⁹ (fft) This is an especially time efficient method of processing the discrete Fourier transform.(dft)

The particular strategy employed in the program used in this thesis is a decimation in time algorithm, for the special case where N, the number of points in the array to be processed, is a power of two.²³ The effectiveness of this algorithm is achieved by the reduction of the number of complex operations (multiplication or addition) necessary to perform the transform. The form of the discrete digital expression for the FT is shown in equation 2.22.

$$(2.22) \quad \begin{aligned} H(f) &= \sum_{t=0}^{N-1} h(t) W_N^{tf} \quad \text{for } f = 0, 1, \dots, N-1 \\ \text{where } W_N &= \exp\left(-\frac{i2\pi}{N}\right) \end{aligned}$$

Intrinsically, it must take N operations to find the value of one H_f , hence N^2 operations to find all $N \cdot H_f$ values.

Using the Cooley-Tukey procedure, the array is split into two sums, one for n even, another for n odd points.

$$(2.23) \quad H(f) = \sum_{t=0}^{N/2-1} h_{2t} w_n^{2tf} + \sum_{t=0}^{N/2-1} h_{2t+1} w_n^{(2t+1)f}$$

The total N-point dFT may be found by combining the two $N/2$ point dFT's according to the relationship,

$$(2.24) \quad H(f) = \sum_{t=0}^{N/2-1} h_{2t} w_{n/2}^{tf} + w_n^f \sum_{t=0}^{N/2-1} h_{2t+1} w_{n/2}^{tf}$$

since $w_{n/2} = w_n^2$

$$(2.25) \quad H(f) = A_f + w_n^f B_f$$

To process the two $N/2$ point arrays requires only $2 * (N/2)^2$ operations.²⁴ If the two $N/2$ point arrays are further divided into $N/4$ point arrays, and so on until each sub-array contains only one point, the transform of which is itself, the complex arithmetic required is only that necessary to recombine the sub-divisions of the array. This is how the $N \log_2 N$ relationship is derived which dictates the number of calculations required to perform a fFT using the Cooley-Tukey algorithm.

Chapter 2
Section 5

CORRELATION

The dFT adheres to the same principal relationships between Fourier transform pairs as does the continuous FT.²⁵ In particular, one of these properties is very useful with respect to our intent, for it states that the convolution of the FT's of two functions is proportional to the FT of the product of the two functions.²⁶ Thus if $H(f) \leftrightarrow h(t)$ and $G(f) \leftrightarrow g(t)$ are both FT pairs then

$$H(f) \otimes G(f) \propto \frac{1}{2\pi} (h(t) * g(t))$$

where \otimes defines the operation of convolution.

This theorem allows the arduous task of a conventional discrete convolution product²⁷ to be replaced by the direct multiplication of the two functions in the Fourier domain. Of further significance is the generalization of the properties of the convolution theorem to generate an equivalent supposition for the correlation operation.²⁸

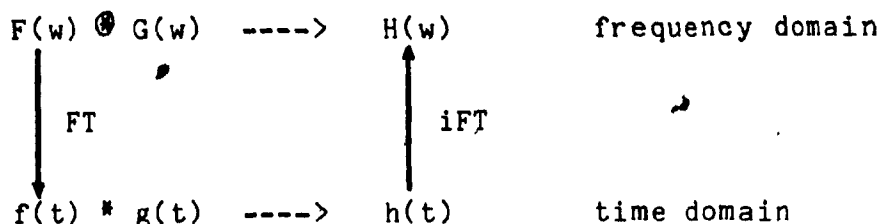
The consequence of this becomes important in light of the fact that the time domain measurement of an NMR signal (the free induction decay) and the frequency domain equivalent (absorption mode) are Fourier transform pairs.²⁹ The result is an elegant data manipulation which allows access to a huge array of digital processing techniques.³⁰

If the data gathered from the experiment, $F(w)$, is in the frequency domain, then upon FT the array is now described as a function of time, $f(t)$. In the time domain our function models a naturally decaying exponential, and may be treated digitally as such.

At this stage the signal can undergo exponential multiplication, convolution,^{31,32,38} cross correlation,³³ trigonometric multiplication,³⁴ digital smoothing,³⁵ and filtering³⁶ or any other operation acting coherently on an exponential function.

The correlation multiplication yields the important components, $h(t)$, without preserving the wiggle beat ringing, and upon retransformation back to the frequency domain we have the signal of interest, $H(w)$. This is illustrated graphically in Figure 2.10.

FIGURE 2.10

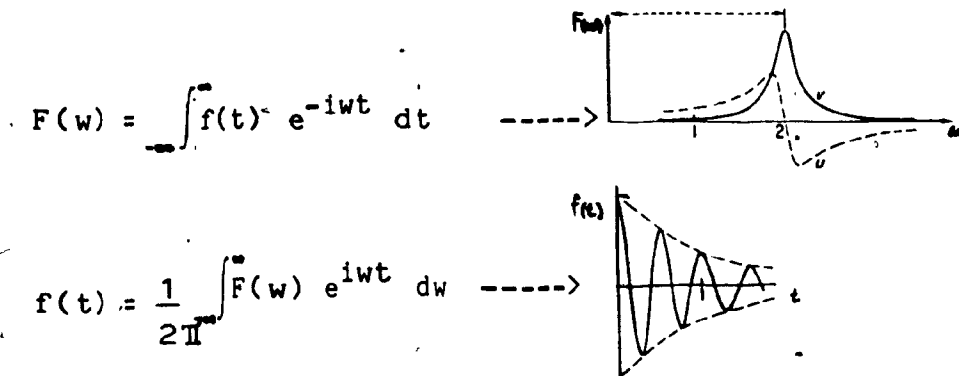


The processing algorithm employed has come under close scrutiny³⁷ and several options are theoretically available. For reasons that will be made evident in latter discussion the physical restraints of the hardware at hand impose criteria for making the decision determining which method to employ.

The derivation will be presented here at a level where these restrictions play no role.

The linear response of a spin system can be written as a Fourier transform pair.²⁹

FIGURE 2.11



In NMR convention, $F(w)$ would be the result obtained from a slow passage experiment while $f(t)$ could represent a typical response from a pulse spectrometer.

The correlation operation may be justified treating the system classically or quantum mechanically, the linear response method will be presented here.¹² In order to show the analytical proof of the correlation operation within the context of the NMR experiment it will first be necessary to describe the spin system, $F(w)$.

The response of the sample to an arbitrary excitation, $E(t)$, can be modeled by

$$(2.26) \quad R(t) = \int_{-\infty}^{\infty} \phi(\tau) E(t-\tau) d\tau$$

where $\phi(\tau)=0$ for $\tau < 0$ (causality condition)

The excitation can be further described as³⁹

$$(2.27) \quad E(t) = e^{i \int_0^t \omega_t dt} = e^{i b t^2 / 2}$$

where $\omega_t = b \cdot t$ for a linear rf field swept at $b \frac{\text{rad}}{\text{sec}^2}$

Substituting into equation 2.26 we get,

$$(2.28) \quad R(t) = \int_{-\infty}^{\infty} \phi(\tau) e^{i b (t-\tau)^2 / 2} d\tau$$

The detected component of the response, $R(t)$, must be in phase and at the same frequency as the applied rf field (H_1). This is obtained by multiplying $R(t)$ by $\exp \frac{-i b t^2}{2}$ and is analogous to phase sensitive detection.⁴⁰

This gives us

$$(2.29) \quad F(\omega) = R(t) * e^{-i b t^2 / 2}$$

which upon substitution by equation 2.28 and factoring, yields,

$$(2.30) \quad F(\omega) = \int_{-\infty}^{\infty} \phi(\tau) e^{i b (\tau^2 - 2t\tau) / 2} d\tau$$

Now taking the forward transform of $F(\omega)$ we have an expression of the system in the time domain.

$$(2.31) \quad f(t) = \frac{1}{2\pi} \int_{-\infty}^{\infty} F(\omega) e^{i \omega t} d\omega$$

Substituting equation. 2.30 into 2.31 and knowing $w_t = b \cdot t$ we get equation 2.32.

$$(2.32) \quad f(t) = \frac{1}{2\pi} \int_{-\infty}^{\infty} \int_{-\infty}^{\infty} \delta(\tau) e^{\frac{1b(\tau^2 - 2w_t\tau)}{2}} e^{1w_t} d\tau dw_t$$

After factoring and rearranging this can be written as equation 2.33.

$$(2.33) \quad f(t) = \frac{1}{2\pi} \int_{-\infty}^{\infty} \underbrace{e^{1w_t(t-\tau)}}_{\delta(t-\tau)} * \int_{-\infty}^{\infty} \delta(\tau) e^{\frac{1b\tau^2}{2}} dw_t d\tau$$

In equation 2.33 the definition for the inverse FT for the Dirac impulse function is underlined. Once recognized,⁴⁰ it provides us with a tool to simplify the equation since by definition⁴² the transform of the product of a function multiplied with an impulse function, is the function itself.⁴³ Substituting the Dirac function into equation. 2.33 we have

$$(2.34) \quad f(t) = \int_{-\infty}^{\infty} \delta(\tau) e^{\frac{1b\tau^2}{2}} * \delta(t-\tau) d\tau$$

and finally, after multiplication, equation 2.35,

$$(2.35) \quad f(t) = \delta(t) e^{\frac{1bt^2}{2}}$$

By inspection, it is obvious that multiplying equation 2.35 by the term $\exp^{-\frac{1bt^2}{2}}$, in this case the function we have designated $g(t)$, the original time response is retrieved to

yield the free induction decay signal $\phi(t)$. This is the justification of the multiplication of our muddled time response by the complex conjugate of the theoretical line shape.

$$h(t) = f(t) * g(t) = \phi(t) e^{\frac{ibt^2}{2}} * e^{-\frac{ibt^2}{2}}$$

$$(2.36) \quad h(t) = \phi(t) !$$

To obtain the final slow passage spectrum it is only necessary to find the inverse FT of $\phi(t)$ in equation 2.36.

$$(2.37) \quad H(w) = \int_{-\infty}^{\infty} h(t) e^{-iwt} dt$$

which yields the approximation to the slow passage spectrum.

Glancing back at Figure 2.10 it is now possible to write down the first rudiments of a flow chart dictating the steps required to perform the actual correlation operation:

- | | |
|--|--------|
| 1. Start with the frequency data | $F(w)$ |
| 2. Perform forward FT to get | $f(t)$ |
| 3. Multiply by $g(t)$ ($\exp \frac{-ibt^2}{2}$) to get | $h(t)$ |
| 4. Perform inverse FT to get | $H(w)$ |

This will be expanded in chapter 4.

Chapter 3

INTRODUCTION

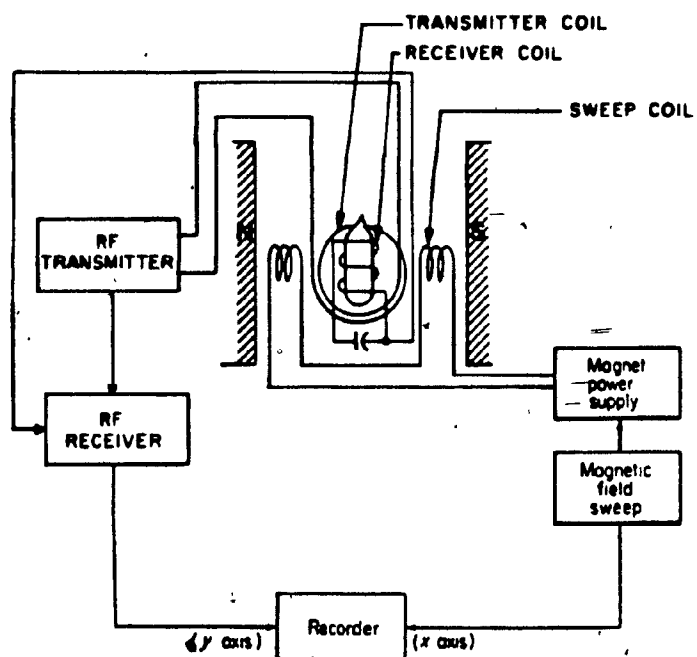
The most basic instrumentation required to perform a modern CW NMR experiment using a crossed coil probe is shown schematically in Figure 3.1.

The theoretical background has already been treated in Chapter 2, the purpose of this chapter is to substantiate the implementation of the experiment with the actual electronic components necessary to meet the criteria established in Chapter 2. A summary is given followed by an explicit description of the system employed in this thesis.

The spectrometer hardware is used to first perturb, then measure the electromagnetic transitions of a population of nuclei (bulk sample), between stationary energy states. The energy levels in the NMR experiment are a consequence of the permanent magnetic field furnished by the magnet pole faces. The stability of the magnet is largely a function of the magnetic power supply and associated monitoring circuitry (magnetic flux stabilizer and temperature controller). The excitation is stimulated by an RF oscillation supplied by the transmitter of Figure 3.1 through a transmitter coil aligned along the x axis. The detection and quantitative measurement of the induced signal is performed by a phase sensitive detector connected to a coil placed on the y axis. Both coils are housed in a probe which sits between the pole faces of the magnet and holds the

Figure 3.1

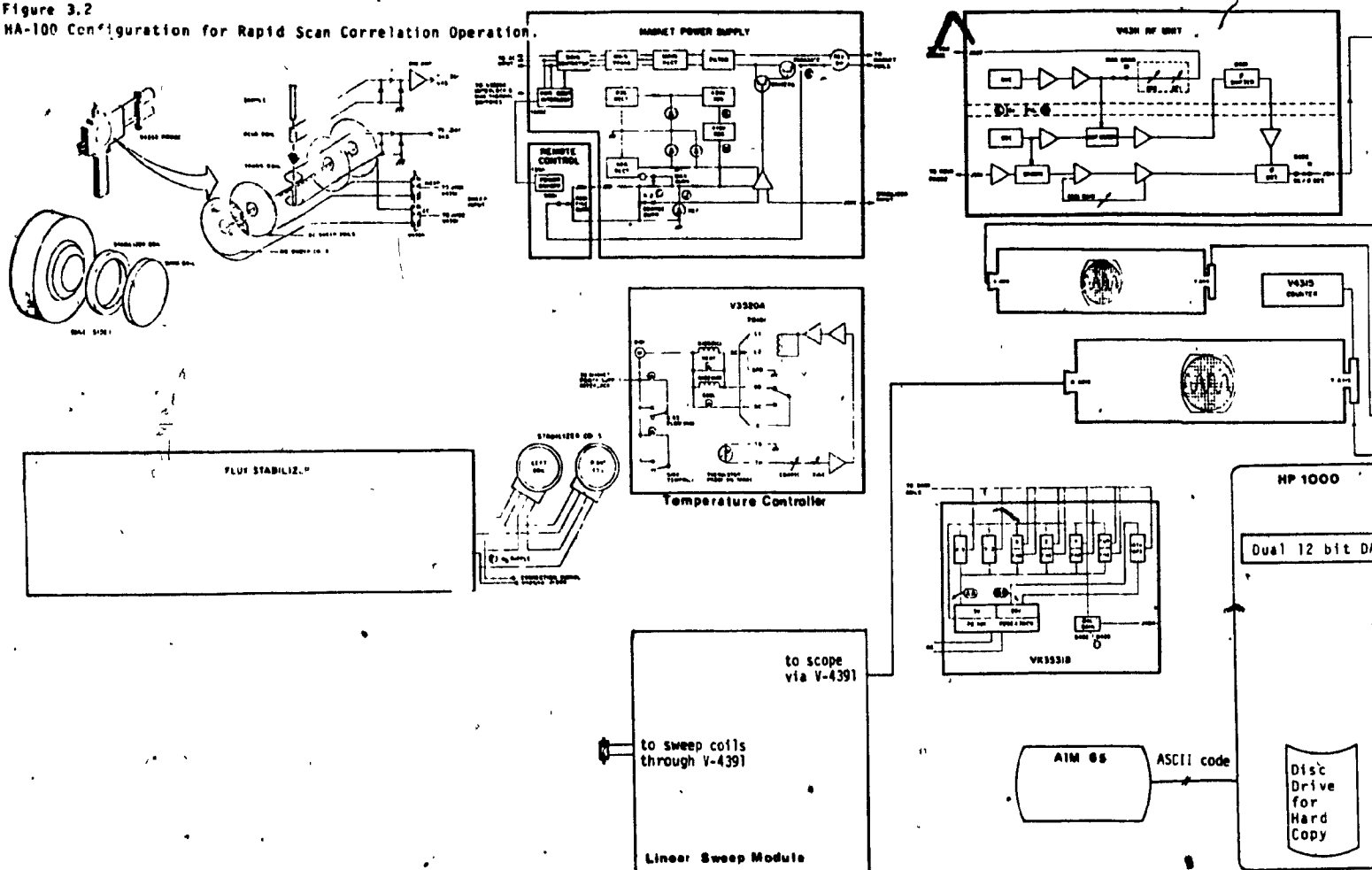
Basic NMR Spectrometer



sample under investigation. At the point of detection both the transmitter and the receiver are tuned to the Larmor frequency, completing the requirements for the resonance condition, and reaching a maximum according to the Bloch equations. The last component to be mentioned, shown in Figure 3.1, is the signal recorder. The recorder receives information derived from two sources, shown clearly in the Figure. Conventionally, the potential from the sweep coils is used to drive an analog motor which moves a bridge proportionally to the x axis. A separate motor drives a slide wire mounted on the bridge, with a pen attached to it. This is driven by the amplified signal from the receiver and draws the y axis absorption plot.

This concludes the general description of an NMR spectrometer, the specific configuration of the instrument used in this thesis will now be discussed. The modified arrangement of an HA-100 spectrometer is shown in Figure 3.2. Each component will be discussed to specify its role in the operation of the entire system.

Figure 3.2
HA-100 Configuration for Rapid Scan Correlation Operation.



Chapter 3
Section 1

The Magnet

A 100 MHz (2.348 Tesla) water cooled electromagnet is employed in this spectrometer along with the original power supply and V3520A temperature controller. The physical dimensions and mechanical criteria conform to the manufacturers specifications⁶⁴ and have been covered in detail in other texts.⁶⁵ The magnetic field must be both stable and homogeneous since, by the Larmor equation, a fluctuation of H_0 by an order of 10^{-9} yields a change in the resonant frequency of .1Hz at 100 MHz, which is significant in a high resolution experiment. When the line broadening governed by the spin-spin and spin-lattice relaxation is less than that caused by the inconsistencies of the magnetic field then the spectrometer contribution is at the limit of resolution. The stability and homogeneity requirements are met by several actions detailed below:

Field Stabilization

The following list comprises the techniques employed in this spectrometer to achieve a stable magnetic field.

1. Insulation and temperature control are provided by a double wall casing and the V3520A temperature controller respectively. The V3520A is solenoid controlled to react to a thermistor resident in a reservoir tank where the water from the magnet cooling coils is continuously cycled.

A large amount of heat is generated from an electromagnet since a high intensity electrical current is routed through two main field coils which are wound around the circuit connected to the pole faces.

2. The output from the main transformer stages going into the magnet is rectified and filtered by current stabilization circuits present in the power supply itself.

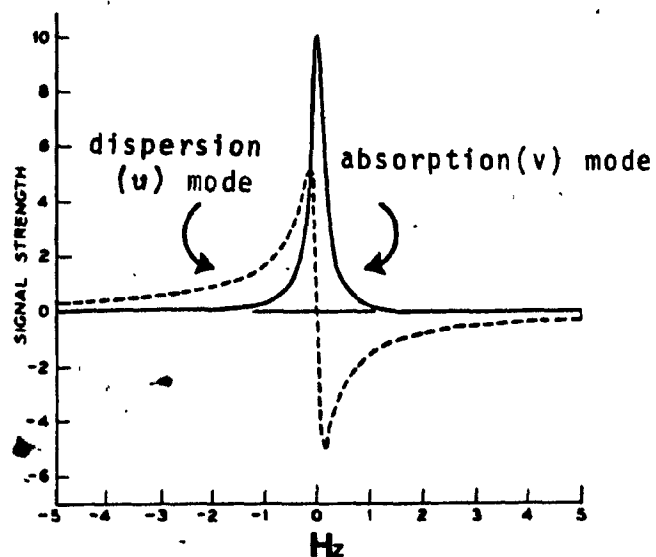
3. Magnetic flux stabilization is supplied by the flux stabilizer which compensates for rapid changes in the magnetic field. This is accomplished by supplying a correction signal to the current stabilizer as a result of monitoring the magnetic flux through stabilizer pick up coils mounted on the pole faces and by supplying a current to the buck-out coils.

4. A field homonuclear lock is used by the V4354A controller with a separate channel provided for the lock modulation. For our purposes, the lock channel was operated at 2500 Hz, the V4354A having a dedicated potentiometer to control the power modulating the lock. The dispersion signal of the chosen reference side band (TMS, DSS, or H_2O) is monitored and current applied to the appropriate stabilizer coil to correct for the shift in magnetic field. See Figure 3.3 for explanation of channel frequency allocation.

Homogeneity

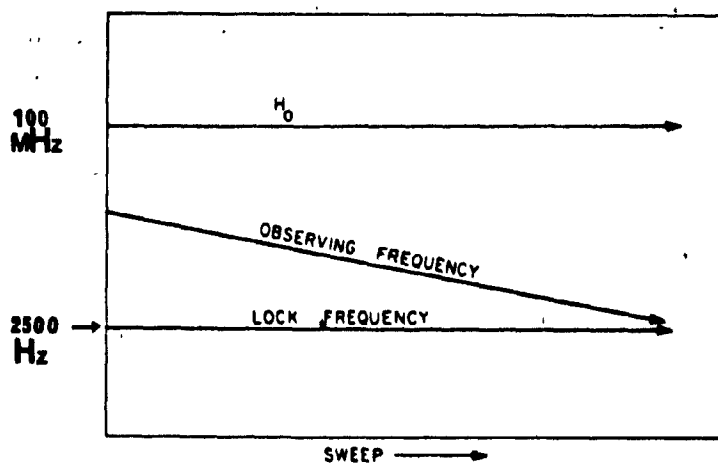
The homogeneity of the magnetic field varies as a result of sample state, sample tube quality, and of course, the

Figure 33



Lock is held at 0. Hz, sign change occurs upon drift.
 Feed back loop monitors sign and applies current to coils.

Figure 34



main field inhomogeneities. Attached to each pole face are shim coils arranged in pairs which apply supplementary fields of concisely regulated strength and geometry controlled by potentiometers housed in the V3531B unit.

Under normal operating procedures, the field homogeneity is shimmed empirically by observing the ringing of an intense singlet.(mentioned in Chapter 2, section 3) This is done before locking such that the signal is maximized to provide the largest possible lock and the most resolved signal possible. Spinning the sample in the probe also increases homogeneity since the magnetic field experienced by any nucleus in the x-y plane will be averaged.

The Sweep System

In order to detect the signal, some method is required to move the resonance condition past the detector. This may be done, as pointed out in Chapter 2, by either sweeping the frequency or the field. The pro's and con's of the two alternatives has recently been questioned in the literature, with the conclusion that both methods are equally sensitive being drawn.⁶⁶ In our case, the lock frequency is held constant, modulated on a separate channel, while a weak ac is supplied to the sweep coils mounted in the probe, from the linear sweep module, originating from the V3530 sweep oscillator. This is represented diagrammatically in Figure 3.4. The V3530 houses the Wavetek oscillator which

responds to a voltage ramp output from the HP-1000 computer (0 to 10 volts) and is initialized by the operator calibrating trim potentiometers on the unit face while observing the V4315 frequency counter. This is the point where the frequency sweep is put under software control. The linear voltage ramp pushes the V3530 output between any two minimum and maximum settings dialed in by the operator viewing the the frequency counter, in response to the polling computer program. This allows discrete digital control of the frequency linear sweep and replaces the usual CW analog drive.

Transmitter, Receiver, Probe.

The HA-100 is a crossed coil spectrometer, where the receiver and transmitter coils are perpendicular to each other, mounted on the x and y axis, respectively. They are housed in the probe body, a single piece of harmonically stable aluminium, this prevents interference from phonons, mentioned in Chapter 2, section 3. Also aligned in the probe are the sweep coils and the receiver preamplifier.

The close proximity of the two coils and local magnetic eddy currents make it necessary to balance the transmitter power with the emf produced in the receiver coil such that a zero potential is passing out of the probe from the receiver coil. This is accomplished with two sets of double paddles, coarse and fine, which tune the coils by changing the inductance of the probe.

Experimentally, the transmitter excitation is caused by applying plane polarized electromagnetic radiation in such a way that a component of the radiation rotates in the same direction as the spin precession, and induces a transition.⁶⁷ The quartz oscillators in the V4311 unit supply the lock, analytical and transmitter channels with the appropriate amplified and attenuated RF energy.

The receiver detection signal is an induced emf potential in the coil which undergoes preamplification in the probe. Once out of the probe, the signal is further amplified and passed into a phase sensitive detector. The abs-

orption (v) or dispersion (u) signal, both present in the output, may then be obtained by the judicious adjustment of the phase angle by rotating a capacitive copper plate between the face of the detector, mounted on a calibrated dial, displayed on the V4311 unit front panel. The output of the phase detector depends upon the phase of the input signal relative to that of the reference signal and the slope of the line. It is well documented that the resistance of the tuned circuit is the absorption (real) mode, while the reactance yields the dispersion (imaginary) mode of data,⁶⁸ and this is electrically how the signal is separated.

Chapter 3

Computer Interface

Any spectrometer using FT techniques requires a computer to process the data digitally. There are many options open to the NMR spectroscopist considering putting a spectrometer under computer control.^{69, 70, 71} In the configuration presented here, there are three obvious functions the computer must perform:

1. Output control signals to run the experiment.
2. Input data from the experiment and output hardcopy.
3. Interface with the operator.

The operating parameters of the computer control network are a function of both the hardware and software involved. The intention here is to discuss the aspects of the computer components which affect the performance of the instrument. The programs are covered in detail in Chapter 4, and that is the most obvious point to discuss the attributes of the entire coordinated system.

HP-1000

The HP-1000 is a Hewlett-Packard minicomputer running under a HP-21MX-E processor with 32K of 16-bit word memory. An HP-7400A disc drive provides 4.9 M bytes of hard copy through one fixed, and one removable disc. Ancillary input-output (I/O) devices include a HP-2645A terminal, Digital

LA-120 terminal(employed as a printer), and a Nicolet Zeta 1553 digital plotter. The I/O between the HP-1000, and the Zeta plotter, or LA-120, is done through an RS-232C interface which is switchable, to allow remote operation from different lines hard wired to various rooms in the Department.

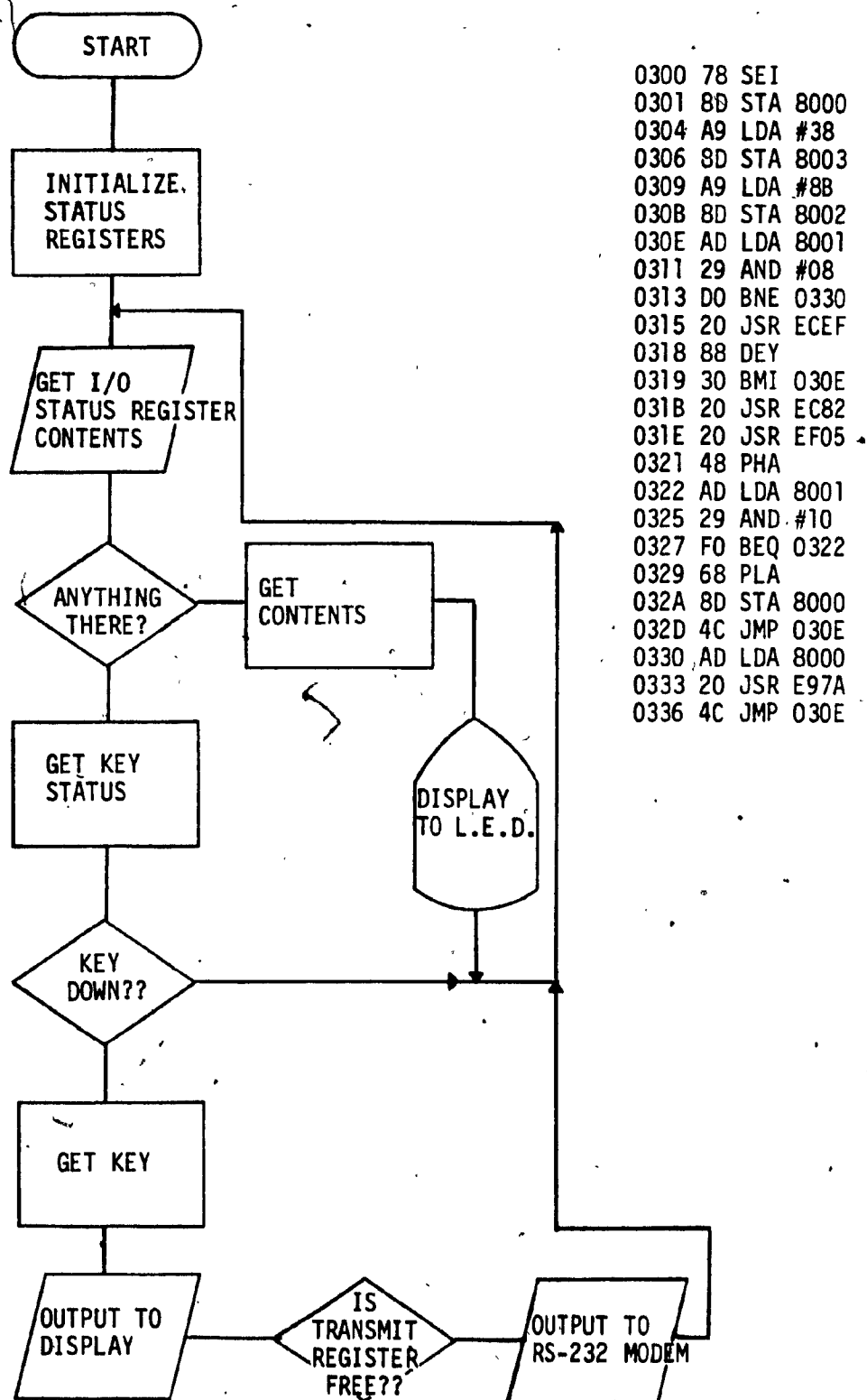
The HP-1000 runs on the HP RTE-2 operating system, and will run Fortran IV and Assembler languages.

AIM-65

The Aim-65 is a single board R-6502 based microprocessor with 4K 8-bit memory. The Aim-65 has an on board dot-matrix thermal printer, a 22 character light emitting diode (LED) display, and a full typewriter style keyboard.

The R6502 central processor unit runs a memory mapped I/O through an 8-bit parallel data bus. Because of the simplicity of the monitor program resident in the Aim, a separate assembly language program was written accessible through a function key on the keyboard. This program, shown in figure 3.5, sets the microprocessor in a polling loop. This loop monitors the keyboard and the designated data lines on the J-3 expansion port, searching for incoming data. In this configuration the Aim acts as a remote terminal, receiving data in both directions. The characters sent by the HP-1000 are input and displayed on the display, while the keyboard data is output on the chip-selected lines.

Figure 3.5 AIM-65 Assembler Program and Flow Chart



INTERFACE

It is now possible to review the original three functions deemed necessary for computer control. The first two, experimental monitor duties, are accomplished by providing a ramp from 0 to 10 volts dc to the Wavetek in the V3530 unit. This allows discrete digital control of the frequency sweep through the experiment with an accuracy imposed by the timer internal to the HP-1000. To a certain degree, the limitations are controlled by the programming efficiency, but the NMR experimental time frame is many orders of magnitude slower than the speed approachable by an optimized assembly language program .

The input signal enters the HP-1000 through the Raytheon 14-bit analog to digital converter(ADC), via a 16-bit duplex register. The output signals exit through two dual 12-bit digital to analog converters(DAC). One DAC line provides the spectrometer sweep and scope x-axis, while the other has the scope y-axis.

The last function, operator interface, is performed through the Aim-65, using the program in Figure 3.5 and the circuitry shown in Figure 3.6. The R6551 is an asynchronous communication interface adapter(ACIA). It is completely programmable, with three internal registers which control the parity, interrupt status, baud rate, and other pertinent handshake parameters which ensure easy interface with a variety of host computers.

Figure 3.6 RS-232 Communication Interface

Aim-65 J-3 port

R6551 chip configuration

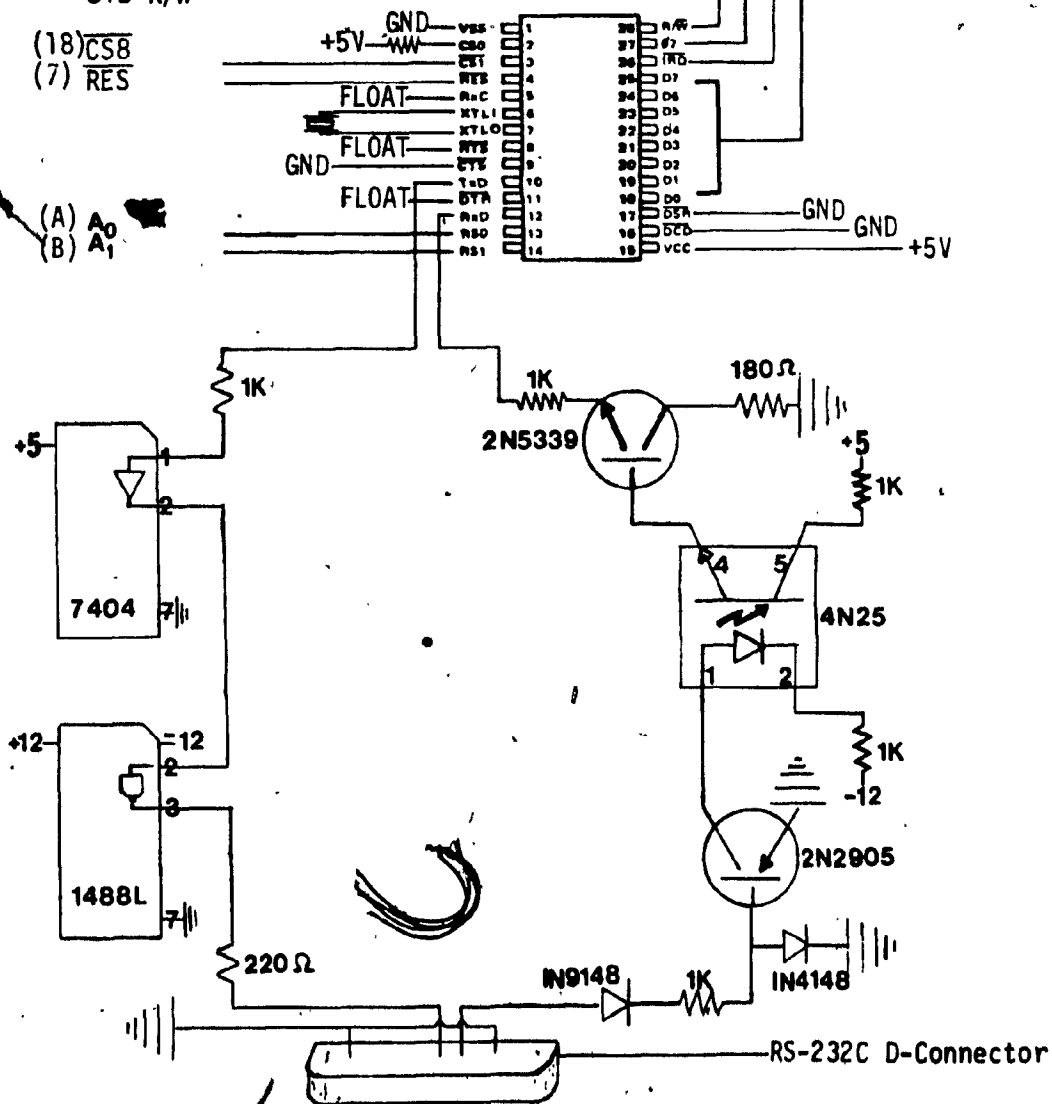
PIN #

- (15) D₀
- (14) D₁
- (13) D₂
- (12) D₃
- (11) D₄
- (10) D₅
- (9) D₆
- (8) D₇

- (4) SYS $\overline{\text{IRQ}}$
- (U) SYS $\phi 2$
- (V) SYS R/W-

- (18) CS8
- (7) RES

- (A) A₀
- (B) A₁



The three functions of the computer control system have been discussed with respect to the hardware components used to implement the net-work. The limiting step is the software, and that is discussed next.

CHAPTER 4

SOFTWARE

Control of the entire correlation process has been divided into three separate programs, each of which is compiled and run distinctly from the others. This is necessary because of the restrictive size of the host computer, but follows a natural separation present in the exclusive nature of each job.

Each program shall be explained presenting the operating algorithm and illustrations of the actual results. The duties of each are summarized here to enable an understanding of how the division of labor is accomplished between them.

1. NMRUN--Actually two programs, a Fortran routine for user interface and calculations, and an assembly language routine which actually runs the spectrometer during the experiment. This program in its entirety allows the user to run the experiment and write the data gathered as a disc file.

2. NMRAN--One large routine which performs all data manipulations necessary for coherent treatment of an NMR data file. This program reads a disc-file (presumably the result of NMRUN), allows processing, and writes the post operative file without affecting the original spectra file.

3. NMPLT--This program reads a disc file and plots the data on the digital Zeta plotter. The routine is in Fortran and utilizes Nicolet Zeta subroutines. The original file is preserved with no additional files created.

The usual sequence of operation is in the order that the routines have been presented. Because of the remote access to the spectrometer, only the programs NMRAN and NMPLT are run local to the HP-1000 and Zeta plotter. This is not inconvenient, since these two routines are run exclusively post manipulative to the experiment itself.

The programs themselves are presented in Appendix 1 for consultation.

Chapter 4
Section 1

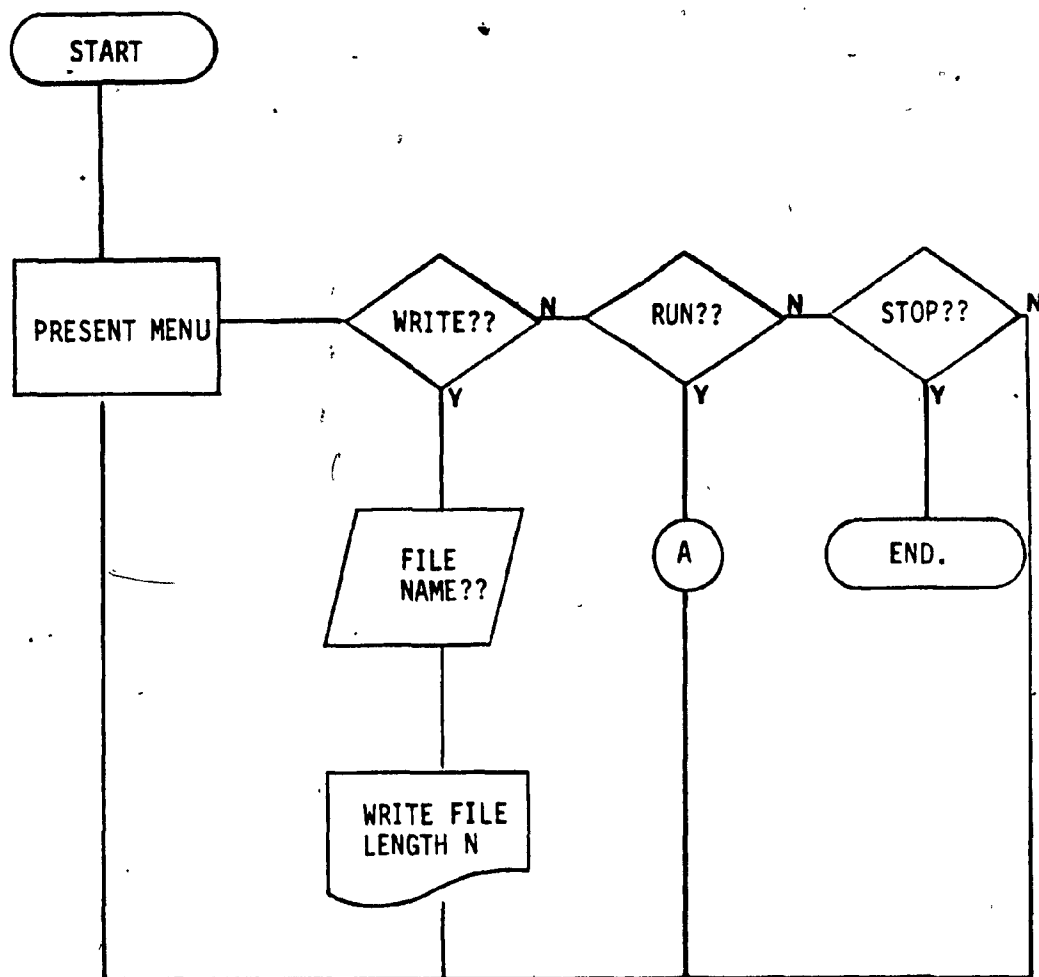
NMRUN

This program runs the spectrometer, and creates a disc file to hold the data recovered from the experiment. There are really two major parts to this code, the controlling Fortran routine and the slave assembler code. Each will be treated separately, taking the lead from their mode of interaction.

It would be most helpful to consult Figure 4.1 for this discourse. The calculation of the running parameters is done to fit the requirements of the assembly language sweep program. The operator is polled for data, of which three responses must be accurate: the two readings off the frequency counter indicating the Wavetek settings, and the number of scans required. All other entries are taken to be estimates, with the real value resultant from the internal calculations returned at the end of the set-up loop. The operator then has the alternative of changing any variable. Because of the hardware configuration, only the acquisition time and the number of sweeps can be altered without repeating the entire set-up routine.

Once the sweep routine has been selected, the keyboard is locked out until the experiment is completed. The assembler routine returns to the calling routine where the acquisition parameters may be immediately changed if the operator was dissatisfied with the original result.

Figure 4.1



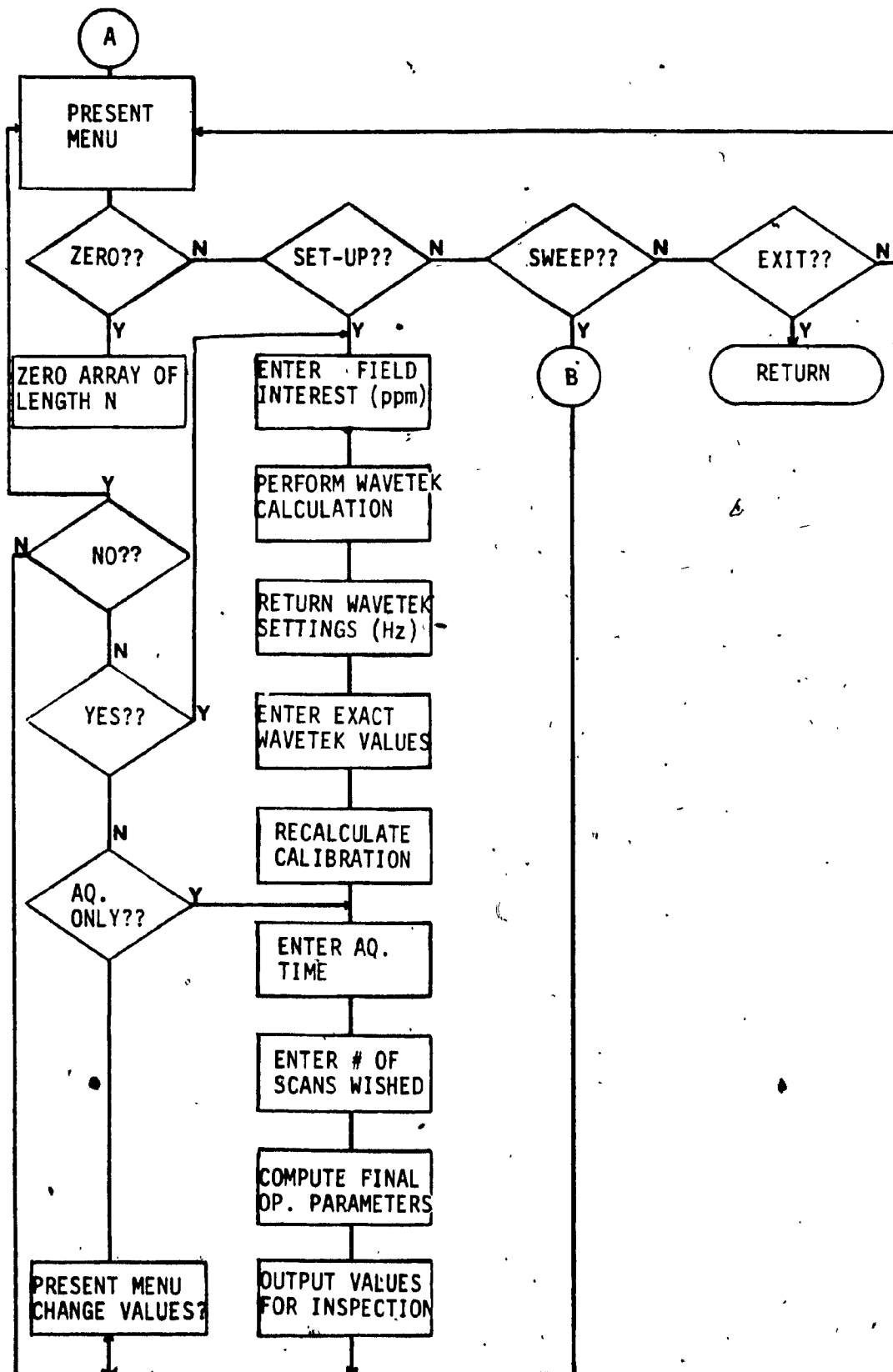
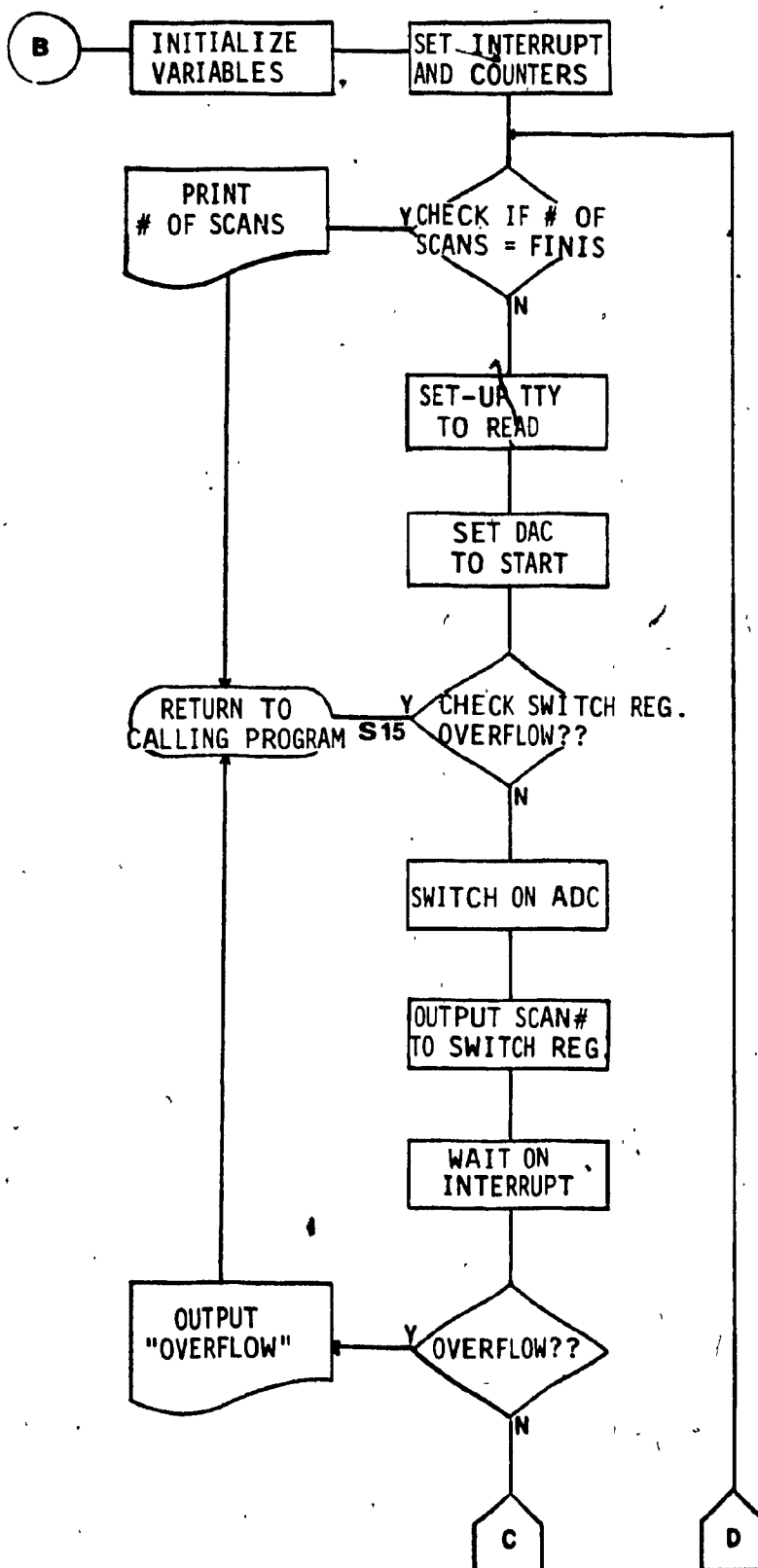
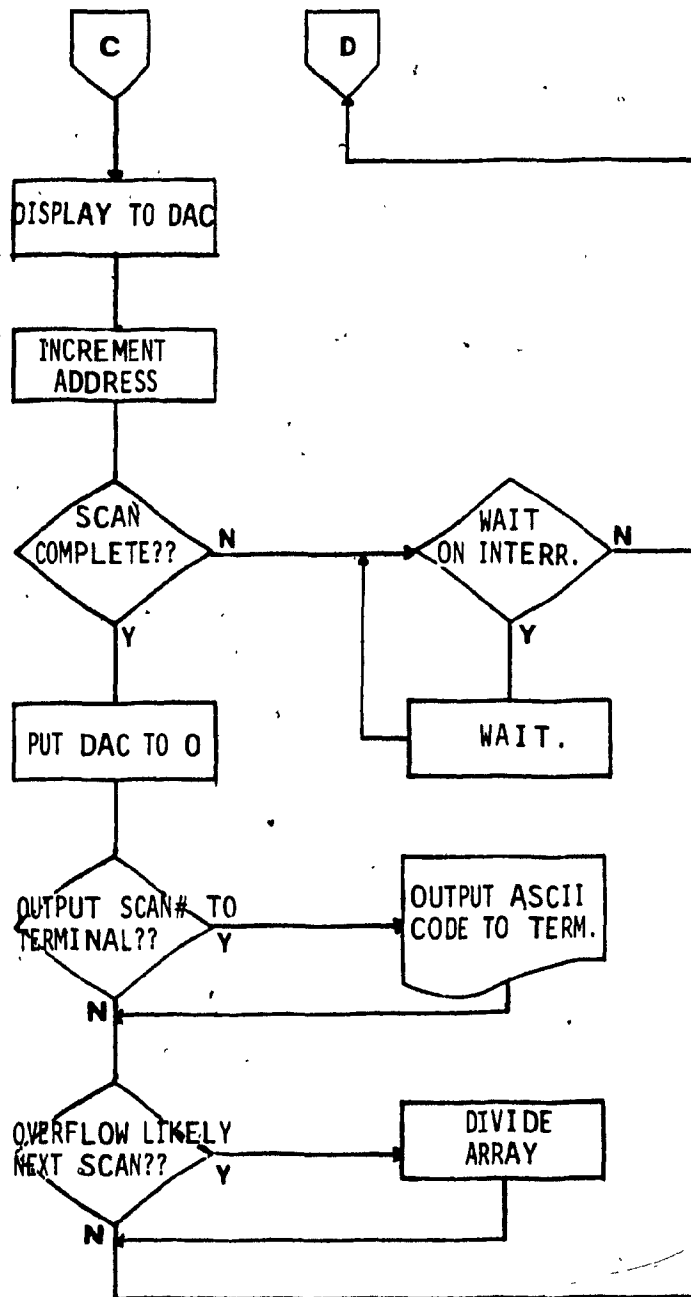


Figure 42





The assembly language code has three Fortran calls from NMRUN which access different subroutines. The three subroutines are responsible for calibration of the V-3530 Wavetek (RMIN,RMAX), and running the experiment on the HA-100 (SWEEP).

The experiment is run by providing a sweep ramp from 0 to 10 volts in 4096 steps, with data collection at each step. The ramp is calibrated by separate calls to RMIN(0V) and RMAX(10V) which are summoned by NMRUN to coincide with the Wavetek adjustment performed by the operator.

The SWEEP code call passes the pertinent values to the assembly routine to run the system clock and count the number of scans. All the calculations are performed in the NMRUN calling routine, the values are simply loaded into the variables with the call, no error checking is done after the call, inside the assembler routine.

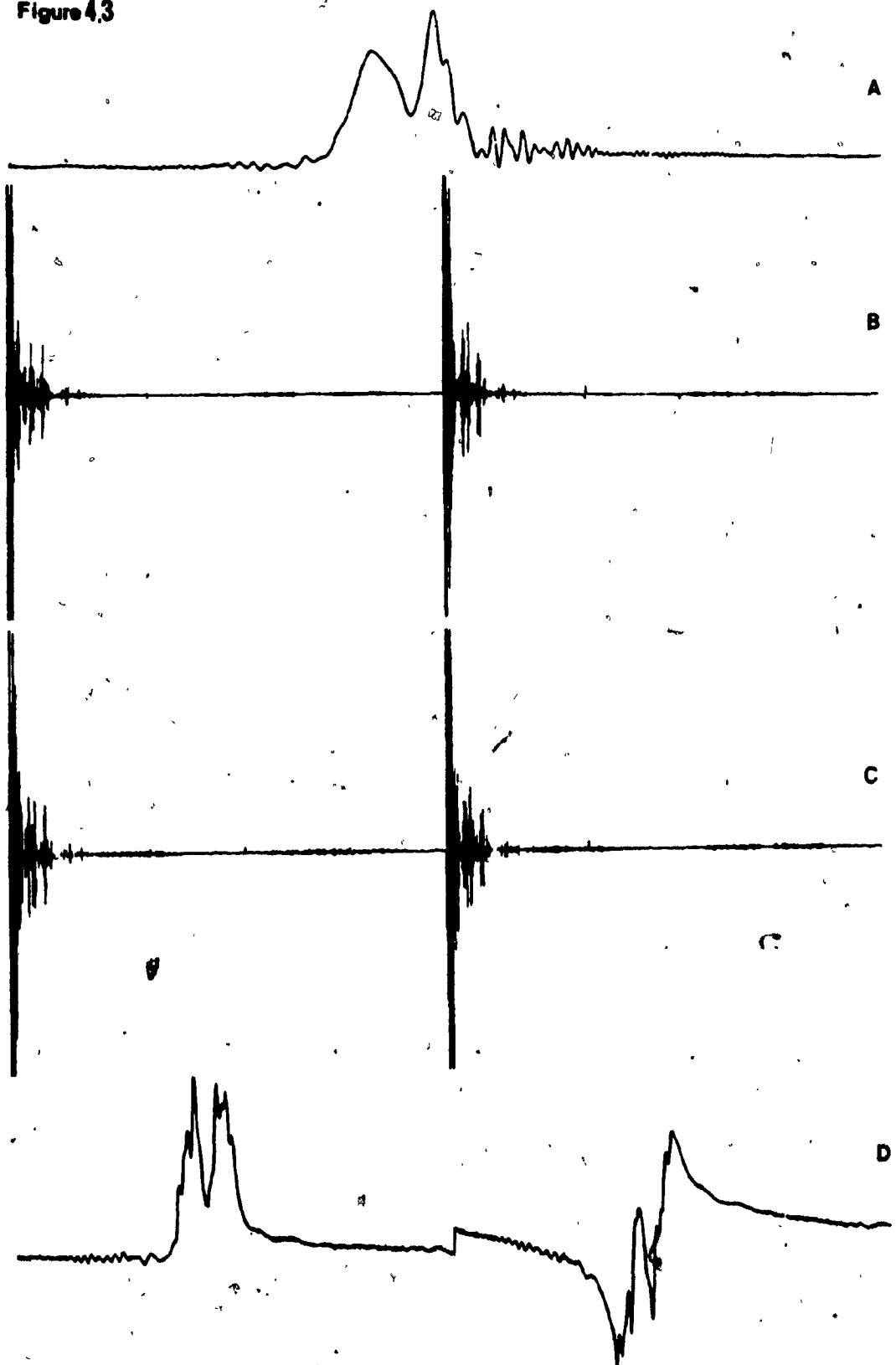
Chapter 4
Section 2

NMRAN

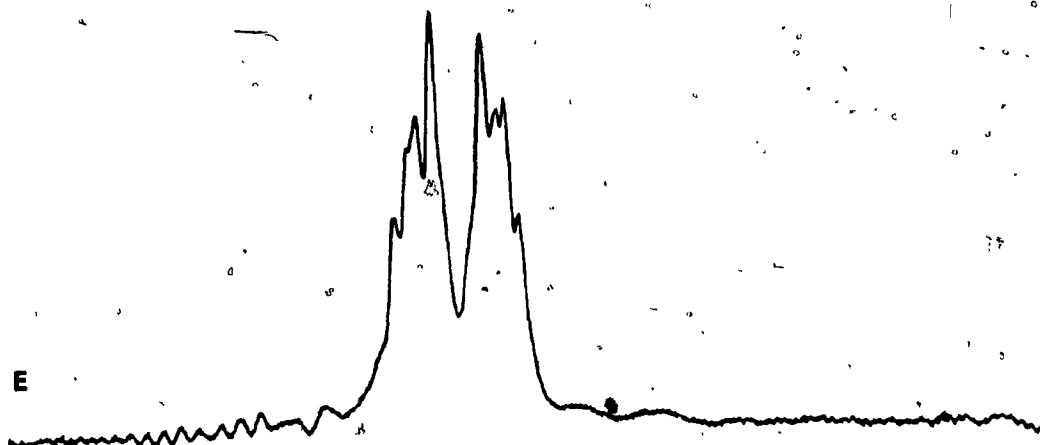
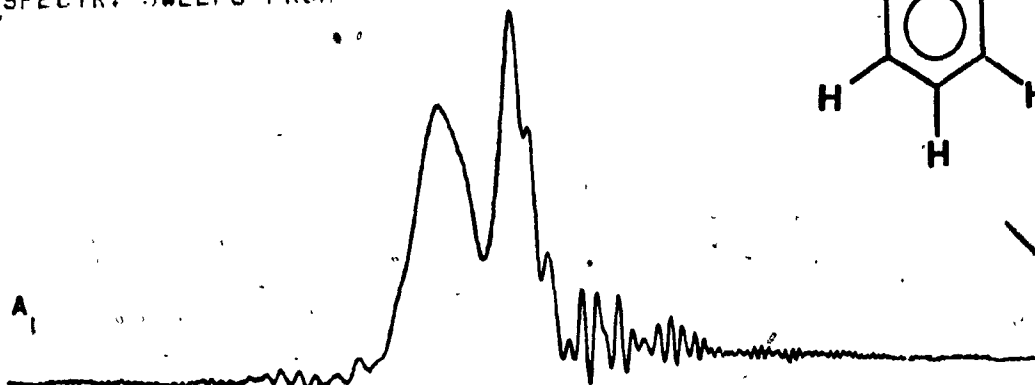
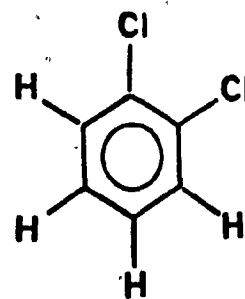
The algorithm is discussed by section, since each processing function operates independently of the others and may be accessed in any sequence. The one assumption which the programmer is responsible for, is that the operator understands what order the different functions should be applied to yield a coherent result. An error checking monitor at this level would be quite complicated unless every step of the processing was put under program control. This would be relatively simple but would restrict the freedom of the operator to experiment with new procedures. There are also hardware memory limitations to be considered.

The actual use of NMRAN is demonstrated in Figure 4.3, which is an illustration of the steps taken typically through the processing of a raw spectrum file to yield the final correlated, phased, slow passage spectrum. No digital massaging was done, so that the final slow passage spectrum of orthodichlorobenzene would be comparable to the fast passage result. Only the sweep rate differs between spectra E and F in Figure 4.3. Obviously, the resolution in the correlated result is not equivalent to that of the slow passage spectrum, but this is simply a question of excessive sweep rate causing line broadening and this case is examined with an example in the experimental Chapter 5.

Figure 4.3



SWEEP RATE- 147.03 HZ/SEC
DIGITAL RESOLUTION = 7.56 PTS/HZ
TRUE ACQUISITION TIME IS 1.84 SEC
SPECTR. SWEEPS FROM 8.53 TO 5.60 PPM



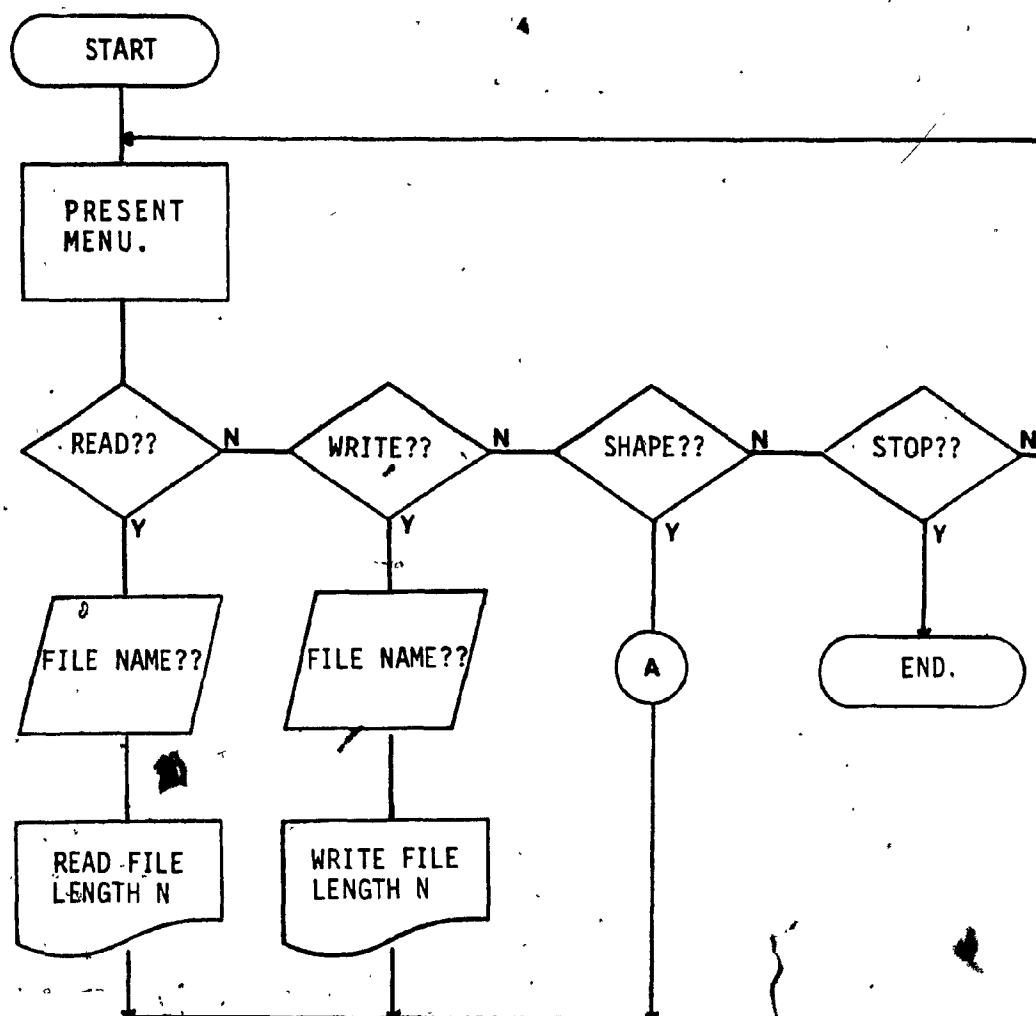
11
SWEEP RATE= 2.26 HZ/SEC
DIGITAL RESOLUTION = 7.56 PTS/HZ
TRUE ACQUISITION TIME IS 119.81 SEC
SPECTR. SWEEPS FROM 8.53 TO 5.60 PPM

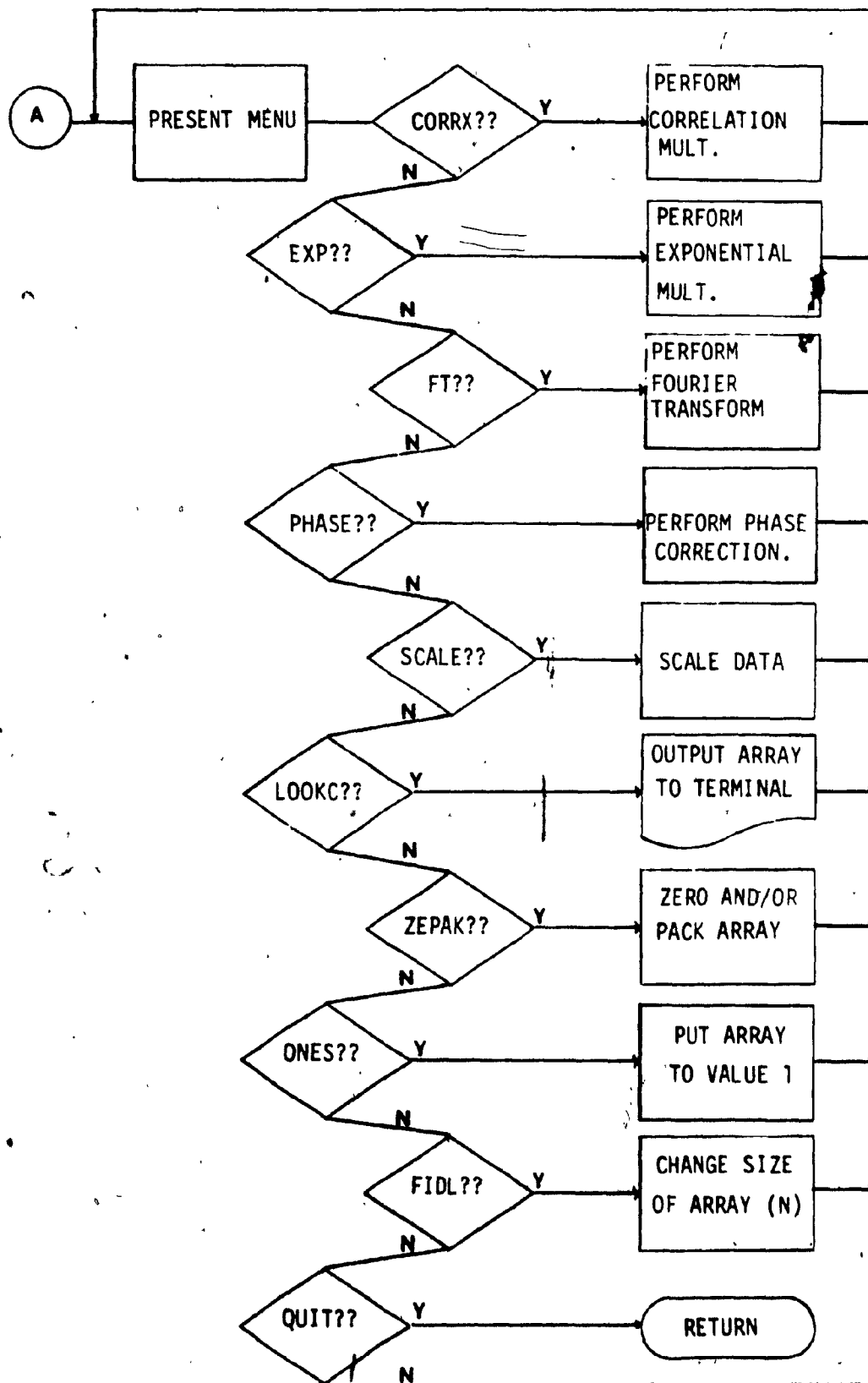
The purpose here is to illustrate the state of the array values at various steps through the processing procedure. The following histogram steps through the exercise typical in correlating a raw spectrum file, the appropriate diagram is indicated for each step alphabetically.

1. read a disc file into the array.
2. scale the array-----> A
3. perform a forward real transform
4. scale the array-----> B
5. perform correlation multiplication-----> C
6. perform an inverse complex transform
7. scale the array-----> D
8. perform phase adjustment
9. pack-plot the result-----> E
10. comparable slow passage plot-----> F

The flow chart is shown in Figure 4.4. The convention is to always present the operator with a menu of alternatives such that the options are plainly before him or her at all times. An unavailable or unintelligible response always returns the menu.

Figure 4.4





CORRELATION

The correlation calculation expects the array to be in first half real - second half imaginary order. The term which represents the theoretical line is not applied directly, but is reduced to a form simpler to implement in the calculation.

From Chapter 2, section 5, it is remembered that

$$g(t) = \exp \left(\frac{-ibT^2}{2} \right) \quad \text{where } b = \text{sweep rate } \frac{\text{rad}}{\text{sec}^2}$$

and T = running time variable.

from Ozawa and Arata³⁷ we know that

$$(4.1) \quad \Delta t = \frac{1}{N \Delta f} = \frac{2\pi}{Nb \Delta t} \quad \text{where } \Delta t = \text{the change in time.}$$

N = number of points.

Δf = change in frequency.

b = sweep rate.

Δt = time increment

by definition in my program

$$b = \frac{2 \pi SW}{AQ}$$

where SW = sweep width.

AQ = aquisition time.

$$\text{and } \Delta t = TCON = \frac{AQ}{N}$$

substituting these into equation 4.1 we get

$$(4.2) \quad \Delta t = \frac{2 \cdot \pi}{N \cdot 2 \cdot \pi \cdot SW \cdot \frac{AQ}{AQ \cdot N}}$$

From Ozawa and Arata³⁷ we also know that $\exp \frac{b (k \Delta t)^2}{2}$
(4.3)

is equivalent to $\exp \frac{b \cdot T^2}{2}$

We can now substitute for b and Δt into equation 4.3 and get

$$(4.4) \quad \frac{2 \cdot \pi \cdot \frac{SW}{AQ} \left(k \left(\frac{2 \pi}{N \cdot 2 \cdot \pi \cdot \frac{SW}{AQ} \cdot \frac{AQ}{N}} \right) \right)^2}{2}$$

which reduces to $\frac{\pi k^2}{SW \cdot AQ}$

where $k \neq$ index of array

SW = sweep width

AQ = aquisition time

It is also much simpler to use Euler's theorem to calculate the value of the exponential term. Thus the operational definition of correlation is realized as:

$$\exp \left(\frac{-i \pi k^2}{SW \cdot AQ} \right) = \cos \left(\frac{\pi k^2}{SW \cdot AQ} \right) + i \sin \left(\frac{\pi k^2}{SW \cdot AQ} \right) \quad (4.4)$$

and is implemented as

$$R_n = R_n \cos () - I_n \sin ()$$

$$I_n = R_n \sin () + I_n \cos ()$$

where R_n represents the real values of the array, and

I_n represents the imaginary values of the array.

This allows the new correlated values to be computed in place without increasing the memory space required. This also allows the total FFT/correlation operation to be completed in $N + 3N \log_2(N)$ multiplications.⁵²

FAST FOURIER TRANSFORM (FFT)

The actual implementation of the Fourier transform is accomplished with a program published by Cooper.⁴⁴ This routine is the result of much optimization^{45,46} and is general in its application. There are many alternatives when searching for an FT algorithm to fit an application, all based on the original work by Cooley-Tukey,⁹ varying from general improvements⁴⁷ to specialized algorithms enhanced specifically for accuracy rather than speed.⁴⁸ This program has seen use in an NMR environment⁴⁹ and hence required few changes to fit turnkey-like into our system.

The program itself is written in Fortran and setup as a subroutine of NMRAN, responding to the menu solicitation for FT. There are three major subroutines internal to the FT code which process the array in three distinct steps and whose order of use determines the type of FT performed by the call. The internal subroutines act separately from each other and do no error checking to supervise the order of deployment, but this is a decision made by the programmer and not the operator. In this case there are only two possible FT calls available to the operator, a real forward FT, and a complex inverse FT, even though the code has the capability to perform all possible variations of calls.

The three subroutines, FFT, POST, and SHUFFL, will be discussed in general, but the bulk of this section must concentrate on the combined effect of all three as they operate on the array. The subroutine is available in the appendix for reference, for further detail the original source is recommended.⁴⁴

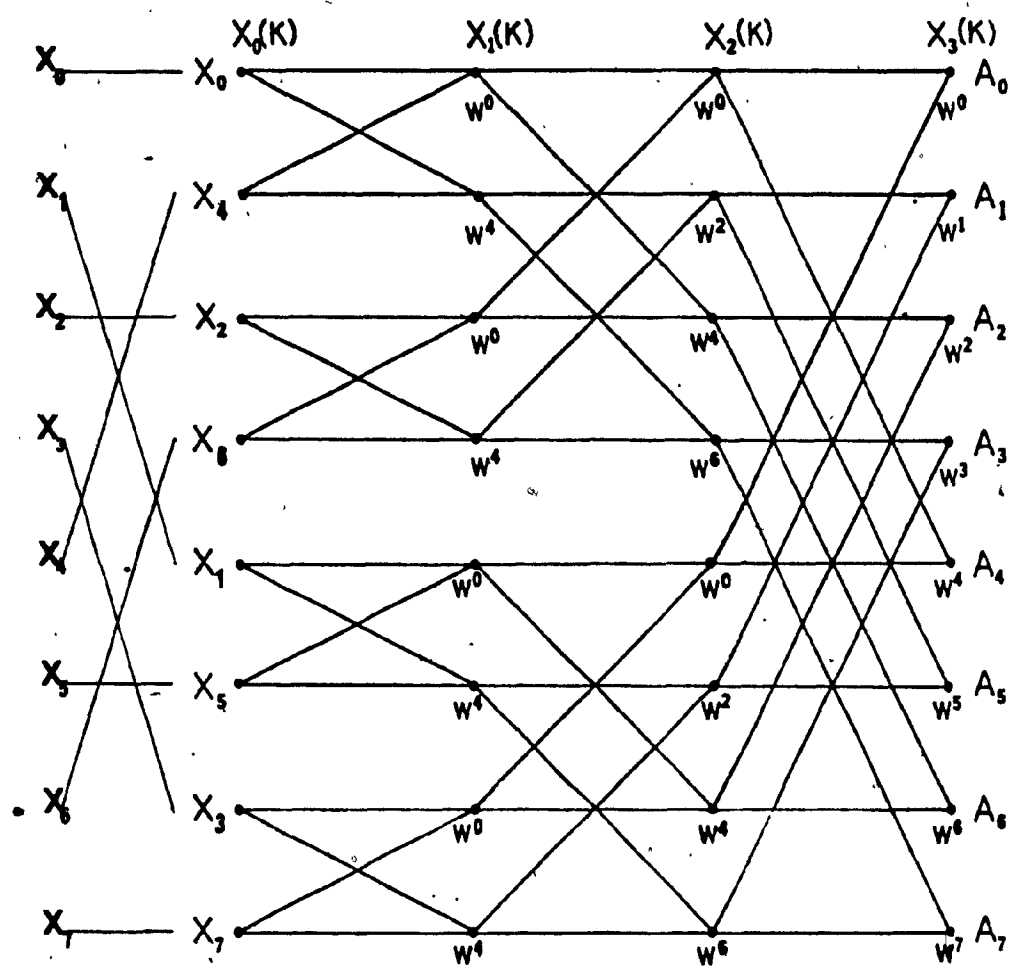
FFT Subroutine

This piece of code actually performs the transformation, the other two being ancillary operations concerned basically with indexing (SHUFFL) and the special treatment of real numbers (POST). The signal flow graph shown in Figure 4.5 illustrates the steps required for an array of $N = 8$. The array is first put into bit-inverted order such that the final sequence is uniform from 0 to 7. This bit-inversion is an artifact of the calculation regimen and is simply an index rearrangement.

In general there will be k passes required for an array of size $N = 2^k$. Each pass constitutes a recombination of points and is indicated on the signal flow graph by each vertical column of dots. During each pass the new value is the result of the following arithmetic:

$$X'_1 = X_1 + X_2 W \quad \text{where } W = \exp \left(\frac{-2\pi i}{N} \right)$$

Figure 4.5



The calculation symmetry can also be used to advantage where

$$X'_2 = X_1 + X_2 W$$

which allows the operation to be done a pair of points at a time, and therefore calculated in place, as opposed to duplicating the array space in memory.

As was done in the correlation method, the exponential term is implemented using Euler's rule. This also allows an elegant way of controlling the direction of the transform, forward or inverse, by changing the state of the variable INV, which simply changes the sign of the trigonometric addition, shown in Figure 4.6.

FIGURE 4.6

$$(4.5) \quad e^{iy} = \cos(y) + i \sin(y) \quad \text{for INV} = 1$$

$$e^{iy} = \cos(y) - i \sin(y) \quad \text{for INV} = -1$$

$$\text{giving } W^y = \cos\left(\frac{-2\pi y}{N}\right) + i \sin\left(\frac{-2\pi y}{N}\right) \quad \text{for INV} = 1$$

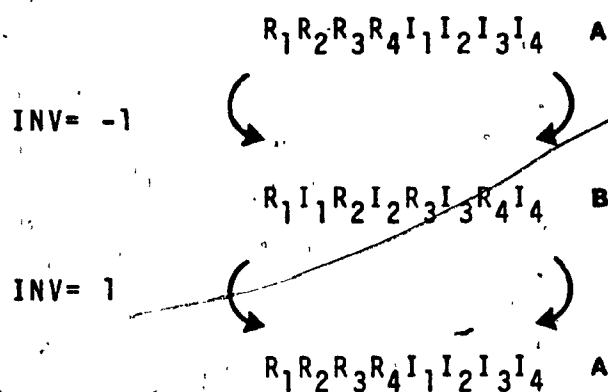
where y is the superscript of W as shown in Figure 4.5.

SHUFFL Subroutine

This subroutine does exactly what the title suggests, it SHUFFLES the array into two different orders depending upon the state of the variable INV. This is illustrated graphically in Figure 4.7, showing the two possible array configurations after SHUFFL processing in A and B for the

Figure 4.7

Action of "Shuffl"



variable $INV = 1$ and -1 , respectively. The significance of this has important implications since the FFT routine expects the data to be in a "first half real, second half imaginary" sequence and generates a complex result accordingly.

POST Subroutine

This routine is employed in a POST-processing function in order to complete the last step of a forward real transform. Again, depending on the sign of INV , it may be used as a pre-processing routine in an inverse real transform, but this format is superfluous to our needs.

The process is a one pass recombinatorial operation which corrects for the fact that the FFT routine acts entirely as if the array were complex.⁵⁰ Thus the real points are calculated by trigonometrically recombining the complex points according to the relationship:

$$(4.6) \quad X_r(n) = R_p + \cos\left(\frac{\pi n}{N}\right) I_p - \sin\left(\frac{\pi n}{N}\right) R_m$$

$$X_i(n) = I_m + \sin\left(\frac{\pi n}{N}\right) I_p - \cos\left(\frac{\pi n}{N}\right) R_m$$

where $n = 0, 1, 2, \dots, N-1$ and $m = N/2$

$$R_p = R_n + R_{m-n}$$

$$I_p = I_n + I_{m-n}$$

$$R_m = R_n - R_{m-n}$$

$$I_m = I_n - I_{m-n}$$

It is now possible to present the FT routine in its entirety. In the final state we have need to perform a forward real FT and an inverse complex FT. The calling sequence for these permutations is

```

call SHUFFL          R1I1R2I2R3I3R4I4
call FFT      ( INV = 1 )  foward real
call POST          R1R2R3R4I1I2I3I4
                  R1R2R3R4I1I2I3I4
call FFT      ( INV = -1 )  inverse complex
                  R1R2R3R4I1I2I3I4

```

PHASE code

The final output from the inverse complex transform leaves the array in the " first half real, second half imaginary " order. The phase correction subroutine expects this, and performs a first order phase correction accordingly. The operator is only required to make a visual appraisal of the phase angle (in degrees) adjustment that it is estimated will result in a perfectly phased spectrum upon application. The equation used to calculate the adjustment is of the form:

$$R_n = \cos(\arg) * R_n + \sin(\arg) * I_n \quad (4.7)$$

$$I_n = -\sin(\arg) * R_n + \cos(\arg) * I_n$$

where $\arg = \frac{\text{phz} * \pi}{180}$

phz = operator entered estimate in degrees..

R_n = the real points of the array.

$n = 1, 2, \dots, N/2$

I_n = the imaginary points of array.

EXPOnential Multiplication

As stated earlier in the theory section, the function which described the array in the Fourier (time) domain is an exponentially decaying free induction decay (fid), and is equivalent to that which would be gathered in a pulse experiment.⁵³ Consequently, the array may undergo the same manipulative techniques employed in pulse FT methods, experiencing the same trade off between resolution and sensitivity as shown in that venue.⁵⁴ The operational difficulties of exponential multiplication can be stated simply:

1. emphasize the start of the fid --> optimum S/N
--> sacrifice resolution
2. emphasize the tail of the fid --> optimum resolution
--> expense of S/N

This translates into line width estimates, which are the required input by the operator. The equation used to model the exponential function is shown in equation 4.8, the calculation itself is done in place. A running total of all line broadening applied against a fid is kept as a book-keeping aid.

$$(4.8) \quad R_n = R_n * \exp - \left(\frac{(n-1) * ELB}{2 * SW} \right)$$

$$I_n = I_n * \exp - \left(\frac{(n-1) * ELB}{2 * SW} \right)$$

where n = index of array

ELB = operator entered line width

SCALE code

This routine allows scaling of the data array to a maximum value entered by the operator. This guards against overflow problems, but is used mainly before a disc file write command is exercised. This ensures that the value of the array falls within the maximum range possible to be encoded for any one value on a disc file(32767).

The operation is a simple search for the largest absolute value in the array, followed by dividing it into the scaling value entered by the operator. This is then multiplied into each array point to yield the scaled array.

LOOKC code

This is essentially a debugging routine which allows the operator to view the array as it is printed out on the terminal. Each value is displayed with the corresponding point number.

ZEPAK code

ZEPAK is a manipulative routine which allows any portion of the array to be zeroed to facilitate the operation of zero filling. The packing option fits a spectrum file into one half the original array size. This was originally done to enable the implementation of a processing algorithm published by Ozawa.³⁷ However there was a loss of resolution by 1/2 because of the missing points, and this was no longer pursued.


ONES code

Another piece of debugging code which simply sets the entire array to the value 1. This is useful when investigating the nature of any of the multiplying functions and searching for artifacts against a reproduction of the function itself.

FIDL code

This routine lets the operator change the size of the array to facilitate debugging and to allow processing of spectra files of an unusual length.

This concludes the description of NMRAN. As previously stated, the programs are presented in the appendix for consultation if desired.

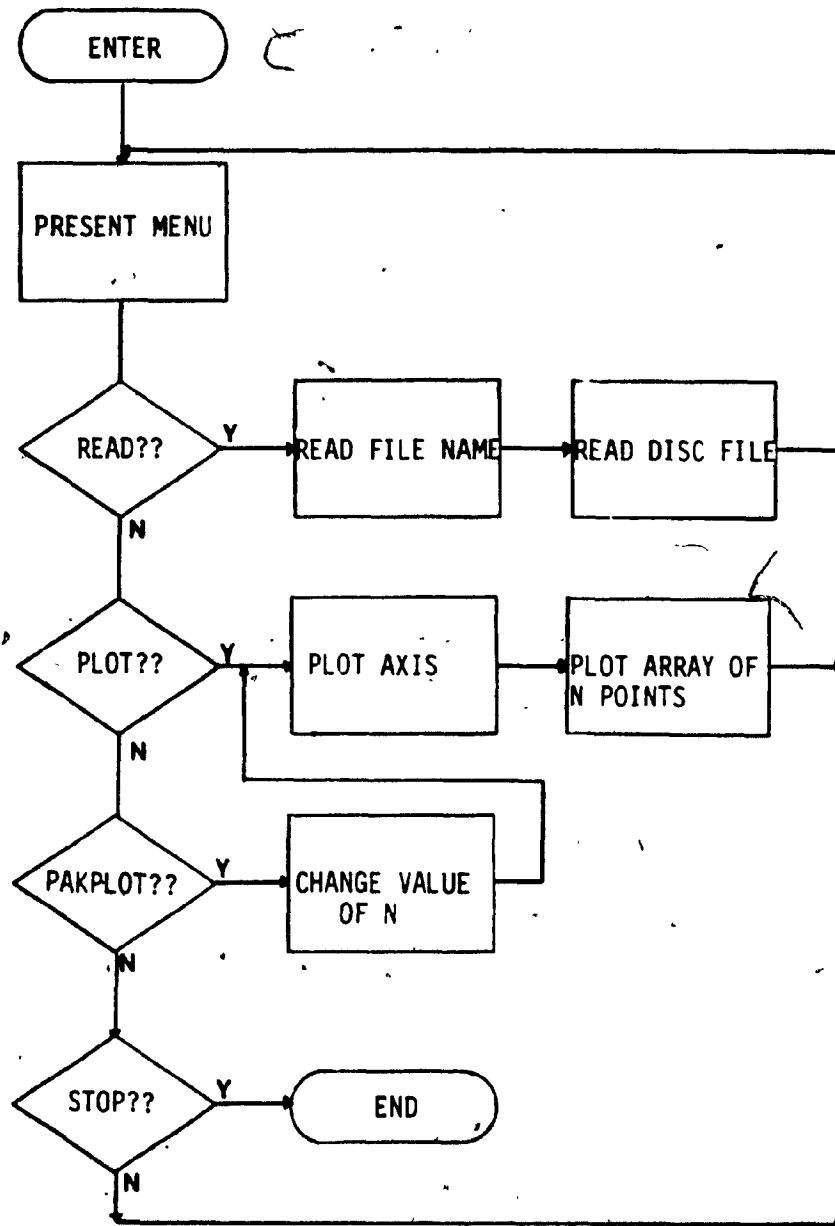


Chapter 4
Section 3

NMPLT PROGRAM

This program is straight forward, the only complexity being hidden in the cryptic format of the Zeta plotter software commands, and to this end the source is referenced.⁵¹ The PAKPLOT option allows the real data to be plotted with out the symmetrical imaginary points. The flow chart is shown in Figure 4.8.

Figure 4.8



Chapter 5

EXPERIMENTAL

The purpose of this Chapter is to present actual spectra obtained from the instrument configured as detailed in the preceding Chapters, which illustrate operation under a variety of conditions. All Figures shown were taken directly from their Zeta-plots after being scaled to 1000.00, and all plotting dimensions are equivalent within any Figure to ensure an accurate comparison. A summary follows.

The effect of sweep rate on the signal-to-noise ratio and saturation parameter was previously mentioned in Chapter 2. This artifact will be investigated using the O.D.C.B. sample employed in Chapter 4 to illustrate the operational flow chart presented there.

Example spectra of some simple organic molecules commonly used for spectrometer calibration will be discussed to demonstrate the system operation when locked on T.M.S.

Aqueous samples will then be explored with the spectrometer locked on both D.S.S. and water. This section clearly demonstrates the advantages of this configuration when investigating systems with strong solvent lines.

Finally, a study of a sparingly soluble thiazolium salt will be presented which exemplifies the type of problem where the unique capabilities of a Correlation Spectrometer find particularly useful applications.

In each case where the fast and slow passage spectra are presented on the same page, the following precautions were taken to allow rigorous comparison:

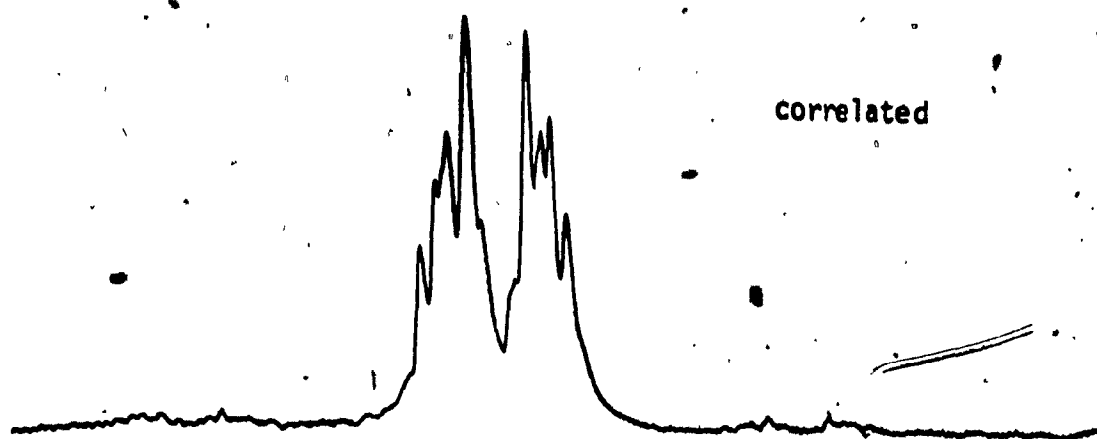
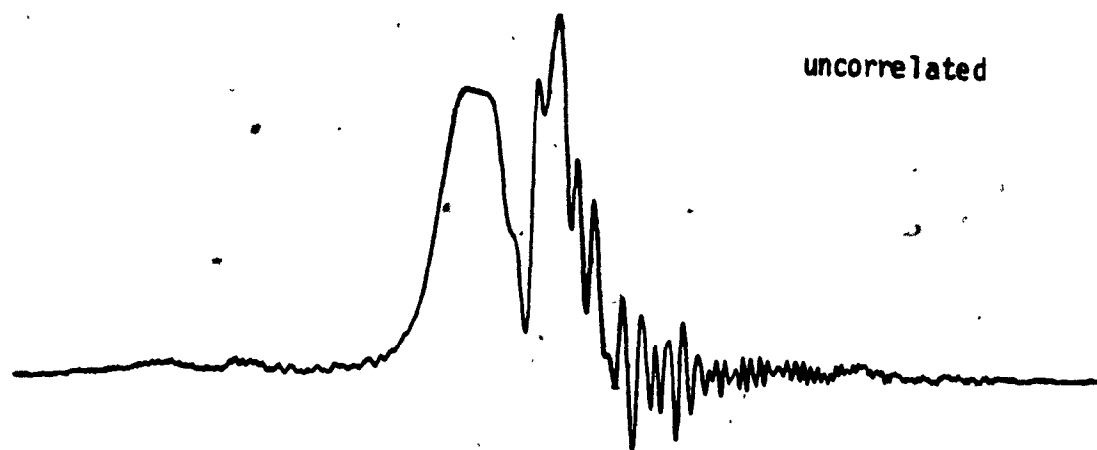
1. The same sample was used in each case.
2. Instrumental settings were equivalent.
3. Digital processing was equal except where phase correction was not required.
4. For each Figure, the fast passage spectrum was run immediately following the slow passage experiment, with no homogeneity adjustments in between. Hence if the field was to degrade over the course of the run the fast passage spectrum would represent the "worst-case" result and consequently the broadest lines.

THE EFFECT OF SWEEP RATE ABERRATIONS

The following short discourse should illustrate the principles originally discussed in Chapter 2 concerning the optimization of the S/N ratio and sensitivity, and the relationship between these parameters and the sweep rate. The O.D.C.B. spectrum has already been presented in Chapter 4. It was noted there that the resolution was not exactly equivalent to that of the slow passage spectrum, although the S/N ratio was slightly better.

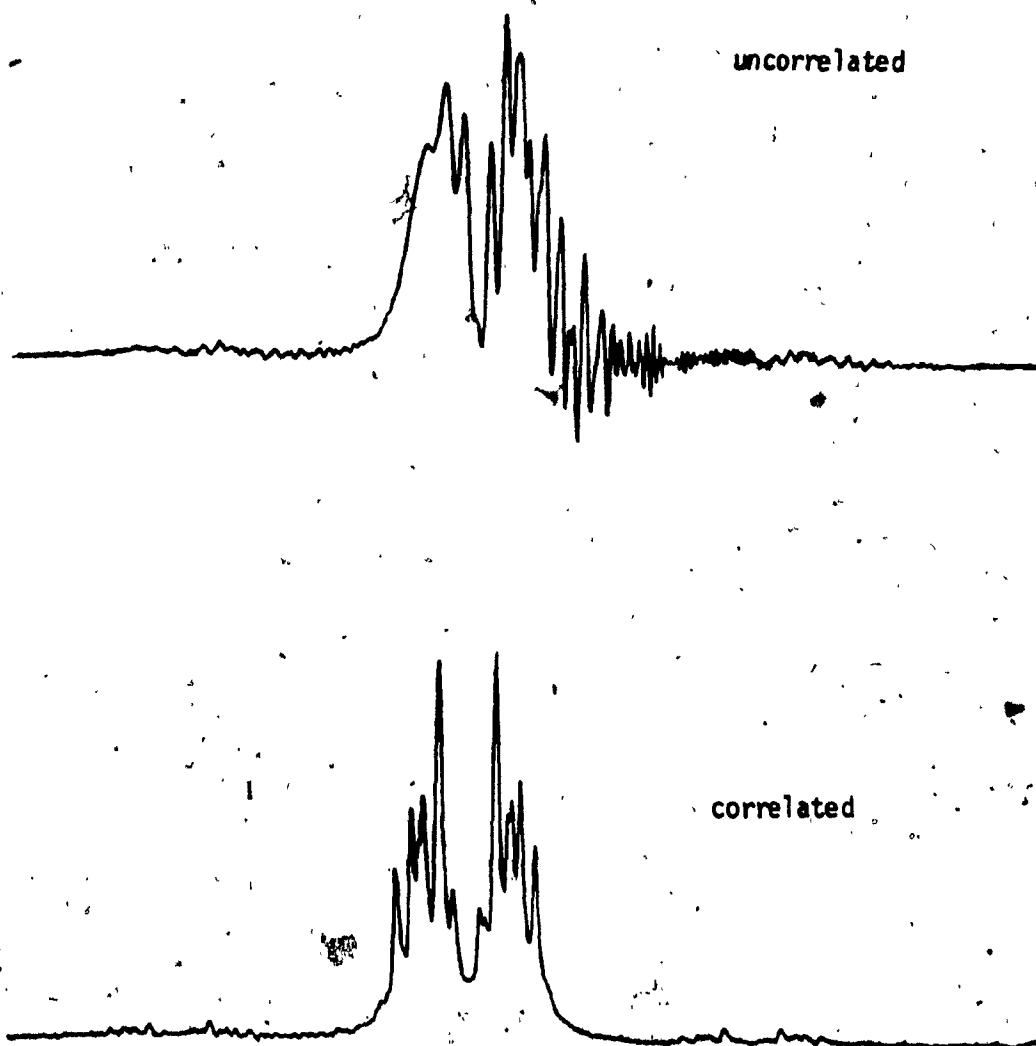
The following series of Figures, 5.1 through 5.4 have equivalent scan parameters with the exception of the sweep rate, which decreases as the Figures proceed. If Figure 5.3 is compared with the slow passage spectrum in Figure 5.5 a

Figure 5.1



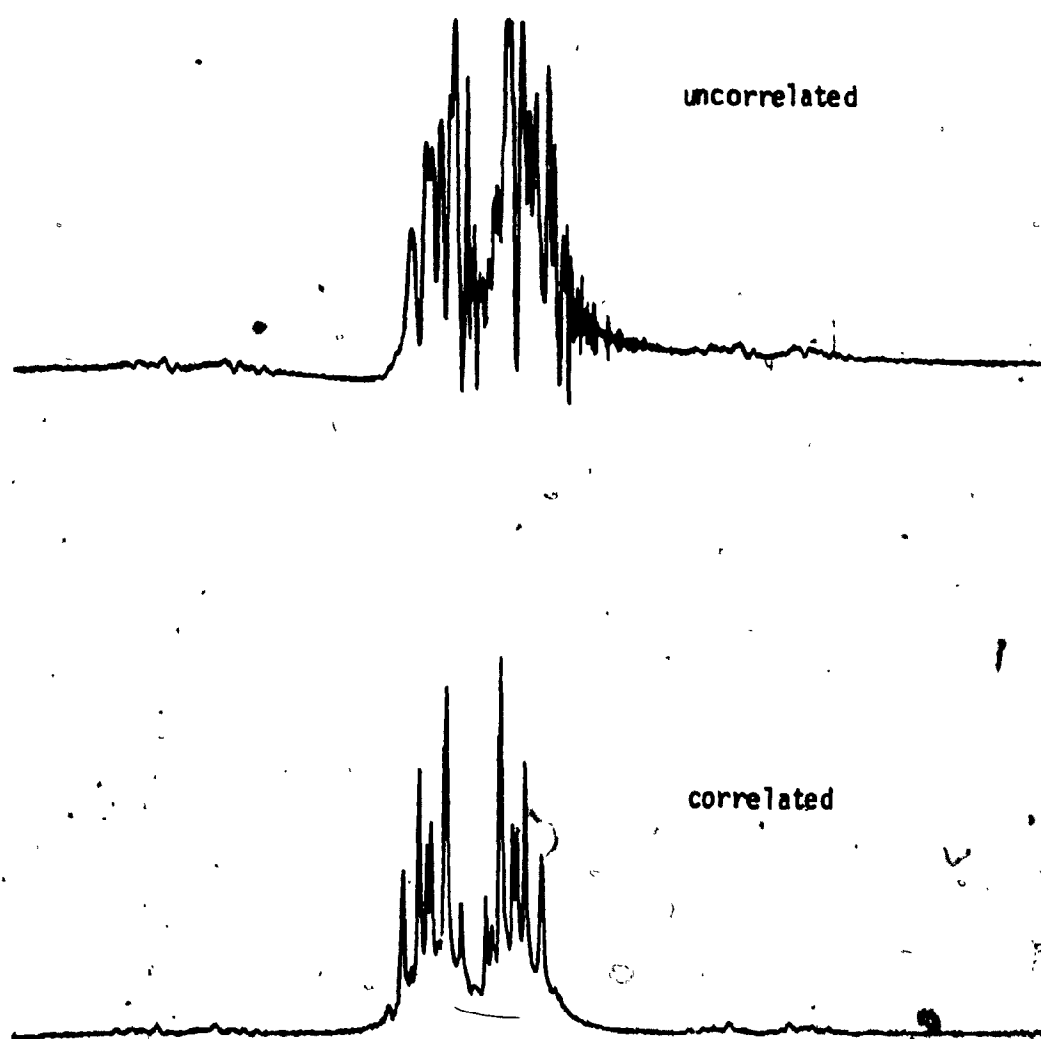
11
SWEEP RATE = 90.90 HZ/SEC
DIGITAL RESOLUTION = 8.46 PTS/HZ
TRUE ACQUISITION TIME IS 2.66 SEC
SPECTR. SWEEPS FROM 8.44 TO 6.02 PPM

Figure 5.2



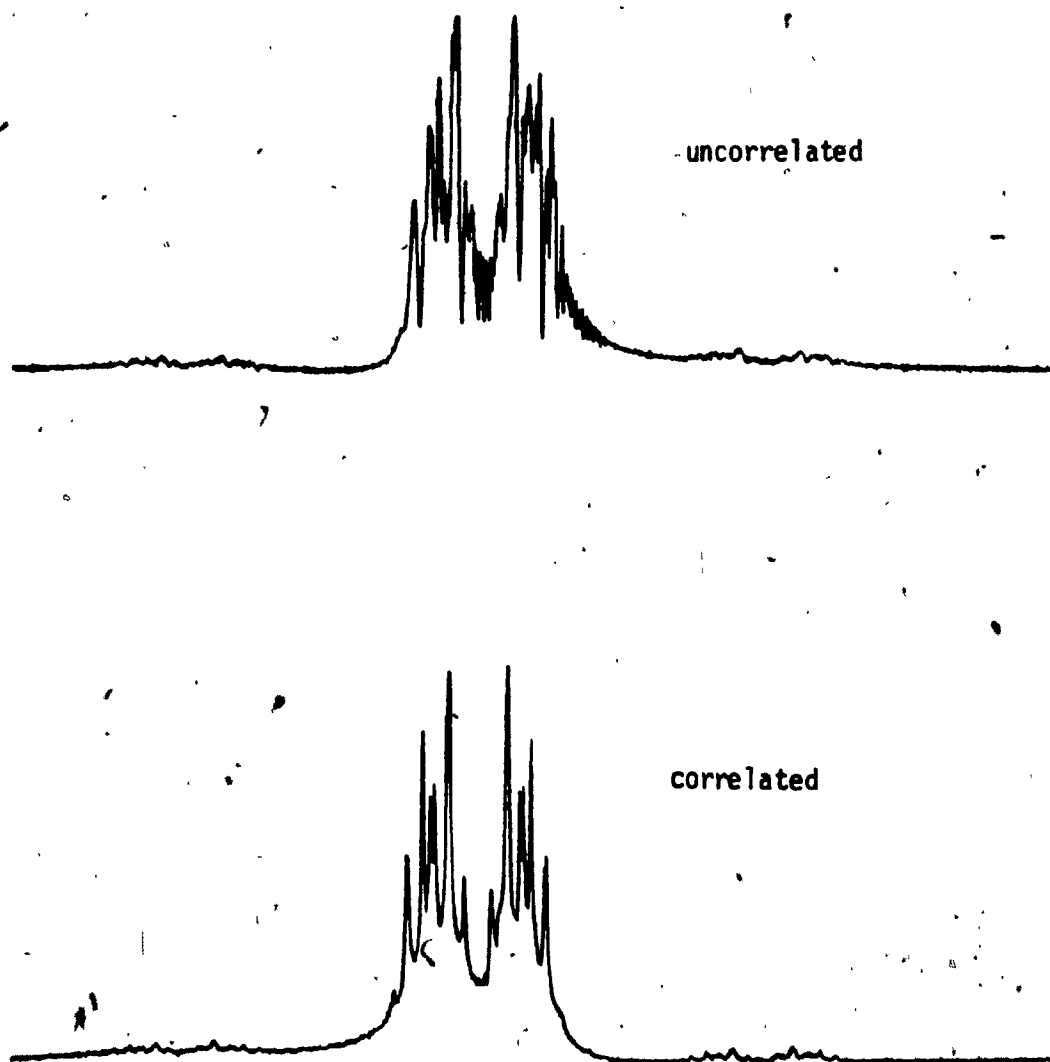
11
SWEEP RATE = 49.24 HZ/SEC
DIGITAL RESOLUTION = 8.46 PTS/MF
TRUE ACQUISITION TIME IS 4.92 SEC
SPECTR. SWEEPS FROM 8.44 TO 6.02 FPK

Figure 5.3



11
SWEEP RATE = 9.59 HZ/SEC
DIGITAL RESOLUTION = 5.45 PTS/HZ
TRUE ACQUISITION TIME IS 24.99 SEC
SPECTR. SWEEPS FROM 5.44 TO 6.02 PK

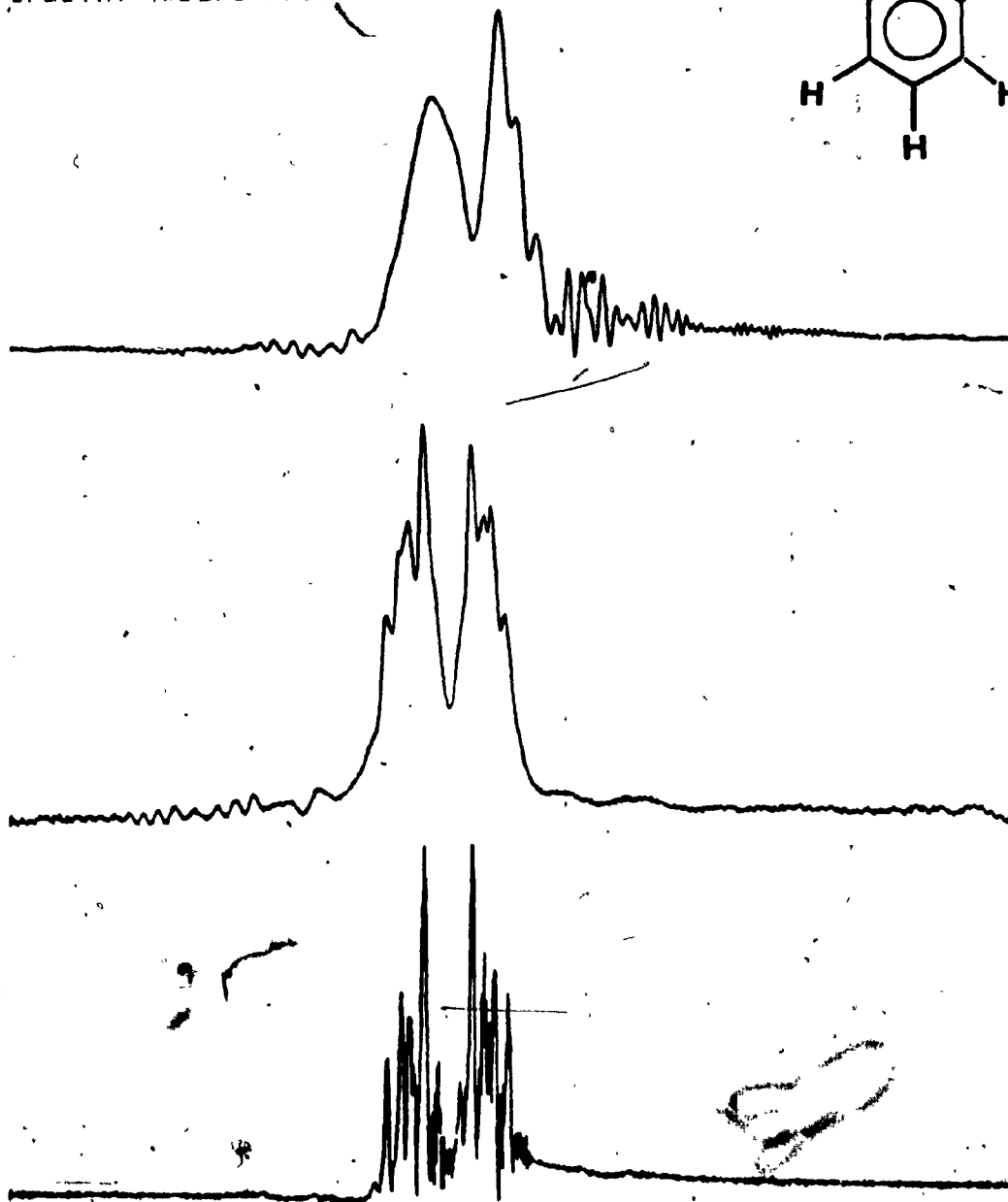
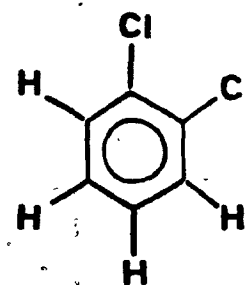
Figure 5.4



11
SWEEP RATE= 4.84 MHz/SEC
DIGITAL RESOLUTION = 8.46 PTS/MHz
TRUE ACQUISITION TIME IS 49.97 SEC
SPECTR. SWEEPS FROM 8.44 TO 6.02 MHz

Figure 5.5

SWEEP RATE- 147.03 HZ/SEC
DIGITAL RESOLUTION = 7.56 PTS/H.
TRUE ACQUISITION TIME IS 1.84 SEC
SPECTR. SWEEPS FROM 8.53 TO 5.82 PPM



11
SWEEP RATE- 2.26 HZ/SEC
DIGITAL RESOLUTION = 7.56 PTS/H.
TRUE ACQUISITION TIME IS 119.81 SEC
SPECTR. SWEEPS FROM 8.53 TO 5.82 PPM

much better correlation is perceived, with assignments becoming distinct.

The measurements were done in reverse order of presentation, Figure 5.4 being the first. Assuming a constant homogeneity contribution, there is an obvious trend with regards to resolution enhancement which nicely illustrates the line broadening effect of excessive sweep rates. This supports the conclusion that the lowest convenient sweep rate should be chosen within the limit of equation 3 of Chapter 2, to yield the greatest sensitivity for the system under investigation.

ORGANIC MOLECULES

The following sample compounds have typically been used in organic N.M.R. spectroscopy as calibration standards to establish resolution and sensitivity performance expectations. In all cases the spectrometer is locked on T.M.S. at 2500 Hz, with the actual print-out stating the scan parameters displayed in each Figure. The abscissa is calibrated by the program and output with the other spectral values.

The intention of this section is to illustrate the normal operation of the instrument using organic solvents. The results are comparable to CW spectra, and demonstrate the time saving inherent in the rapid passage experiment.

ETHYL BENZENE

The first system under scrutiny is that of a 5% ethyl benzene, 10% T.M.S., in CDCl_3 . Figure 5.6 presents the spectrum of what might be an initial scan of the expected area of interest. The assignments are trivial, but if greater digital resolution is desired it is a simple task to adjust the spectral scan width to increase the number of points defining a unit Hz. This is shown in Figure 5.7, the definition of the absorbance is significantly enhanced. The wiggle in the baseline observed as the sweep approaches 0 ppm is caused by high lock modulation beating against the analytical channel as the spectrometer approaches T.M.S.

CROTONALDEHYDE(trans)

Figures 5.8 and 5.9 illustrate the absorbance spectra of trans-crotonaldehyde shown in the same format as ethyl benzene. In Figure 5.8 the methyl group signal has been truncated, presumably by the A.D.C. Interestingly, this demonstrates the fact that the information coherent to the fine structure, normally absent in the RP spectrum, must be contained in the oscillation following the main peak. Otherwise restoration by correlation multiplication would be impossible. In this case the only feature affected by the truncation is possibly the peak height. Figure 5.9 has a shorter spectral width allowing better definition of the down-field peaks.

Figure 5.6

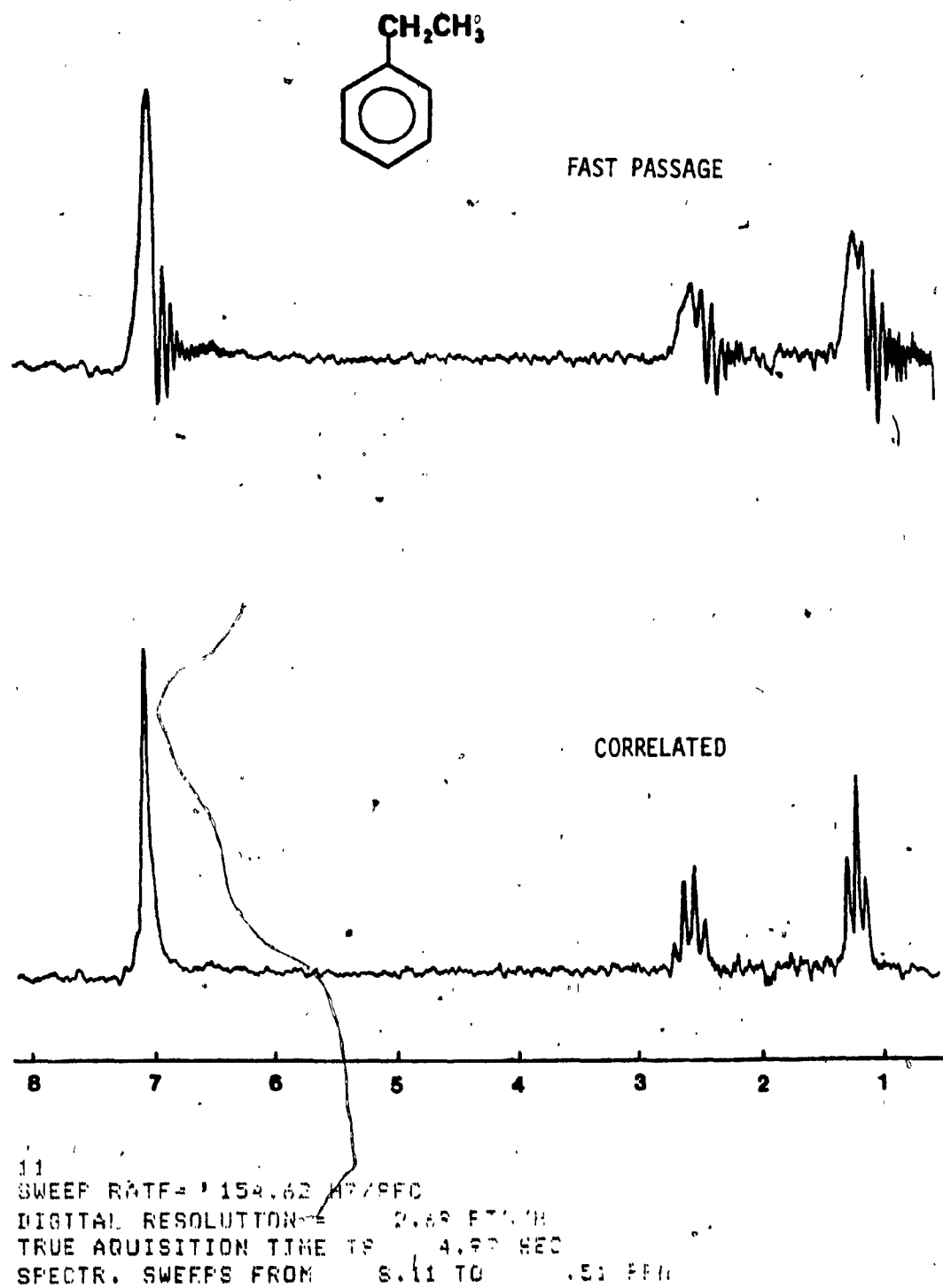
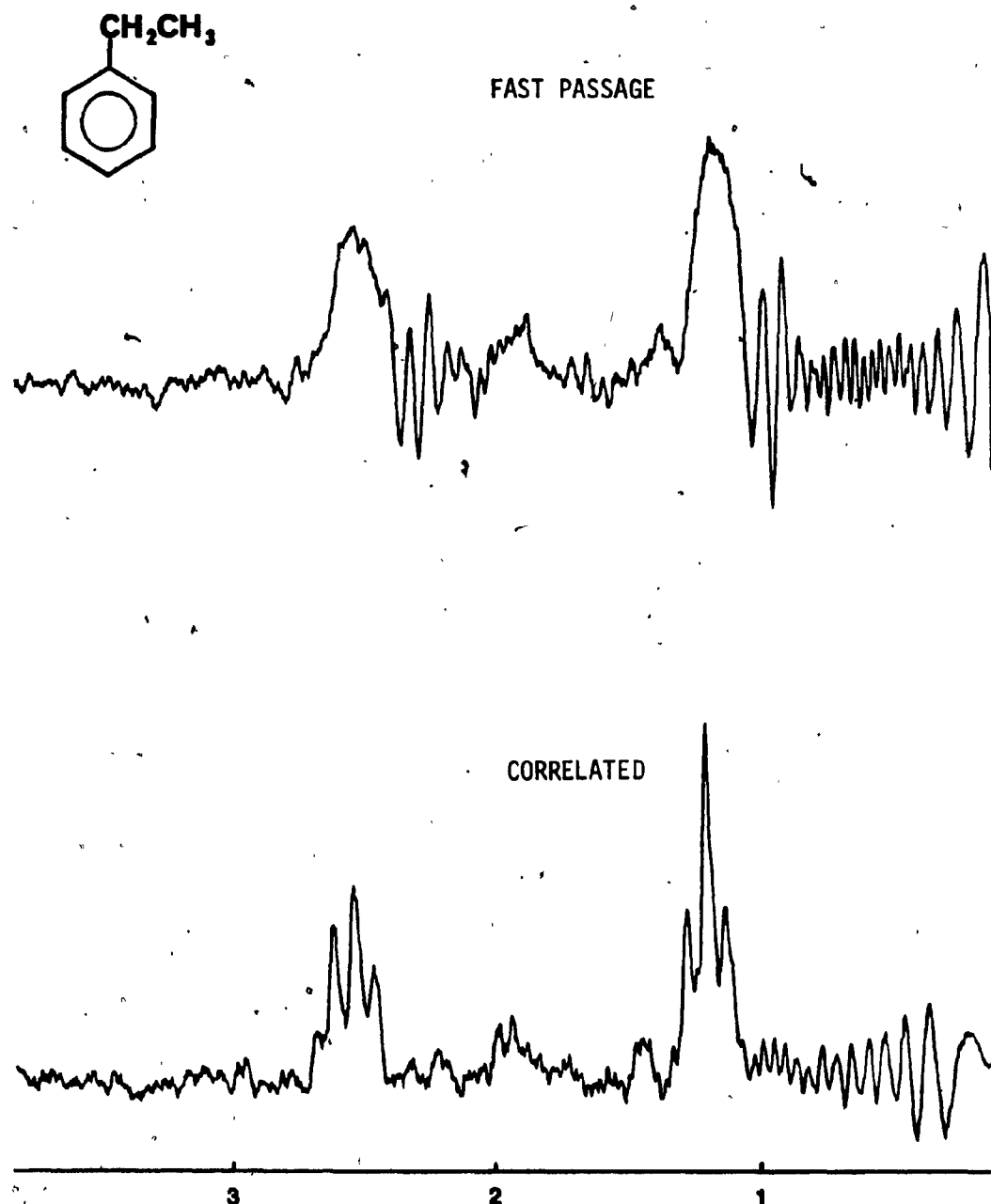


Figure 5.7



11

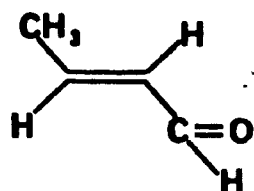
SWEEP RATE = 200.37 HZ/SEC

DIGITAL RESOLUTION = 5.40 FT/Hz

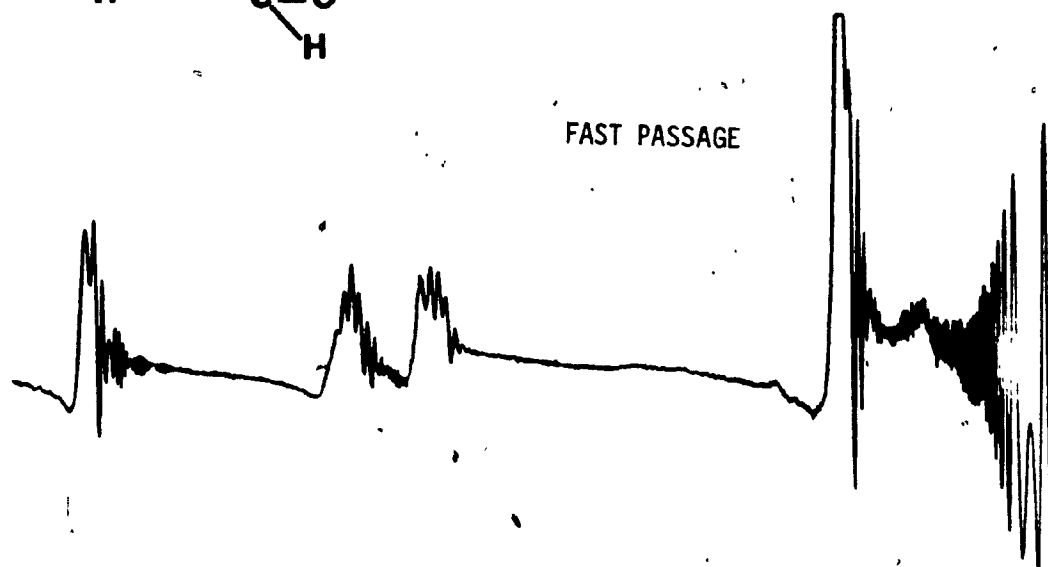
TRUE ACQUISITION TIME = 1.84 SEC

SPECTR. SWEEPS FROM 3.83 TO 1.10 MHz

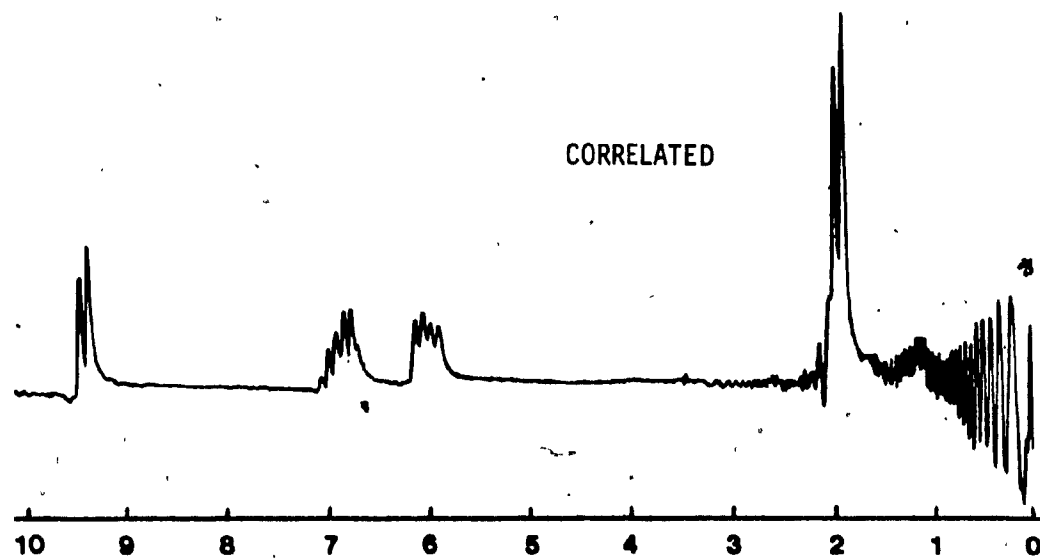
Figure 5.8



FAST PASSAGE

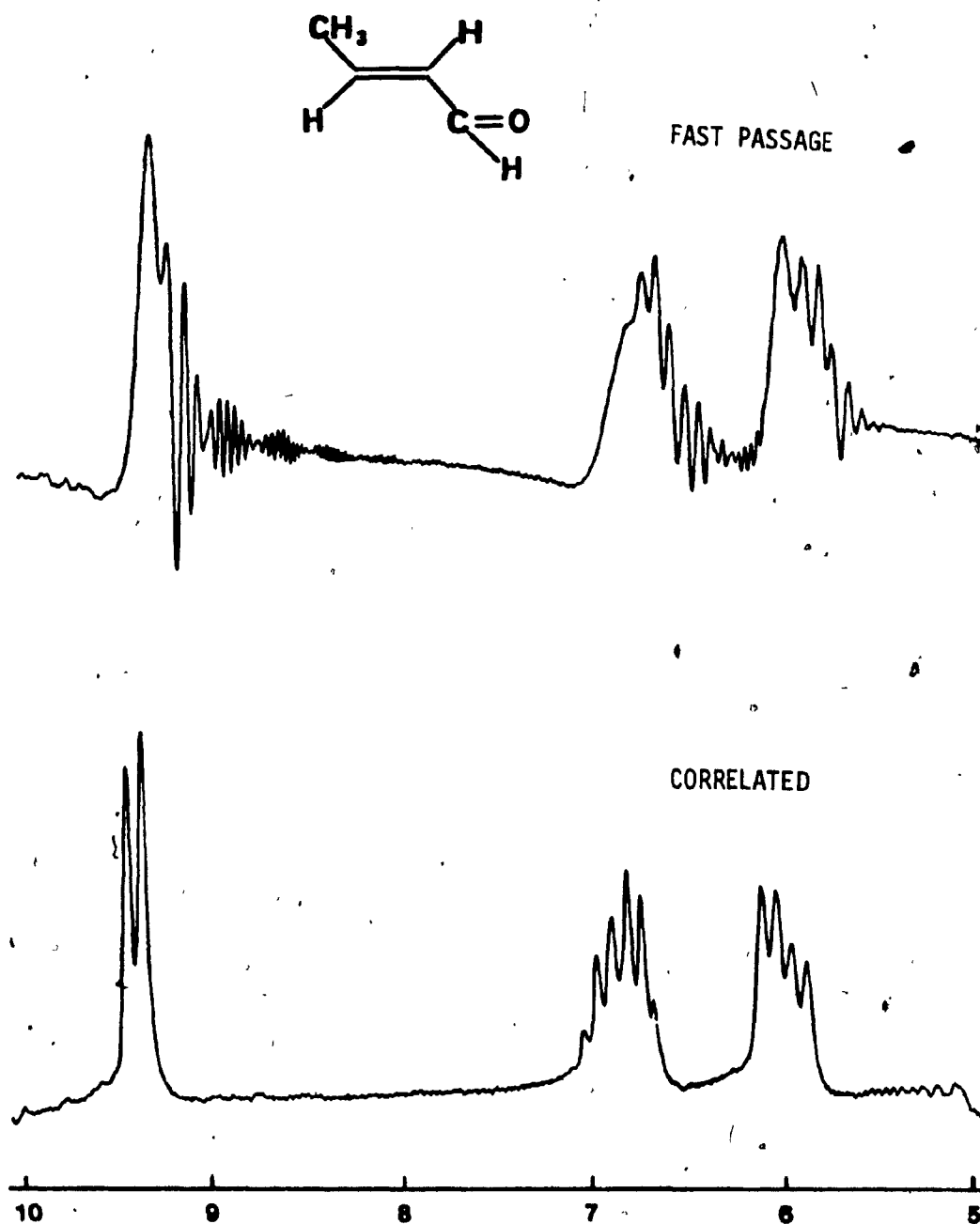


CORRELATED



11
SWEEP RATE- 126.29 Hz/SEC
DIGITAL RESOLUTION = 1.96 Hz
TRUE ACQUISITION TIME IS 0.94 SEC
SPECTR. SWEEPS FROM 10.11 TO -0.35 Hz

Figure 5.9



11

SWEEP RATE = 209.10 HZ/SEC
DIGITAL RESOLUTION = 3.98 PTS/HZ
TRUE ACQUISITION TIME IS 2.46 SEC
SPECTR. SWEEPS FROM 10.10 TO 4.95 MHz

ETHYL TOLUENE(meta)

A sample of 10% ethyl toluene, 10% T.M.S., in CDCl_3 is examined in Figures 5.10 and 5.11. The spectrum has enough resolution to enable easy assignment of the aliphatic region, and the splitting of the aromatic protons is evident.

ORTHODICHLOROBENZENE

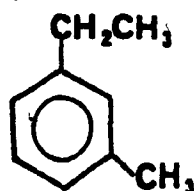
The spectrum of O.D.C.B. should now be familiar. Figure 5.12 exhibits the original scan of the entire field to contrast the increased digital resolution available in Figure 5.13. As previously discussed in this Chapter, better sensitivity could be obtained by lowering the sweep rate.

CHLOROFORM

Finally, the trivial spectrum of chloroform is shown in Figure 5.14, the spinning side bands clearly present. The two spikes just poking out of the baseline are caused by trace ethanol added as a stabilizer at 0.7%. They are not resolved by the correlation multiplication because the ringing is hidden in the noise of the baseline.

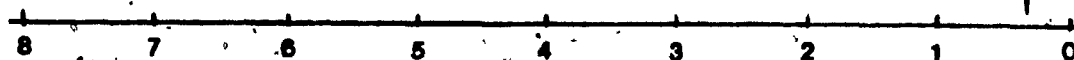
I have been particularly brief here because the sample compounds under scrutiny are all well studied and warrant little interest other than that inherent in their presentation, as evidence of the spectrometer operation.

Figure 5.10



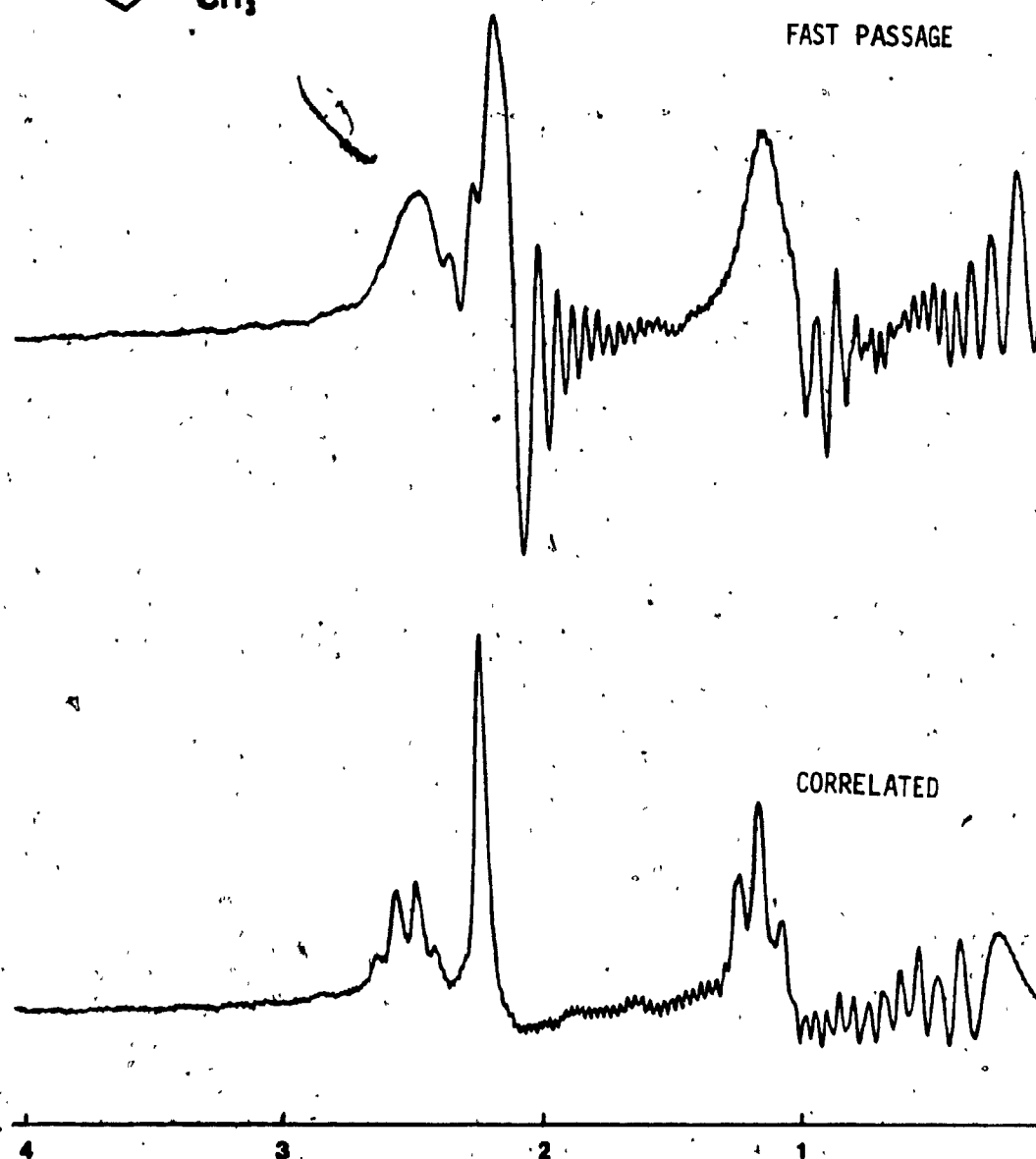
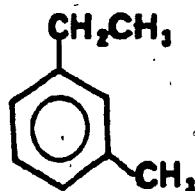
FAST PASSAGE

CORRELATED



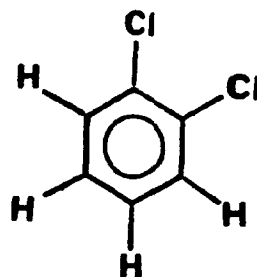
11
SWEEP RATE = 163.98 HZ/SEC
DIGITAL RESOLUTION = 2.54 PTS/HZ
TRUE ACQUISITION TIME IS 4.90 SEC
SPECTR. SWEEPS FROM 8.00 TO .00 PPM

Figure 5.11

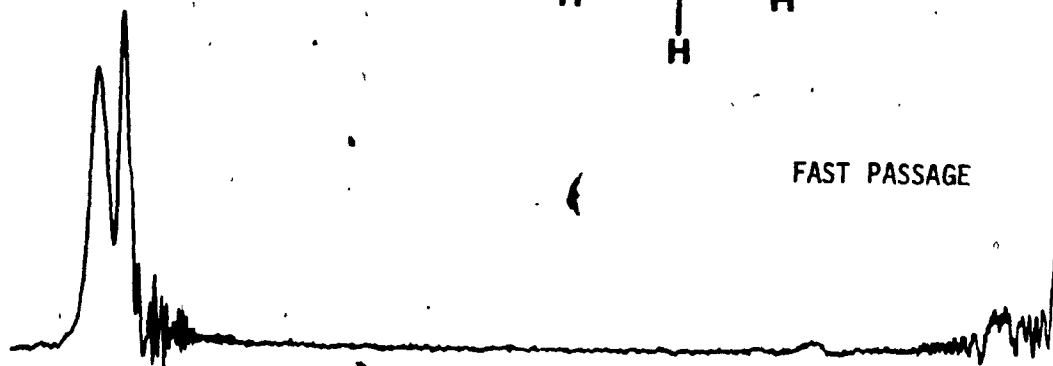


11
SWEEP RATE - 217.01 HZ/SEC
DIGITAL RESOLUTION = 5.12 PPM
TRUE ACQUISITION TIME IS 1.84 SEC
SPECTR. SWEEPS FROM 4.05 TO 0.05 PPM

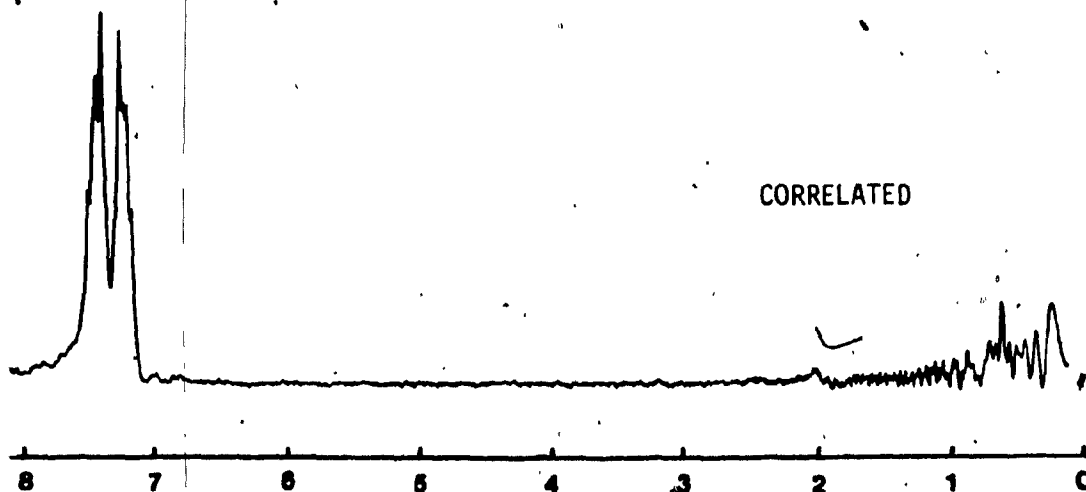
Figure 5.12



FAST PASSAGE

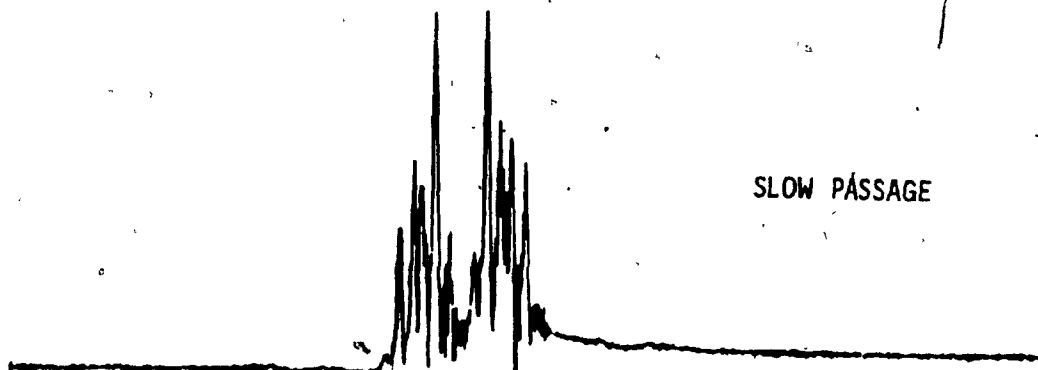
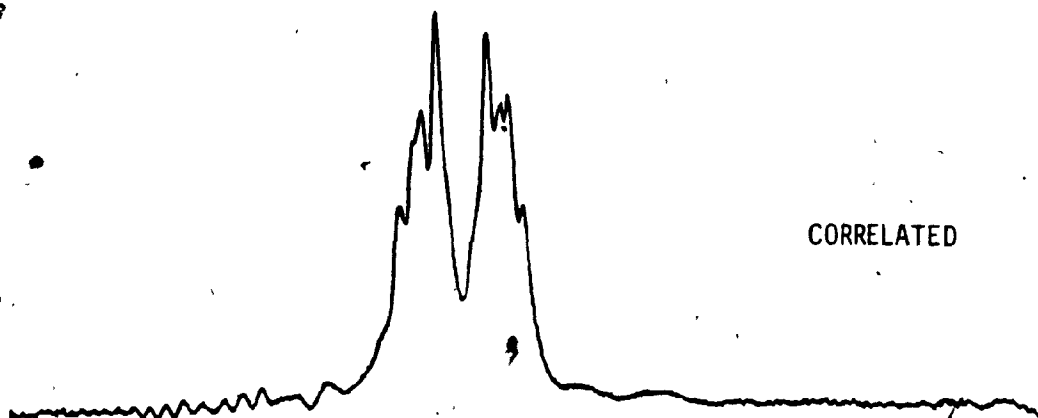
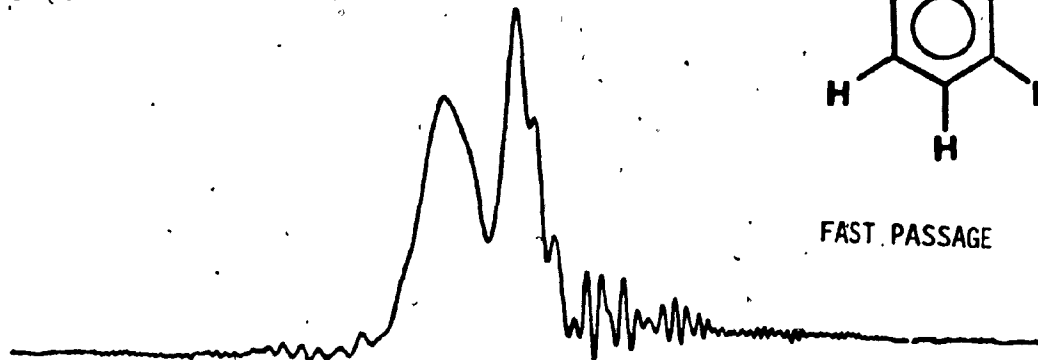
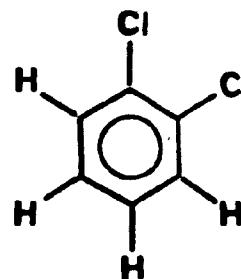


CORRELATED



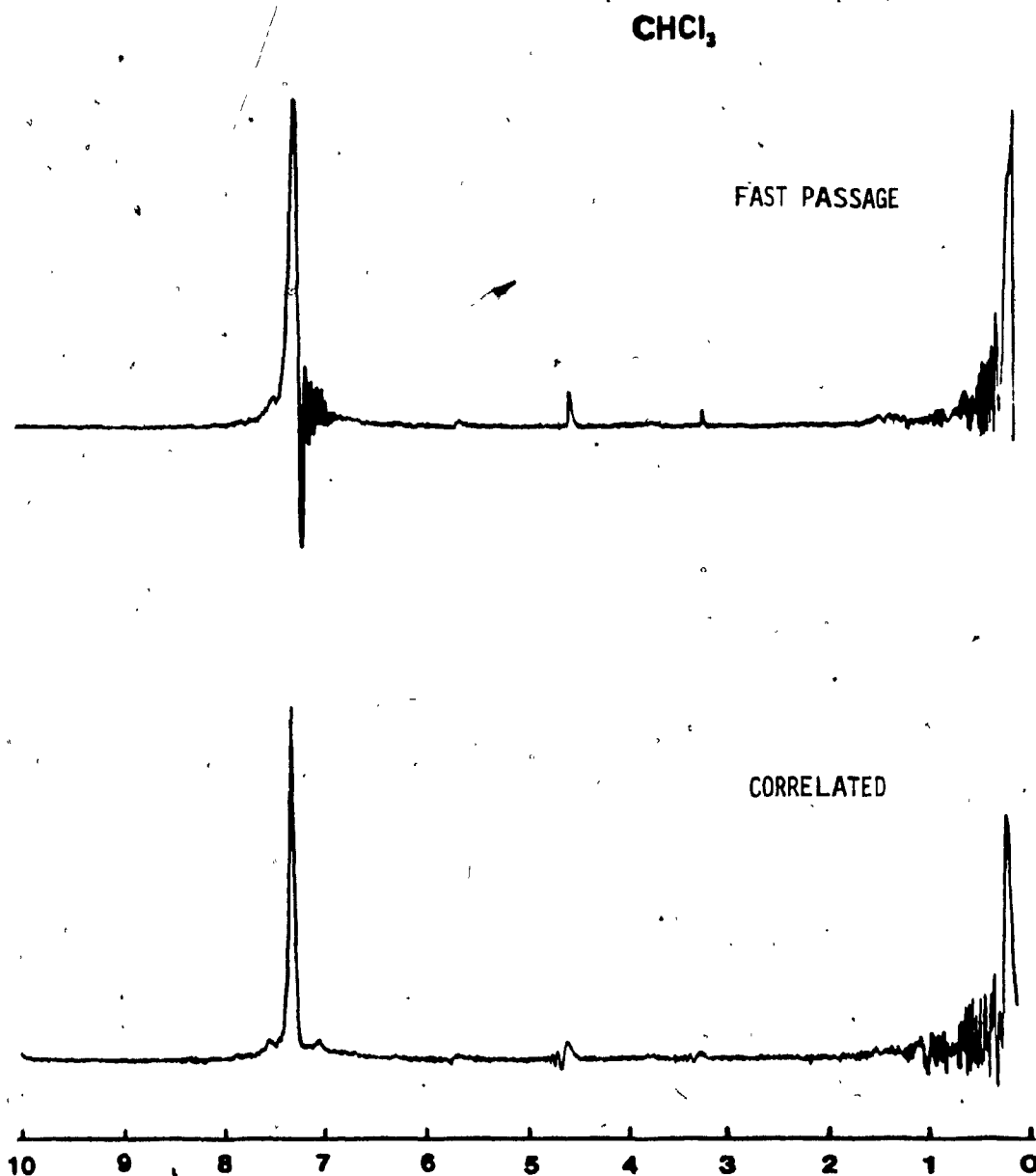
11
SWEEP RATE - 143.98 HZ/SEC
DIGITAL RESOLUTION = 2.54 PTS/HZ
TRUE ACQUISITION TIME IS 4.92 SEC
SPECTR. SWEEPS FROM 8.09 TO .03 PPM

Figure 5.13
SWEEP RATE- 147.03 HZ/SEC
DIGITAL RESOLUTION = 7.56 PTS/H.
TRUE ACQUISITION TIME IS 1.84 SEC
SPECTR. SWEEPS FROM 8.53 TO 5.82 PPM



11
SWEEP RATE= 2.26 HZ/SEC
DIGITAL RESOLUTION = 7.56 PTS/H.
TRUE ACQUISITION TIME IS 119.81 SEC
SPECTR. SWEEPS FROM 8.53 TO 5.82 PPM

Figure 5.14



11
SWEEP RATE= 102.54° HZ/SEC
DIGITAL RESOLUTION = 2.03 PTS/HZ
TRUE ACQUISITION TIME IS 9.83 SEC
SPECTR. SWEEPS FROM 10.04 TO -0.04 PPM

AQUEOUS ENVIRONMENTS

Water has always presented a problem in the realm of proton N.M.R. spectroscopy. Where it is present as the principal solvent, it has a number of undesirable characteristics which cause problems:

1. High abundance of H_2O protons.
2. Wide line width relative to most absorbances.
3. Chemical shift is pH dependent.

The first point nominates water as a useful spectral feature to lock the spectrometer onto. Unfortunately points two and three oppose this since a wide line width allows the lock mechanism to drift somewhat, affecting field stability. The dependence of the chemical shift on pH means that the lock placement cannot be precalibrated in the program unless the pH of the sample was to be standardized. This is too stringent a restriction to place on sample preparation to be useful, hence D.S.S. must always be present in the sample tube for calibration purposes, if shift assignment is necessary.

In the following spectra, no digital massaging was done other than phase correction where required. All samples were run with a 20 Hz hardware filter in place. Since the exact position of the water resonance cannot be predicted a priori, the chemical shift scales are calculated after the experiment using D.S.S. as a reference, where the spectrometer was locked on the water signal.

ETHANOL IN WATER

The first example presented is a spectrum of 5% ethanol in water with 5% D.S.S. added to calibrate the abscissa. Figure 5.15 is organized such that the RP response along with scan parameters is shown on top, followed by the correlated result. The slow passage spectrum is given at the bottom for comparison. Again, instrumental settings were equal, the rapid passage experiment run immediately after the slow passage run.

In both final spectra the well known triplet/quartet features are easily identifiable. Contrasting the results, the S/N ratio is significantly better in the correlated spectrum, but the line width is perhaps narrower in the SP example. In the rapid passage result the quartet is much clearer than in the equivalent slow passage response.

The time required for each scan is also notable since the rapid passage spectrum was gathered in only 42.79 sec, while the slow passage experiment took 2hrs 13min. This is a significant saving realized and is what makes the technique superior to pulse methods when the dynamic range problem avoided is taken into account.

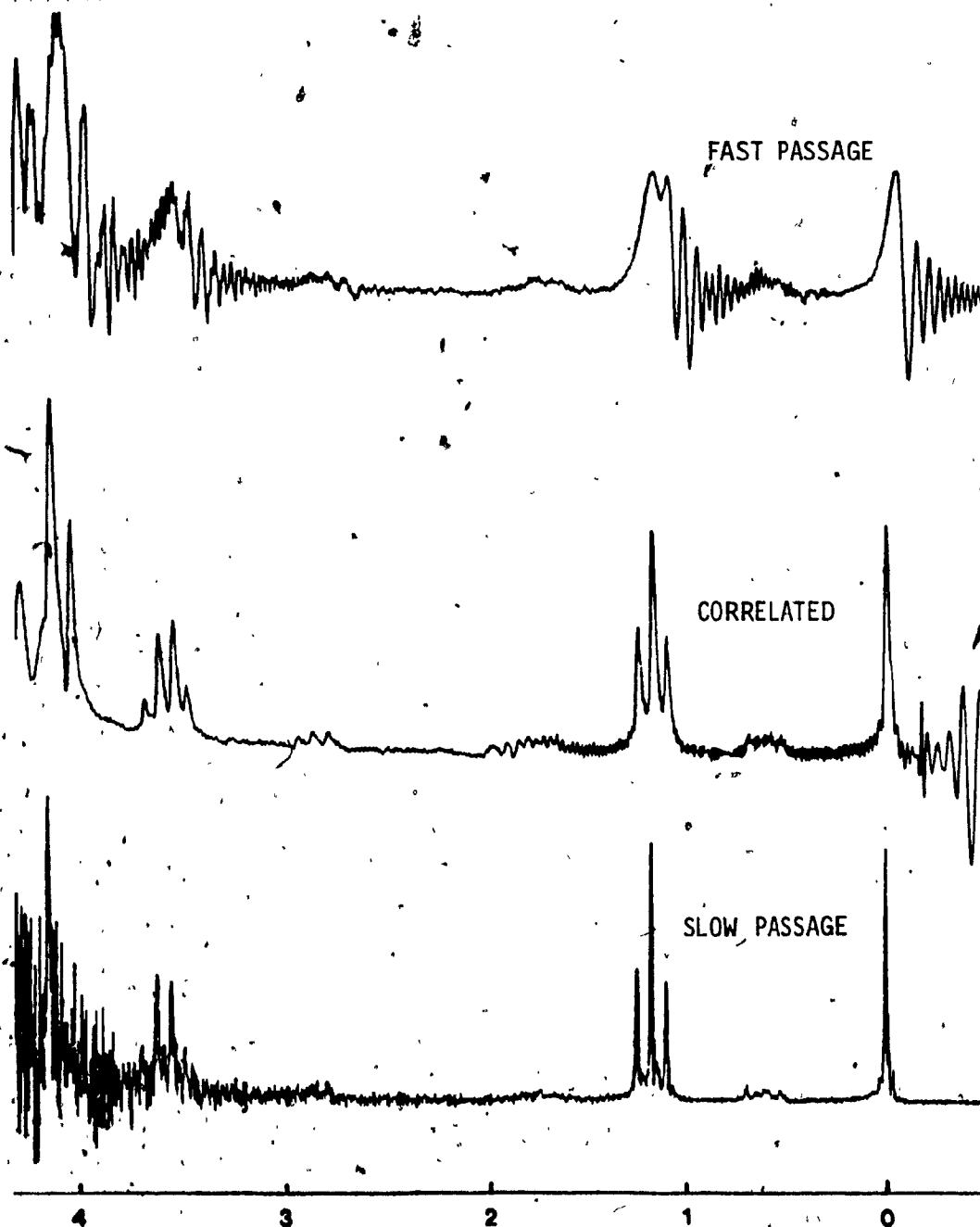
PROLINE AND IMIDAZOLE

The object of the next series of spectra is to demonstrate the usefulness of a correlation spectrometer in biochemical applications. One molar solutions of proline and imidazole were studied in D_2O and H_2O with 10% D.S.S.

Figure 5.15

SWEEP RATE 126.44 HZ/SEC
DIGITAL RESOLUTION 4.17 PTS/HZ
TOTAL ACQUISITION TIME IS 3.60 SEC
SPECTRUM SWEEPS FROM 4.16 TO -0.70 PPM

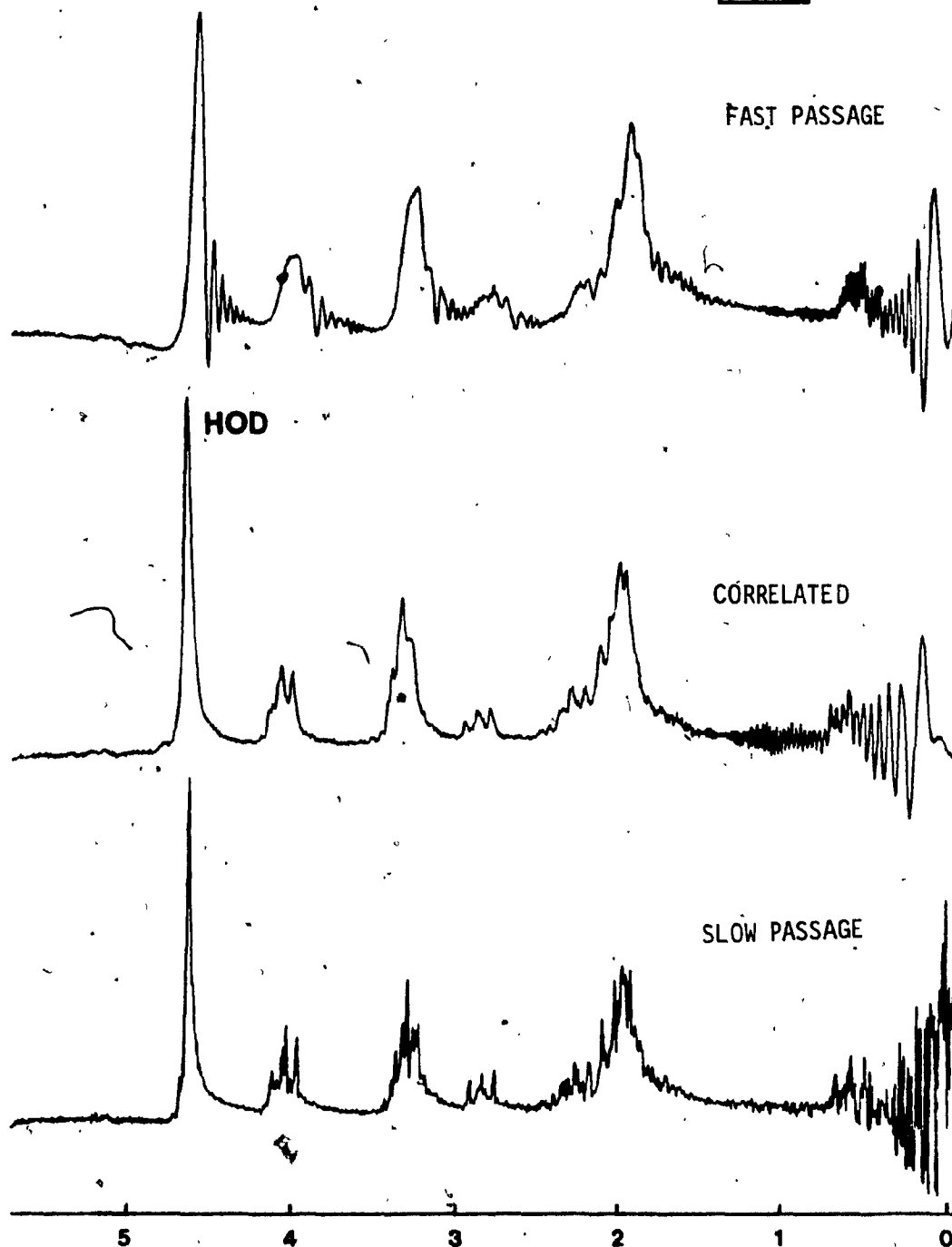
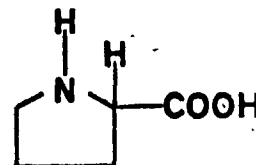
CH3CH2OH



20
SWEEP RATE 1.23 HZ/SEC
DIGITAL RESOLUTION 4.17 PTS/HZ
TOTAL ACQUISITION TIME IS 399.97 SEC
SPECTRUM SWEEPS FROM 4.16 TO -0.70 PPM

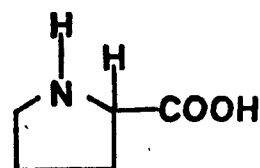
Figure 5.16

SWEEP RATE = 100.00 Hz/sec
DIGITAL RESOLUTION = 3.51 pps/ppm
SINE ACQUISITION TIME IS 4.99 SEC
SPECTRA SWEEP FROM 5.77 TO 0.07 PP



SWEEP RATE = 100.00 Hz/sec
DIGITAL RESOLUTION = 3.51 pps/ppm
SINE ACQUISITION TIME IS 4.99 SEC
SPECTRA SWEEP FROM 5.77 TO 0.07 PP

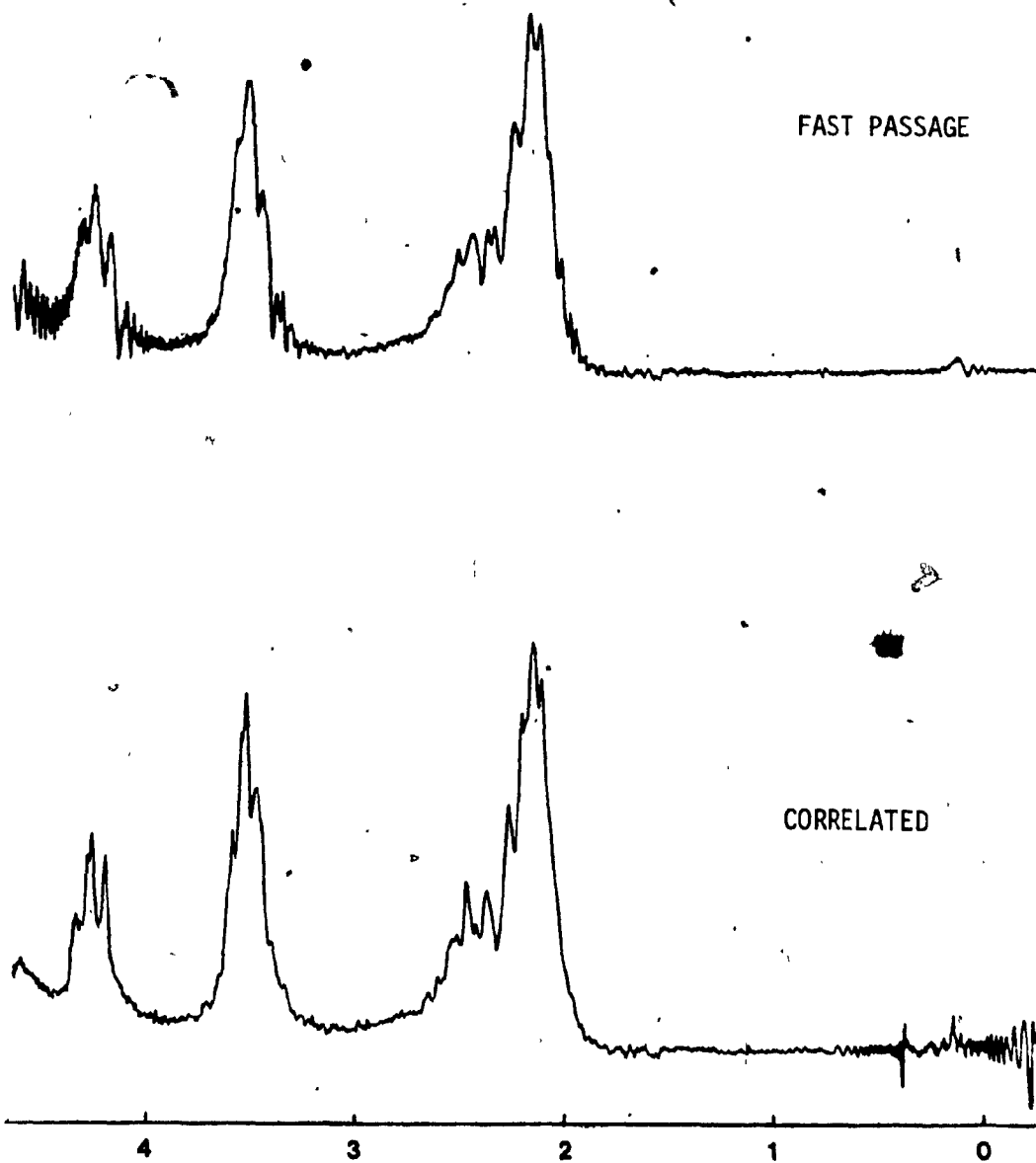
Figure 5.17



in H₂O

FAST PASSAGE

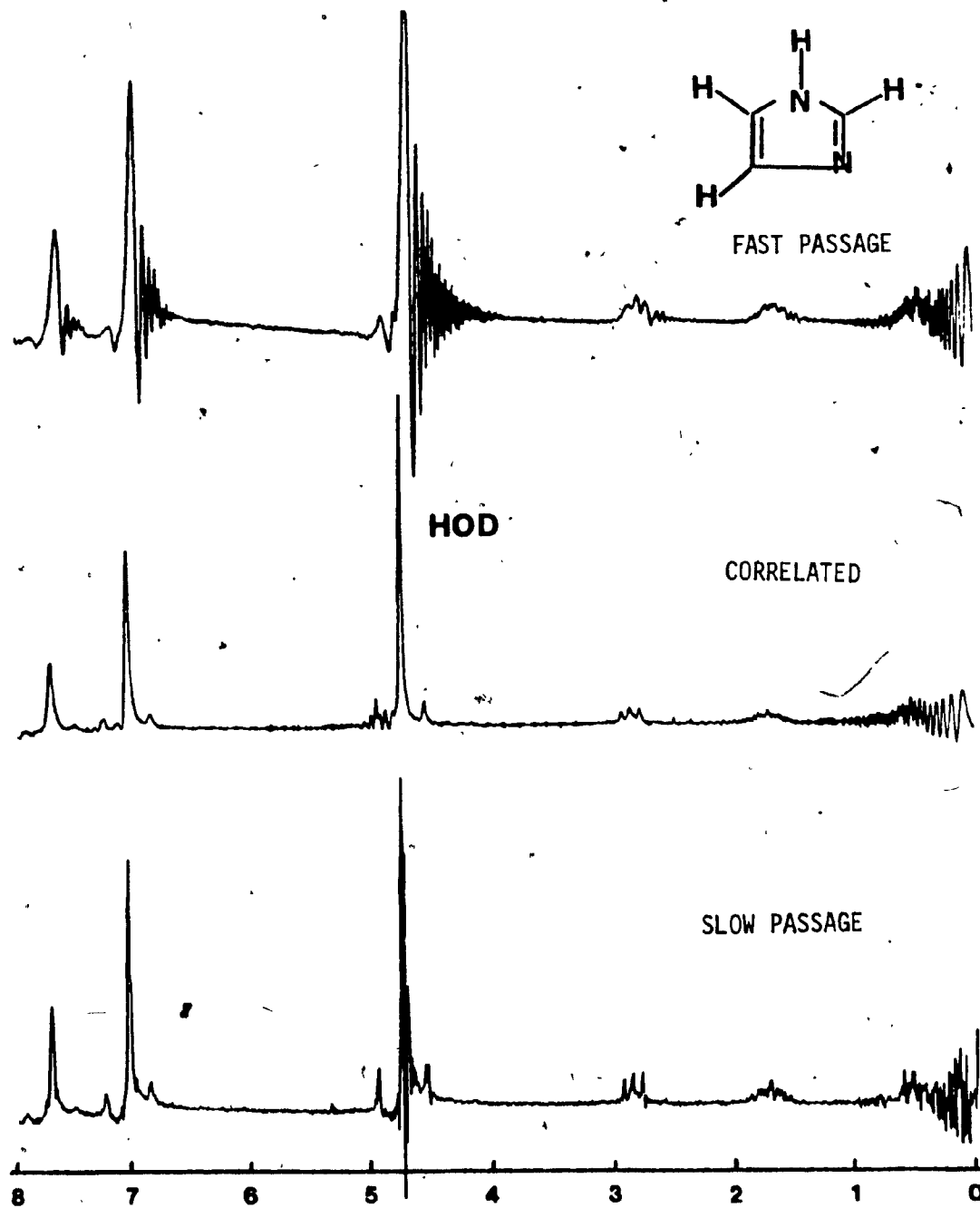
CORRELATED



11
SWEEP RATE 40.64 HZ SEC
DIGITAL RESOLUTION 1.20 HZ
TRUE ACQUISITION TIME 11.00 SEC
SPECTR. SWEEP FROM 4.6 TO 0.0

Figure 5.18

SWEEP RATE = 100.29 HZ/SEC
DIGITAL RESOLUTION = 0.56 PTS/HZ
Pulse ACQUISITION TIME IS 7.99 SEC
SPECTR. SWEEPS FROM 8.04 TO 0.03 PPM



SWEEP RATE = 4.01 HZ/SEC
DIGITAL RESOLUTION = 0.05 PTS/HZ
TRUE ACQUISITION TIME IS 197.84 SEC
SPECTR. SWEEPS FROM 8.04 TO 0.03 PPM

present for calibration. In D_2O the spectrometer can easily be locked on the D.S.S. signal, the residual water is small enough not to knock the lock box off the D.S.S. at 10%.

In Figure 5.16, the slow and rapid passage spectra of proline in D_2O are compared. The presence of the D.S.S. complicates the example a little by overlapping with the proline lines, the proton sitting on the nitrogen has exchanged with D_2O , and is not seen. The slow passage result exhibits better resolution but the S/N ratio is not equal to that of the correlated spectrum.

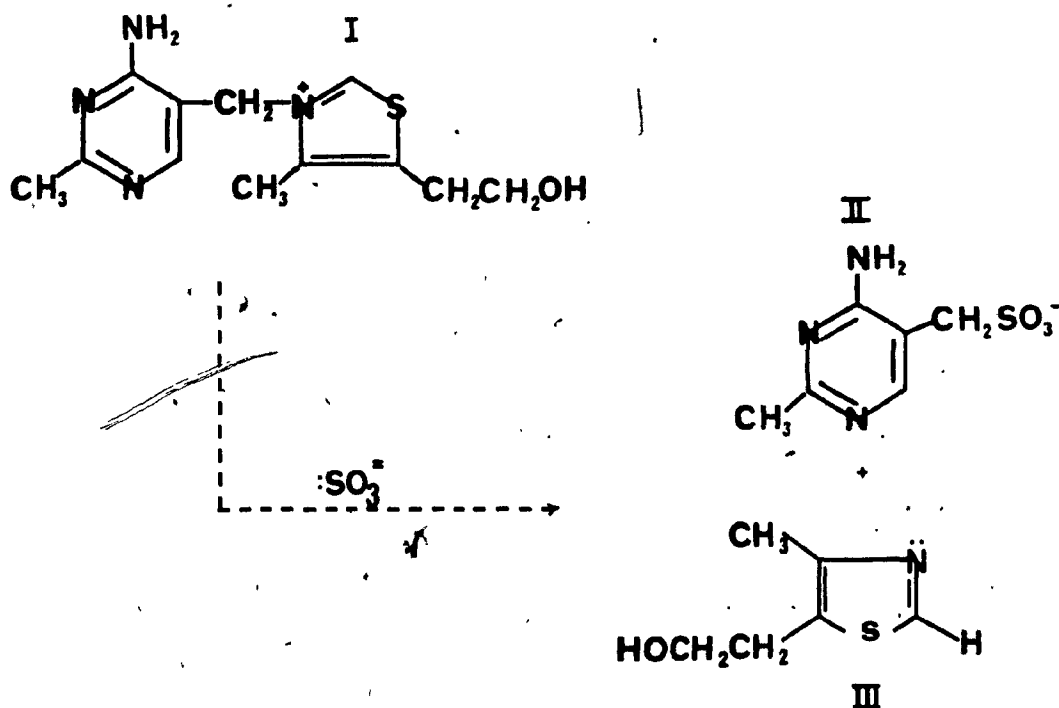
The fast passage spectrum run in water, presented in Figure 5.17, has better resolution. This is probably a consequence of the slower sweep rate and resulting optimization of the saturation parameter. The time difference between the two sweep rates indicates a substantial saving, with the rapid passage taking only 25 sec while the equivalent slow passage experiment required 7 minutes.

The spectrum of imidazole was run in D_2O with the resolution easily comparable between the slow and rapid passage results. Spinning side bands are observed in both spectra, the slow passage result exhibits a slight ringing even at 4 Hz/sec. The time difference for the two is similar to the proline result.

STUDY OF A THIAZOLE

The labile exchange of the C-2 proton in the thiazolium ion has been shown to be requisite to the catalytic ability of thiamin.⁵⁵ The soluble thiazole (III) has been isolated as the result of cleavage of thiamin (I) in the presence of :SO_3^- .⁵⁶ (Figure 5.22)

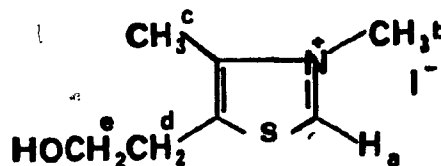
Figure 5.22.



The mechanism of this reaction has received attention kinetically⁵⁷ and corroborative evidence has been furnished by N.M.R..⁵⁸ The study of the mechanism of the base catalyzed opening of the thiazole ring in thiamin has previously been studied using stopped-flow N.M.R. at 60 MHz on a C.W. instrument.⁵⁹

Figure 5.19

99 MHz
DIGITAL RESOLUTION = 4.71 Hz
TIME ACQUISITION TIME IS 4.00 sec
SPECTRA SWEEP FROM 5.00 TO 0.00 Hz



FAST PASSAGE

HOD

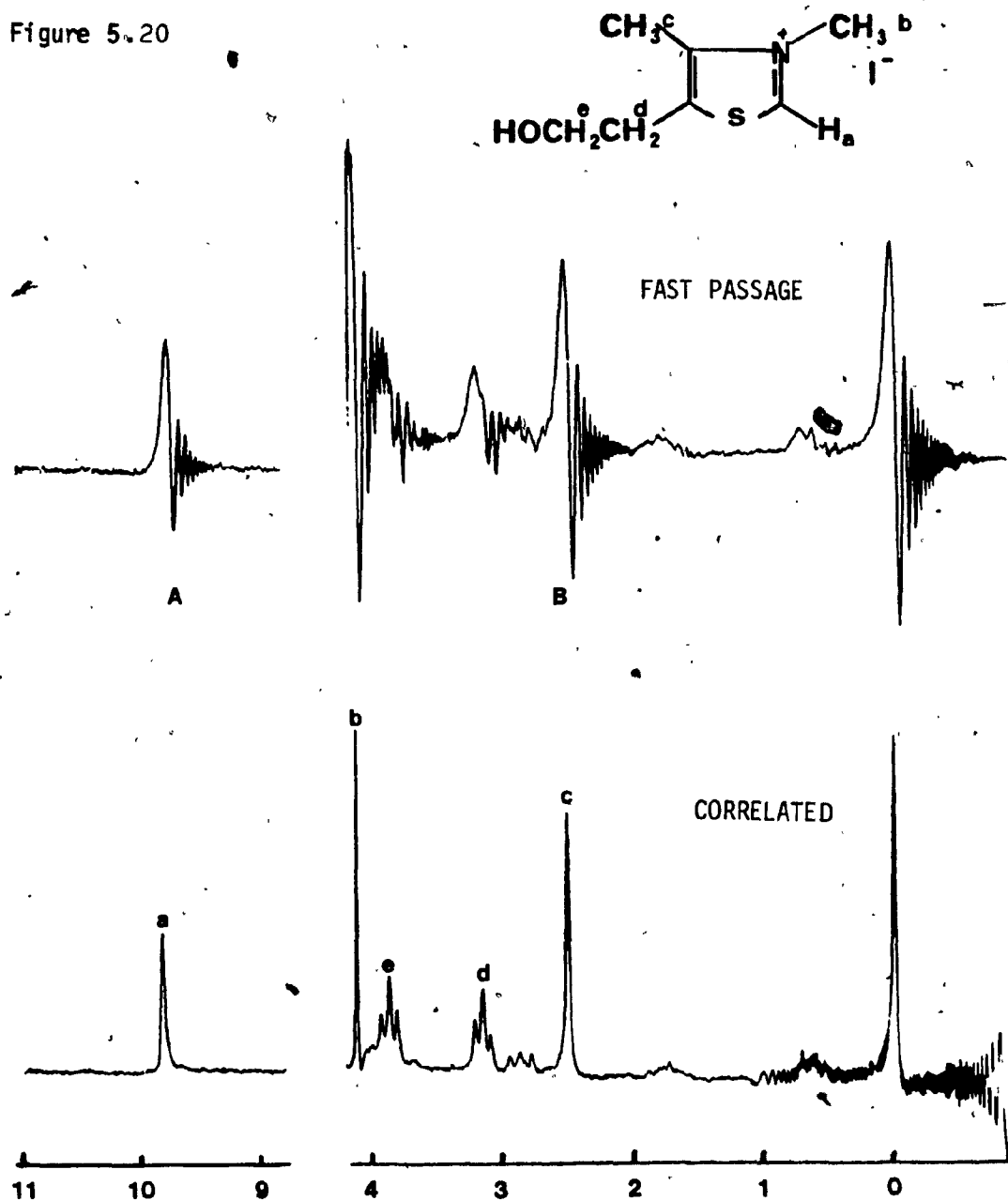
CORRELATED

SLOW PASSAGE

5 4 3 2 1 0

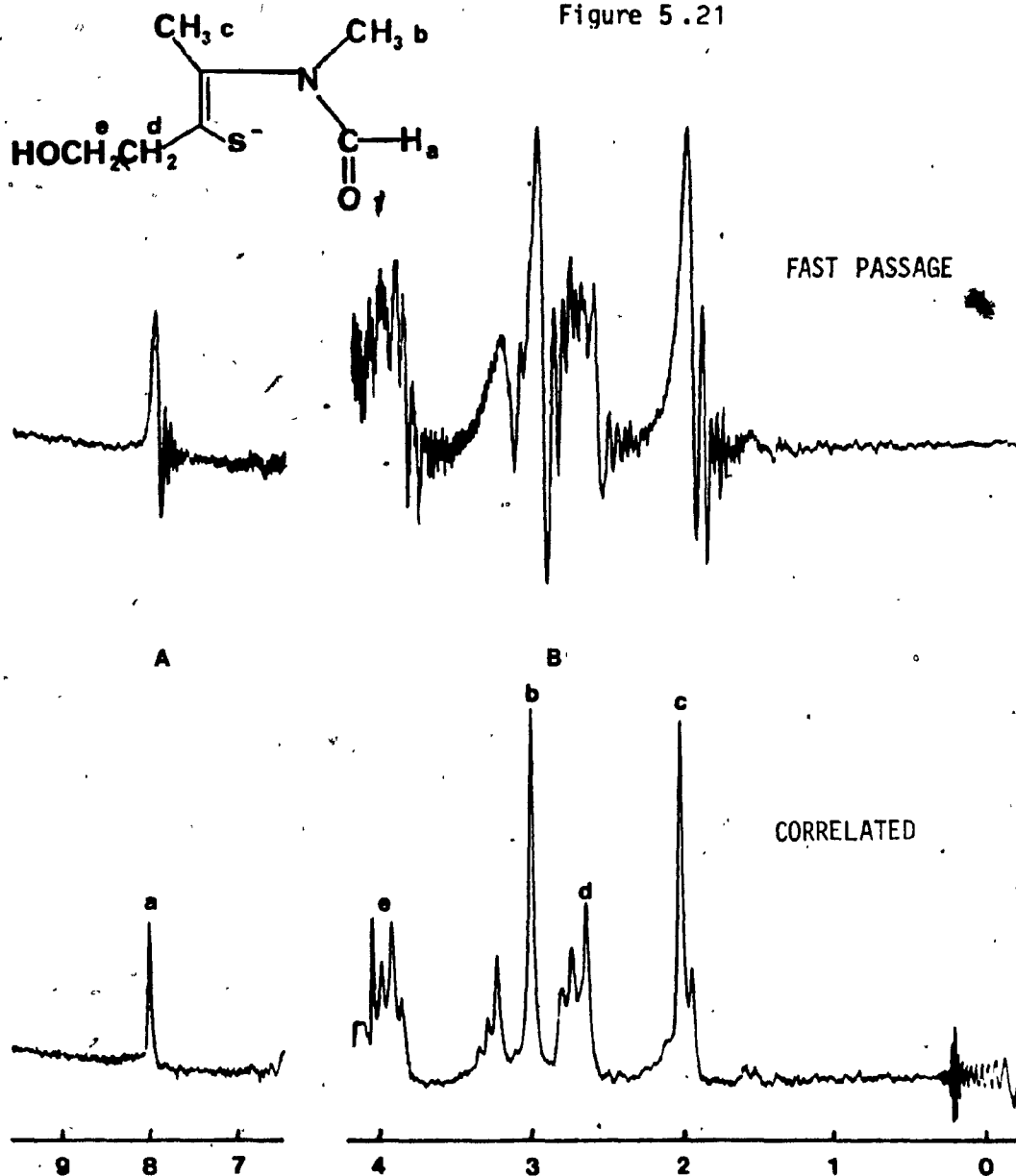
5.00 MHz
DIGITAL RESOLUTION = 4.71 Hz
TIME ACQUISITION TIME IS 4.00 sec
SPECTRA SWEEP FROM 5.00 TO 0.00 Hz

Figure 5.20



11
SWEEP RATE 100.76 HZ/SEC
DIGITAL RESOLUTION 8.90 HZ/SEC
TRUE ACQUISITION TIME 15 1.00 SEC
SPECTR. SWEEP FROM 11.01 TO 0.00
11
SWEEP RATE 100.76 HZ/SEC
DIGITAL RESOLUTION 8.90 HZ/SEC
TRUE ACQUISITION TIME 15 4.92 SEC
SPECTR. SWEEP FROM 4.18 TO 0.00

Figure 5.21



A
 SWEEP RATE 100.32 HZ/SEC
 DIGITAL RESOLUTION 2.04 Hz
 TRUE ACQUISITION TIME 15 2.40 SEC
 SPECTR. SWEEPS FROM 9.40 TO 2.00 Hz

B
 SWEEP RATE 114.32 HZ/SEC
 DIGITAL RESOLUTION 4.54 Hz
 TRUE ACQUISITION TIME 10 2.40 SEC
 SPECTR. SWEEPS FROM 4.00 TO 0.00 Hz

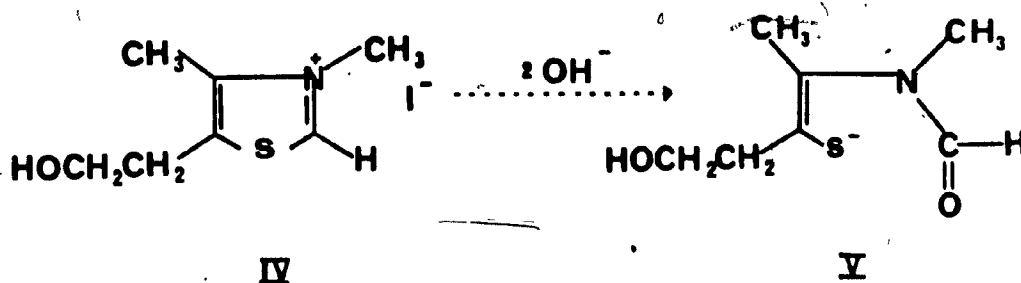
Work progressing in this department was involved in the investigation of the kinetic properties of the isolable thiazolium ring (III). This study deals with the application of correlation N.M.R. as a corroborative tool to supply evidence supporting a previous mechanistic hypothesis.⁶⁰

Figure 5.19 illustrates comparable fast and slow passage spectra run in D_2O of the iodide salt of the ring(III). Nothing is observed to low field of HOD, the proton H_a is assumed exchanged with the solvent D_2O .


Figure 5.20 is a spectrum of the same salt (IV), this time run in water. The H_a proton is clearly visible at 9.8 ppm unexchanged. The contribution from the non-bonding electrons on the nitrogen atom has shifted the peak significantly downfield, as expected.⁶¹

Figure 5.21 gives positive evidence that the base catalyzed ring opening does, in fact, end in the structure shown(V). The formyl proton, H_a , is found where we would expect an equivalent system⁶², at 8.1 ppm.

Figure 5.23



The Experimental section has demonstrated that the instrument does in fact function in a variety of operating conditions and has furnished useful results that would not have been possible by pulse methods because of the severe dynamic range problems caused by the solvent, water.



Chapter 6

FUTURE APPLICATIONS AND CONCLUSIONS

It has taken the duration of this thesis to bring this project to the point where it is a viable research grade spectrometer in the chosen configuration. The more interesting potential of system development and evolution has just become realizable. The areas of development lie in two obvious sectors:

1. General enhancement of instrument capabilities on existing features.
2. Extension of facility to new experiments.

Under the first heading there are a number of published advanced software programs which would benefit the system. Cooper has published a peak-picking routine,⁵² and there has been continuous development in the literature of digital methods for handling dynamic range problems,^{72,73} correlation development,⁷⁴ and truncation artifacts.⁷⁵ The entire range of traditional pulse data massaging techniques such as Gaussian multiplication⁵³ and trigonometric multiplication³⁴ are available. Further, a wing processing method enabling extraction of data out of the shoulder of the water signal has been published specifically for a correlation system.⁷⁶ The software at hand currently has no baseline correction routine, this should warrant attention.

Unfortunately, before any further software development should progress to any extent, serious thought should be given to increasing the HP-4000 memory capabilities. The existing software runs as three separate programs by necessity because of memory protect errors issued when attempting to load too large a program. One alternative is the rather complicated procedure of writing overlays which allow an extremely efficient use of memory and disc.

With regards to new experiments, it should be plain that the forte of this spectrometer configuration is in the study of aqueous systems. To this end, it compliments the pulse spectrometer already resident in the Department in providing a more extensive range of capabilities to the users.

Specifically, the study of chemical exchange by rapid scan FT NMR has already been dealt with theoretically in the literature.⁷⁷ Flow,⁷⁸ and stopped-flow NMR⁷⁹ have been well demonstrated as perfectly viable as corroborative evidence and in kinetic studies as well. As of yet, the advantages of Rapid Scan Correlation FT NMR have not been brought to bear on kinetic problems in aqueous systems, a perfectly viable and possibly superior method of investigation. Less obvious is the development of already existing variable temperature capabilities to run non-isothermal kinetics.⁸⁰ Spin lattice relaxation measurements have also been demonstrated, with potential advantages over pulse techniques.⁸¹

CONCLUSION

In conclusion the following statements can safely be made with respect to the objectives of this thesis:

1. The configuration detailed in this text does function successfully as a Rapid Scan Correlation FT NMR spectrometer.

2. The instrument operation has been demonstrated in a variety of experimental conditions and returned respectable results.

3. The system has proven useful in elucidating the solution to a problem unobtainable or difficult to obtain by pulse techniques.

4. The spectrometer has very promising prospects with regards to further developments and provides an important compliment to the NMR facilities of the department.

5. What has for most universities become scrap metal⁸⁴ has been transformed here into a viable research spectrometer.

REFERENCES

1. Bloch, F., Hansen, W.W., Packard, M.E.,
Phys. Rev. 69, 127, (1946).
2. Purcell, E.M., Torrey, H.C., Pound, R.V.,
Phys. Rev. 69, 37, (1946).
3. Arnold, J.T., Packard, M.E., Dharmatti, S.S.,
J. Chem. Phys. 19, 507, (1951).
4. Bloch, F. Phys. Rev. 70, 474, (1946).
5. Ernst, R.R., Anderson, W.A., Rev. Sci. Instru. 37, 93,
(1966).
6. Torrey, H.C. Phys. Rev. 76, 1059, (1949).
7. Hahn, E.L. Phys. Rev. 80, 580, (1951).
8. Fourier, J.B.J. Theorie Analytique de la Chaleur,
Paris, 1982.
9. Cooley, J.W., Tukey, J.W., Math.Comp. 19, 297, (1965).
10. Ernst, R.R. Adv. Mag. Res. 2, 1, (1966).
11. Dadok, J., Sprecher, R.F. J. Mag. Res. 13, 243, (1974).
12. Gupta, R.J., Ferretti, J.A., Becker, E.D.
J. Mag. Res. 13, 275, (1974).
13. Arata, Y., Ozawa, H. Chem. Lett. 1257, (1974).
14. Ogino, T., Arata, Y., Fujiwara, S.,
J. Mag. Res. 39, 381, (1980).
15. Ozawa, H., Arata, Y. Chem. Lett. 239, (1975).
16. IDEM, J. Mag. Res. 21, 67, (1976).
17. Arata, Y., Ozawa, H., Fujiwara, S., Ogino, T.
Pure and Appl.Chem. 50, 1273, (1978).
18. Pople, J.A., Schneider, W.G., Bernstein, H.J.
High Resolution NMR, pg.31-43, McGraw-Hill, 1959
19. Becker, E.D. High resolution NMR, Theory and Chemical Appl.
pg.23, Academic Press, NY., 1980, 2nd ed.
20. Slichter, C.P., Principles of Magnetic Resonance
pg.16-22, Harper, NY., 1963

21. Boas, M.L., Mathematical Methods in the Physical Sciences. pg.60, J.Wiley, 1983, 2nd ed.
22. Bracewell, R., The Fourier Transform and its Applications. following convention "method 2" McGraw-Hill, NY, 1965
23. Tretter, S.A., Intro. to Discrete Time Signal Proc. J.Wiley, NY, 1976
24. Cooper, J.W., Transform Tech. in Chemistry pg.84, Plenum Press, NY, 1978
25. Champeney, D.C., Fourier Transforms and their Phys. Appl. pg.16, Academic Press, London, 1973
26. IBID, pg.18
27. Bracewell, R.N., The Fourier Transform and its Appl. pg.36-40, McGraw-Hill, NY, 1978, 2nd ed.
28. Brigham, E.O., The Fast Fourier Transform pg.119 Prentice Hall, N.J., 1974
29. Lowe, I.J., Norberg, R.E., Phys. Rev. 107, 46, (1957).
30. Hieftje, G.M., Horlick, G., "Corr. Methods in Chem. Data Measurement" in Contemp. Topics in Anal. and Clinical Chemistry, Vol.3, pg.153, Plenum, 1978
31. Jones, R.N., Shimokoshi, K., Appl.Spectr. 37, 59, (1983).
32. IBID 37, 67, (1983).
33. Ng, R.C.L., Horlick, G., Spectr. Acta. 36b, 543, (1981).
34. Gueron, M., J. Mag. Res. 30, 515, (1978).
35. Bromba, M.U.A., Ziegler, H., Anal.Chem. 55, 648, (1983).
36. Clin, B. J. Mag. Res. 33, 457, (1979).
37. Ozawa, H., Arata, Y. Bull.Chem.Soc.Jpn. 55, 411, (1982).
38. Gassner, M. J. Mag. Res. 30, 141, (1978).
39. Bloch, F. Phys. Rev. 102, 104, (1956).
Phys. Rev. 105, 1206, (1956).
40. Ernst, R.R. J. Mag. Res. 1, 7, (1969).
41. Boas, M.L., Math. Meth. in the Phys. Sci. pg.669 J.Wiley 1983, 2nd ed.

42. IBID pg.668
43. Riley, K.F., Math. Meth. for the Phys. Sci. pg.215
Cambridge Univ. Press, 1974
44. Cooper, J.W., Intro. to Pascal for Scientists pg.211
J.Wiley 1981
45. Cooper, J.W., J. Mag. Res. 22, 345, (1976).
46. Cooper, J.W., J. Mag. Res. 28, 405, (1977).
47. Singleton, R.C., IEEE Trans. Audio. and Elec.,
AU-17, No.2, (1969).
48. Makinen, S., Rev. Sci. Instru. 53(5)., 627, (1982).
49. Cooper, J.W., Spect. Tech. for Organic Chemists
J.Wiley, NY, 1981
50. Brigham, E.O., The Fast Fourier Transform pg.169
Prentice Hall, N.J., 1978
51. Nicolet Zeta Corp., Fundamental Plotting Subroutines
Fortran Reference Manual, Pub.No.431-014, 5.3 March 1978
52. Cooper, J.W., The Minicomputer in the Lab. pg.278
Wiley Interscience, 1978
53. Bruker Spectrospin Canada, WP80-SY Manual
54. Roeder, S.B.W., Fukushima, E., Exptl. Pulse NMR, A Nuts
and Bolts Approach, pg.88, Addison-Wellsly, 1981
55. Haake, P., J. Am. Chem. Soc. 91, 1113, (1969).
56. Williams, R.R., J. Am. Chem. Soc. 57, 1856, (1935).
57. Zoitewicz, J.A., Ann.N.Y.Acad.Sci. 378, 7, (1982).
58. Jordan, F., IBID, pg.17
59. Ashai, Y., Mizuta, E., Talanta 19, 567, (1972).
60. Ashai, Y., Nagaoka, M., Chem.Pharm.Bull. 19, 1017, (1971).
61. Jackman, L.M., Sternhall, S., Appl. of NMR in Organic
Chemistry, pg.209, Pergamon Press, 1969, 2nd ed.
62. IBID pg.191
63. Ernst, R.R., J. Mag. Res. 3, 10, (1970).
64. Varian Instruments Canada, HA-100 Operating Manual.

65. Martin, M.L., Martin, G.J., Delpeuch, J.J., Pract. NMR Spectroscopy, pg.52, Heyden, NY, 1980
66. Dulcic, A., Rakvin, B., J. Mag. Res. 52, 323, (1983).
67. Shaw, D., Fourier Transform NMR Spectroscopy, Elsevier, NY., 1976.
68. Hoult, D.I., Prog. NMR. Spectr. 12, 41, (1978).
69. Adder, R.E., J. Mag. Res. 29, 105, (1978).
70. Landers, P.C., J.Phys.E.Sci.Instru. 6, 552, (1978).
71. Redfield, A.G., Rev. Sci. Instru. 54(4)., 503, (1983).
72. Roth, K., J. Mag. Res. 302, (1980).
73. Marchal, J.P., J. Mag. Res. 33, 469, (1979).
74. Horlick, G., Ng, R.C.L., Spectrochim. Acta. 36B, 529, (1981).
75. Marshall, A.G., J. Mag. Res. 551, (1979).
76. Kyogoku, Y., Bull.Chem.Soc.Jpn. 53, 904, (1980).
77. Jen, J., J. Mag. Res. 45, 257, (1981).
78. Fyfe, C.A., Cocivera, M., Damji, S.W.H., J. Mag. Res. 23, 377, (1976).
79. Ernst, R.R., J. Mag. Res. 35, 39, (1979).
80. Martin, G.J., Martin, M.L., J. Phys. Chem. 84, 414, (1980).
81. Ferretti, J.A., Becker, E.D., J. Mag. Res. 16, 505, (1974).
82. Reilly, C.A., J. Chem. Phys. 25, 604, (1956).
83. Bovey, F.A., NMR Spectroscopy, pg.42, Acad.Press, NY, 1969.
84. Pers.Comm. Paul Cote, Instr. Division, Varian Canada May 1982.

APPENDIX

```

C*****
C      PROGRAM NMRUN
C*****
C
C  SOURCE FILE IS GRUN::11
C  BINARY FILE IS RRUN
C  PROGRAM COMES UP ON RU,NMRUN.
C  PROGRAM LOADS ON TR,TRUN
C  BINARY FILE IS RRUN
C  THIS PROGRAM RESPONDS AT TERMINAL #7 (REMOTE)
C
C
C  THIS IS THE MAIN PROGRAM FOR CONTROL OF THE HA-100
C  IN THIS CONFIGURATION THE INSTRUMENT IS RUN AS A
C  RAPID PASSAGE ADIABATIC CONTINUOUS WAVE SPECTROMETER.
C  THE WAVETEK IS DRIVEN BY THE SWEEP SUBROUTINE
C
C  INITIALIZE THE VARIABLES
C
C      COMMON XDATA(2048), NN
C      COMMON SW, AQ, SWPRT
C      EQUIVALENCE (XDATA(1),IDATA(1))
C      INTEGER IDATA(4096)
C      ISTRT=0
C      KLOK=0
C      IRATE=1
C      NSCAN=10
C      NN=2048
C      DO 4 I=1,4096
C      IDATA(I)=0
C  4      CONTINUE
C      WDOH=10.00
C      WDOL=2.00
C  THE ARRAY HAS BEEN ZEROED!!!!
C
C  DECIDE WHICH OF THREE MAIN FUNCTIONS TO PERFORM
C*****
C
C  1      WRITE(7,100)
C  100     FORMAT("READ,WRITE,RUN, OR STOP??")
C         READ(7,101)IRES
C  101     FORMAT(A2)
C         IF (IRES.EQ.2HRU) GO TO 108
C         IF (IRES.EQ.2HWR) GO TO 550
C         IF (IRES.EQ.2HRE) GO TO 500
C         IF (IRES.EQ.2HST) STOP
C         GO TO 1
C
C  FIRST FUNCTION IS RUNNING THE EXPERIMENT
C*****
C
C  108     WRITE(7,109)
C  109     FORMAT("ZERO, SET-UP, SWEEP, OR EXIT ??")
C         READ(7,110)IREP

```

```

IF(IREP.EQ.2HSE) GO TO 120
IF(IREP.EQ.2HSW) GO TO 170
IF(IREP.EQ.2HZE) GO TO 180
IF(IREP.EQ.2HEX) GO TO 1
GO TO 108

```

C

C*****

```

120 WRITE(7,121)
121 FORMAT("ENTER SPECTRAL RANGE OF INTEREST")
WRITE(7,122)
122 FORMAT("ENTER DESIRED HIGH FIELD LIMIT IN PPM")
READ(7,*)WDOH
WRITE(7,123)
123 FORMAT("ENTER DESIRED LOW FIELD LIMIT IN PPM")
READ(7,*)WDOL
DOH=(WDOH*100.0)+2500.00
DOL=(WDOL*100.0)+2500.00
WRITE(7,124)DOH
124 FORMAT("SET WAVETEK MAX. TO ",F7.2," HZ")
WRITE(7,125)
125 FORMAT("ENTER EXACT VALUE IN HZ, OFF FREQ. CNTR")

```

CALL RMIN

```

READ(7,*)DOH
WRITE(7,126)DOL
126 FORMAT("SET WAVETEK MIN. TO ",F7.2," HZ")
WRITE(7,127)
127 FORMAT("ENTER EXACT VALUE IN HZ, OFF FREQ. CNTR")

```

CALL RMAX

```

READ(7,*)DOL
CALL RMIN
139 WRITE(7,128)
128 FORMAT("ENTER EST. AQUISITION TIME")
READ(7,*)AQEST
WRITE(7,129)
129 FORMAT("ENTER THE NUMBER OF SCANS WISHED")
READ(7,*)NSCAN

```

C

```

WDOL=(DOL-2500.00)/100.00
WDOH=(DOH-2500.00)/100.00
SW= ABS(DOL-DOH)
RES= 2048.00 /SW
DWLEST=AQEST/2048.00
RATE=DWLEST/0.000100
IRATE=IFIX(RATE)
IF(IRATE.LT.1) GO TO 137
DWELL=FLOAT(IRATE)*0.000100
AQ=DWELL*2048.00
SWPRT=SW/AQ

```

C

WRITE(7,130)SWPRT


```

WRITE(7,131)RES
131  FORMAT("DIGITAL RESOLUTION = ",F7.2," PTS/HZ")
      WRITE(7,132)AQ
132  FORMAT("TRUE AQUISITION TIME IS ",F7.2," SEC")
      WRITE(7,133)WDOH,WDOL
133  FORMAT("SPECTR. SWEEPS FROM ",F7.2," TO ",F7.2," PPM")
C
134  WRITE(7,135)
135  FORMAT("CHANGE PARAMETERS??, YES,NO, OR JUST AQ. TIME?")
      READ(7,136)IHRU
136  FORMAT(A2)
      IF (IHRU.EQ.2HYES) GO TO 120
      IF (IHRU.EQ.2HNO) GO TO 108
      IF (IHRU.EQ.2HAQ) GO TO 139
      GO TO 134
137  WRITE(7,138)
138  FORMAT("ERROR -/DWELL TIME TOO SMALL/")
      GO TO 134
C
C*****
C
170  DO 171 I=1,4096
      IDATA(I)=0
171  CONTINUE
      ISTRT=0
      NON=2047
C
C SWEEP SUBROUTINE IN ASSEMBLER
C*****
      CALL SWEEP(ISTRT,NON ,KLOK,IRATE,NSCAN)
C*****
C
C  FLOAT IS DONE ON PREMISE THAT IDATA IS PACKED USING
C  EVERY SECOND DATA LOCATION VIA THE ASSMBLR ROUTINE SWEEP
C
      WRITE(7,173)
173  FORMAT("SWEEP DATA FLOATING")
      J=1
      DO 172 I=1,2048
      XDATA(I)=FLOAT(IDATA(J))
      J=J+2
172  CONTINUE
      GO TO 134
C
C  ZERO ARRAY
180  DO 181 I=1,4096
      IDATA(I)=0
181  CONTINUE
      GO TO 108
C
C*****
C
500  CALL DSCRD
      GO TO 1

```

C*****

C
550 CALL DSCRT
GO TO 1
END

C

C

C*****

C

C

SUBROUTINE DSCRD
DIMENSION IDCB(144), IBUF(1), NAME(3)
COMMON XDATA(2048), NN
COMMON SW, AQ, SWPRT

C

WRITE(7,505)
505 FORMAT("ENTER NAME OF FILE YOU WISH TO BE READ")
READ(7,510)NAME
510 FORMAT(3A2)

C

CALL OPEN(IDCB, IERR, NAME, 0, 0, 0)
IF (IERR.LT.0) GO TO 540

C

CALL READF(IDCB, IERR, IBUF, 1)
IF (IERR.LT.0) GO TO 540

C

NN=IBUF(1)
MN=2*NN

C

CALL READF(IDCB, IERR, XDATA, MN)
IF (IERR.LT.0) GO TO 540

C

C

CALL CLOSE(IDCB, IERR)
IF (IERR.GE.0) GO TO 545

C

540 WRITE(7,541)
541 FORMAT("ERROR IN FILE HANDLING(IERR)!")

C

545 WRITE(7,546)
546 FORMAT("FILE READ COMPLETED")

C

RETURN
END

C*****

C

SUBROUTINE DSCRT
DIMENSION IDCB(144), IBUF(1), NAME(3)
COMMON IDATA(2048), NN
COMMON SW, AQ, SWPRT
REAL IDATA

C

WRITE(7,555)
555 FORMAT("ENTER NAME OF FILE TO BE WRITTEN ")


```

C*****:
C      PROGRAM NMRAN
C*****:
C
C  SOURCE FILE IS GRAN::11
C  BINARY FILE IS RRAN
C  PROGRAM COMES UP ON RU,NMRAN
C  PROGRAM LOADS ON TR,TRAN
C  THIS PROGRAM RESPONDS AT TERMINAL #6 (REMOTE) -
C
C  THE DSCRT AND DSCRD ROUTINES PROVIDE HARD COPY
C  STORAGE AND RETREVAL FOR THE SPEC. FILES ON THE
C  REMOVABLE DISC.
C  THE DSHAP SUBROUTINE PERFORMS THE CORRELATION MULTI-
C  PPLICATION AND ACCESS TO THE FOURIER TRANSFORM ROUTINE
C  AND ALL OTHER DATA MANIPULATION ROUTINES.
C
C  INITIALIZE THE VARIABLES
C
C      COMMON XDATA(2048), NN
C      COMMON SW, AQ, SWPRT
C      EQUIVALENCE (XDATA(1),IDATA(1))
C      INTEGER IDATA(4096)
C      NN=2048
C      TLB=0.00
C      DO 4 I=1,4096
C      IDATA(I)=0
4      CONTINUE
C      WDOH=10.00
C      WDOL=2.00
C      AQ=0.0
C      SW=0.0
C
C  DECIDE WHICH OF THREE MAIN FUNCTIONS TO PERFORM
C*****:
C
C  1      WRITE(6,100)
C  100     FORMAT("READ,WRITE,SHAPE, OR STOP??")
C         READ(6,101)IRES
C  101     FORMAT(A2)
C         IF (IRES.EQ.2HSH) GO TO 200
C         IF (IRES.EQ.2HWR) GO TO 550
C         IF (IRES.EQ.2HRE) GO TO 500
C         IF (IRES.EQ.2HST) STOP
C         GO TO 1
C
C  FIRST FUNCTION IS RUNNING THE EXPERIMENT
C*****:
C
C  SHAPE SUBROUTINE CALL
C*****:
C
C  200     CALL DSHAP
C         GO TO 1

```

C*****

C

500 CALL DSCRD
GO TO 1

C

C*****

C

550 CALL DSCRT
GO TO 1
END

C

C

C*****

C

SUBROUTINE DSHAP
COMMON IDATA(2048), NN
COMMON SW, AQ, SWPRT
REAL IDATA,ISRG, ICRG
INTEGER HWDO
RDTN=0.00
PHZ=90.00

C

C*****

C

PRESENT THE MAIN MENU

C

201 WRITE(6,202)
202 FORMAT("CORX,EXPX,FT,PHASE,SCALE,LOOKC,ZEPK,ONES,FIDL,QUIT?")
READ(6,203)IRAP
203 FORMAT(A2)
IF (IRAP.EQ.2HPH) GO TO 210
IF (IRAP.EQ.2HCO) GO TO 220
IF (IRAP.EQ.2HON) GO TO 230
IF (IRAP.EQ.2HEX) GO TO 240
IF (IRAP.EQ.2HZE) GO TO 250
IF (IRAP.EQ.2HFT) GO TO 260
IF (IRAP.EQ.2HSC) GO TO 270
IF (IRAP.EQ.2HLO) GO TO 280
IF (IRAP.EQ.2HFI) GO TO 290
IF (IRAP.EQ.2HQU) GO TO 299
GO TO 201

C

C*****

C

PHASE ADJUSTMENT AND RECONSTRUCTION

C

210 WRITE(6,211)PHZ
211 FORMAT("CURRENT PHASE ANGLE = ",F7.2," DEG. ENTER NEW VALUE")
READ(6,*)PHZ
NO2=NN/2
RG=(PHZ/180.00)*3.141592654
CRG=COS(RG)
SRG=SIN(RG)

C

J=NO2+1
DO 212 I=1,NO2

```

        ISRG=SRG*IDATA(J)
        RSRG=SRG*IDATA(I)
        ICRG=CRG*IDATA(J)
        IDATA(I)=RCRG+ISRG
        IDATA(J)=-RSRG+ICRG
        J=J+1
212    CONTINUE
        WRITE(6,213)PHZ
213    FORMAT("FINISHED PHASE ADJUST TO ",F7.2," DEG.")
        GO TO 201
C
C*****
C
C    CORRELATION MULTIPLICATION
C    EXPECTS ARRAY IN FORM      RRRR/IIII
C
220    CONTINUE
C
        NO2=NN/2
        WRITE(6,222)SW,AQ
222    FORMAT("SW= ",F7.3," HZ.  AQ= ",F7.3," SEC.")
C
        JDX=NO2+1
        AR=3.141592654/(AQ*SW)
        IDATA(1)=0.00
        IDATA(JDX)=0.00
C
        DO 229 IDX=1,NO2
            RDX=FLOAT(IDX)
            ARG=AR*RDX**2
            ARGC=COS(ARG)
            ARGS=SIN(ARG)
            HOLDI=IDATA(IDX)
            HOLDJ=IDATA(JDX)
            IDATA(IDX)=(HOLDI*ARGC)-(HOLDJ*ARGS)
            IDATA(JDX)=(HOLDI*ARGS)+(HOLDJ*ARGC)
            JDX=JDX+1
229    CONTINUE
        GO TO 201
C
C*****
240    CONTINUE
C    EXPOTENTIAL MULTIPLICATION
C
        ELB=0.00
        NO2=NN/2
        J=NO2+1
        WRITE(6,241)TLB
241    FORMAT("TOTAL LB IS ",F7.2," -ENTER ADDITIONAL LB")
        READ(6,*)ELB
        TLB=TLB+ELB
        DO 242 I=1, NN
            BRKT= -((I-1)*ELB)/(2*SW)
            PNT= EXP(BRKT)

```

```

      IDATA(J)=IDATA(J)*PNT
      J=J+1
242  CONTINUE
      WRITE(6,243)TLB
243  FORMAT("FID HAS TOTAL OF ",F7.2," HZ LB BY EXP *")
      GO TO 201
C
C*****
C      JUMP TO FOURIER TRANSFORM SUBROUTINE
C
260  CONTINUE
      CALL FFTN
      GO TO 201
C*****
C
230  CONTINUE
      WRITE(6,231)
231  FORMAT("THE ARRAY HAS BEEN .1111111'D")
      DO 232 I=1, NN
      IDATA(I)=1.0
232  CONTINUE
      GO TO 201
C
C*****
C
C      ROUTINE ZEROS WINDOW IN ARRAY
250  CONTINUE
      LWDO=0
      HWDO=NN
      ISKP=1
      WRITE(6,256)
256  FORMAT("ZERO, PACK OR QUIT??")
      READ(6,257)IREP
257  FORMAT(A2)
      IF(IREP.EQ.2HZE) GO TO 258
      IF(IREP.EQ.2HQA) GO TO 259
      IF(IREP.EQ.2HQU) GO TO 201
      GO TO 250
258  CONTINUE
      WRITE(6,251)
251  FORMAT("ENTER THE ZEROING WINDOW PARAMETERS BY POINT NUMBER")
      WRITE(6,252)LWDO
252  FORMAT("THE LOWER WINDOW IS POINT NUMBER ",I5).
      READ(6,*)LWDO
      WRITE(6,253)HWDO
253  FORMAT("THE HIGH WINDOW IS POINT NUMBER ",I5)
      READ(6,*)HWDO
      WRITE(6,263)ISKP
263  FORMAT("ZERO BY EVERY ",I5," PTS??")
      READ(6,*)ISKP
      DO 254 I=LWDO, HWDO, ISKP
      IDATA(I)=0
254  CONTINUE
C

```

```

255  FORMAT("ARRAY HAS BEEN ZEROED FROM ",I5," TO ",I5," BY ",I5)
C
      GO TO 201
259  CONTINUE
      NO2=NN/2
      J=2
      DO 261 I=1,NO2
      IDATA(I)=IDATA(J)
      J=J+2
261  CONTINUE
      WRITE(6,262)
262  FORMAT("ARRAY PACKED: RRRR/GBGE")
      GO TO 250
C*****
270  CONTINUE
C      THIS ROUTINE DOES A SCALING FUNCTION
C
C      SORT FOR THE MAX VALUE OF THE ARRAY
C
      YMAX=ABS(IDATA(1))
      DO 271 I=1, NN
      VABS=ABS(IDATA(I))
      IF (YMAX.GE.VABS) GO TO 271
      YMAX=ABS(IDATA(I))
271  CONTINUE
      WRITE(6,272)YMAX
272  FORMAT("THE MAX. VALUE OF THE ARRAY IS ",F7.2)
      WRITE(6,273)
273  FORMAT("ENTER SCALING VALUE(32767 IS MAX)")
      READ(6,*)SKL
C
C      SCALE THE ARRAY
C
      DO 274 I=1, NN
      IDATA(I)=(IDATA(I)/YMAX)*SKL
274  CONTINUE
      WRITE(6,275)SKL
275  FORMAT("THE ARRAY HAS BEEN SCALED TO ",F7.2)
      GO TO 201
C
C*****
280  CONTINUE
C
C
C
      WRITE(6,281)NN
281  FORMAT("CURRENT # OF PTS IN ARRAY= ",I5)
C
C      WRITE THE ARRAY
C
      DO 283 I=1,NN
      WRITE(6,282) I,IDATA(I)
282  FORMAT("PT NMBR ",I5," HAS THE VALUE ",F7.2)
283  CONTINUE

```



```

      WRITE(6,284)
284  FORMAT("THE END OF THE ARRAY")
      C
      GO TO 201
      C
      C*****
      C
290  CONTINUE
      WRITE(6,291)NN
291  FORMAT("CURRENT #OF PTS = ",I5," -ENTER NEW VALUE!")
      READ(6,*)NN
      WRITE(6,292)NN
292  FORMAT("ARRAY NOW CONTAINS ",I5," PTS!")
      GO TO 201
      C
      C*****
      C
299  CONTINUE
      RETURN
      END
      C
      C*****
      C
      SUBROUTINE DSCRD
      DIMENSION IDCB(144), IBUF(1), NAME(3)
      COMMON XDATA(2048), NN
      COMMON SW, AQ, SWPRT
      C
      WRITE(6,505)
505  FORMAT("ENTER NAME OF FILE YOU WISH TO BE READ")
      READ(6,510)NAME
510  FORMAT(3A2)
      C
      CALL OPEN(IDCB, IERR, NAME, 0, 0, 0)
      IF (IERR.LT.0) GO TO 540
      C
      CALL READF(IDCB, IERR, IBUF, 1)
      IF (IERR.LT.0) GO TO 540
      C-
      NN=IBUF(1)
      MN=2*NN
      C
      READ TOTAL # OF PTS, NN IS # OF REAL PTS!
      C
      CALL READF(IDCB, IERR, XDATA, MN)
      IF (IERR.LT.0) GO TO 540
      C
      MN=2
      CALL READF(IDCB, IERR, AQ, MN)
      IF (IERR.LT.0) GO TO 540
      CALL READF(IDCB, IERR, SW, MN)
      IF (IERR.LT.0) GO TO 540
      C
      C
      CALL CLOSE(IDCB, IERR)

```

```

C
540 WRITE(6,541)
541 FORMAT("ERROR IN FILE HANDLING(IERR)!")
C
545 WRITE(6,546)
546 FORMAT("FILE READ COMPLETED")
C
      RETURN
      END
C*****
C
      SUBROUTINE DSCRT
      DIMENSION IDCB(144), IBUF(1), NAME(3)
      COMMON IDATA(2048), NN
      COMMON SW, AQ, SWPRT
      REAL IDATA
C
      WRITE(6,555)
555 FORMAT("ENTER NAME OF FILE TO BE WRITEN (REMOVABLE DISC)")
      READ(6,560)NAME
560 FORMAT(3A2)
C
      ISIZE=-1
      ITYPE=3
      IERR=0
      ICR=11
C
      CALL CREAT( IDCB, IERR, NAME, ISIZE, ITYPE, 0, ICR)
      IF (IERR.LT.0) GO TO 590
C
      IL=1
      IBUF(1)=NN
C
      CALL OPEN(IDCB,IERR,NAME)
      IF (IERR.LT.0) GO TO 590
C
      CALL WRITF(IDCB, IERR, IBUF, IL)
      IF (IERR.LT.0) GO TO 590
C
      IL=2*NN
      CALL WRITF(IDCB, IERR, IDATA, IL)
      IF (IERR.LT.0) GO TO 590
C
      IL=2
      CALL WRITF(IDCB, IERR, AQ, IL)
      IF (IERR.LT.0) GO TO 590
      CALL WRITF(IDCB, IERR, SW, IL)
      IF (IERR.LT.0) GO TO 590
C
      CALL LOCF(IDCB,IERR,IERR,IRB,IOFF,JSEC)
      IF (IERR.LT.0) GO TO 590
C
      ITRUN=JSEC/2-IRB-1
C

```

```

      IF (IERR.GE.0) GO TO 595
C
590  WRITE(6,591)
591  FORMAT("FILE HANDLING ERROR(IERR)")
C
595  WRITE(6,596)
596  FORMAT("FILE WRITE COMPLETED!!")
      RETURN
      END
C
C*****
C
C
C  THIS PROGRAM PERFORMS A FAST FOURIER TRANSFORM
C  SIMILAR TO THE COOLEY-TOOKEY ALGORITHM.
C  THE CODE WAS TRANSLATED INTO FORTRAN FROM A
C  PASCAL LISTING WRITTEN BY JAMES COOPER WITH
C  SOME MODIFICATIONS.
C
C  THIS PROGRAM HAS THREE SUBROUTINES WITH IN IT, EACH
C  OF WHICH PERFORM AN ENTIRELY SEPERATE FUNCTION.
C  WHAT FOLLOWS IS A FLOW CHART OF THE INDEXING SYSTEM
C  USED FOR THIS APPLICATION TO CORRELATION PROCESSING.
C
C  REAL ARRAY-----      RRRRRRRR-----FREQ. DOMAIN
C
C
C
C
C  (REAL)  SHUFL-----
C  (FWD)   FFT-----      TO
C  (TRFRM) POST-----
C
C
C  COMPLEX ARRAY--      RRRRIIII-----TIME DOMAIN
C
C  (COMPLX)
C  (INV)   FFT-----      TO
C  (TRFRM)
C
C  COMPLEX ARRAY--      RRRRIIII-----FREQ. DOMAIN
C
C*****
C
C  SUBROUTINE FFTN
C  COMMON X(2048), N
C  COMMON SW, AQ, SWPRT
C  INTEGER CMBK
C  DATA PI2/1.570796327/
C
C  INV=1
C
106  WRITE(6,101)

```

```

      READ(6,102)CMBK
102  FORMAT (A2)
      IF (CMBK.EQ.2HFO) GO TO 104
      IF (CMBK.EQ.2HIN) GO TO 103
      IF (CMBK.EQ.2HST) GO TO 108
      GO TO 106
C
103  INV=-1
      CALL FFT (INV,PI2)
      GO TO 107
104  CONTINUE
C
      CALL SHUFL(INV)
      CALL FFT ( INV, PI2 )
      CALL POST( NU, INV, PI2)
107  WRITE(6,109)
109  FORMAT("TRANSFORM COMPLETED")
108  RETURN
      END
C
C  SUBROUTINES BEGIN*****
C
C  FIRST A FUNCTION WHICH PERFORMS "BIT INVERSION"
C
      FUNCTION IBITR (J,NU)
      IB=0
      DO 25 IN=1, NU
      J2=J/2
      IB=IB*2+(J-2*J2)
25  J=J2
      IBITR=IB
      RETURN
      END
C
C  NEXT SUBROUTINE IS DEBUG *****
C  OUTPUTS THE DATA ARRAY DURING PROGRAM DEVELOPMENT
C
      SUBROUTINE DEBUG
      COMMON X(2048), N
      COMMON SW, AQ, SWPRT
      DO 15 I3=1, N
15  WRITE(6,105) X(I3)
105  FORMAT ( F7.2 )
      RETURN
      END
C
C  NEXT SUBROUTINE IS POST *****
C  ACTION IS PENDANT ON THE STATE OF "INV"
C  IF INV=1 THEN DO POST PROCESSING FOR FORWARD REAL TRANSFORM
C  IF INV=-1 THEN DO PRE PROCESSING FOR INVERSE REAL TRANSFORM
C  THIS SUBROUTINE WORKS THROUGH THE ARRAY BY CUTTING IT IN
C  HALF AND PROCESSING FROM THE ENDS TO THE MIDDLE.
C  THE INDEX I AND M WORK THE FIRST HALF OF THE ARRAY.
C  THE INDEX IPN2 AND MPN2 WORK THE 2ND HALF OF THE ARRAY.

```

```

SUBROUTINE POST ( NU, INV ,PI2)
COMMON X(2048), N
COMMON SW, AQ, SWPRT
REAL IPCOS, IPSIN, IC, IS1, IP, IM
NN2=N/2
NN4=N/4
DO 35 L=1,NN4
  I=L+1
  M=NN2-I+2
  IPN2=I+NN2
  MPN2=M +NN2
  RP= X(I)+X(M)
  RM= X(I)-X(M)
  IP= X(IPN2)+ X(MPN2)
  IM= X(IPN2)- X(MPN2)
C  TAKING COSINE OF PI/2N
  ARG= (PI2 / NN4)*(I-1)
  IC= COS (ARG)
C  THE COSINE WILL BE -VE IF DOING INV. FT.
  IF (INV.EQ.-1) IC=-IC
  IS1= SIN(ARG)
  IPCOS= IP*IC
  IPSIN= IP*IS1
  RMSIN= RM*IS1
  RMCOS= RM*IC
C  PROCESSING REAL(R___) AND IMAGINARY(I___) POINTS
  X(I)= RP + IPCOS - RMSIN
  X(IPN2)= IM-IPSIN-RMCOS
  X(M)= RP- IPCOS+ RMSIN
  X(MPN2)= -IM -IPSIN -RMCOS
35  CONTINUE
  RETURN
  END

C
C  NEXT SUBROUTINE IS SHUFFL *****
C                                RIRIRIRI
C                                TO
C                                RRRRIIII
C
C      IN PREPARATION FOR FORWARD TRANSFORM, OTHERWISE REVERSE
C
C  THE DIRECTION OF SHUFFLE DEPENDS ON STATUS OF INV.
C
C  INV IS 1 THEN: LARGE CELLS AND WORK DOWN ARRAY
C  INV IS -1 THEN: SMALL CELLS AND WORK UP ARRAY.
C
C
SUBROUTINE SHUFL (INV)
COMMON X(2048), N
COMMON SW, AQ, SWPRT
INTEGER CELNUM, CELDIS, PASS, PARNUM
C
  IF (INV.EQ.-1) GOTO 43
  CELDIS = N/2
  CELNUM= 1

```

```

      GOTO 47
43    CONTINUE
      CELDIS= 2
      CELNUM= N/4
      PARNUM= 1
47    CONTINUE
C
C    PERFORM THE FIRST PASS
C
      I= 2
      DO 45 J= 1, CELNUM
      DO 41 K= 1, PARNUM
      XTEMP= X(I)
      IPCM1= I+ CELDIS -1
      X(I)=X(IPCM1)
      X(IPCM1)=XTEMP
      I=I+2
41    CONTINUE
      I=I+ CELDIS
45    CONTINUE
C
C    CHANGE VALUES FOR 2ND PASS
C
      IF (INV. EQ. -1) GOTO 42
      CELDIS= CELDIS/2
      CELNUM= CELNUM*2
      PARNUM= PARNUM/2
      GOTO 44
42    CONTINUE
      CELDIS= CELDIS*2
      CELNUM= CELNUM/2
      PARNUM= PARNUM*2
44    CONTINUE
      IF(( CELDIS.LT.2.AND.INV.EQ.1).OR.(CELCUM.EQ.0.AND.INV.EQ.-1) )
1     GOTO 49
      GOTO 47
49    RETURN
      END
C
C    NEXT SUBROUTINE IS FFT *****
C    THIS IS IT !!!!!!!!!!!!!!!
C
      SUBROUTINE FFT( INV, PI2 )
      COMMON X(2048), N
      COMMON SW, AQ, SWPRT
      REAL I2COSY, I2SINY, K1, K2
      INTEGER CELNUM, CELDIS, PASS, PARNUM
C
      NU=0
      N1=N/2
      N2=N1
50    CONTINUE
      NU=NU+1
      N1=N1/2

```

```

DO 51 I=1, N2
  II=I-1
  K=IBITR(II,NU) +1
  IF (I.LE.K) GOTO 51
  IPN2= I+ N2
  KPN2= K+ N2
  TR= X(K)
  TI= X(KPN2)
  X(K)= X(I)
  X(KPN2)= X(IPN2)
  X(I)= TR
  X(IPN2)= TI
51 CONTINUE
  I=1
C THE FIRST PASS IS DONE ALONE.
52 IF (I.GT.N2) GOTO 53
  K= I+ 1
  KPN2= K + N2
  IPN2= I + N2
  K1 = X(I) + X(K)
  X(K) = X(I) - X(K)
  X(I) = K1
  K1 = X(IPN2) + X(KPN2)
  X(KPN2) = X(IPN2) - X(KPN2)
  X(IPN2) = K1
  I = I + 2
  GOTO 52
53 CONTINUE
  CELNUM = N2/4
  PARNUM = 2
  CELDIS = 2
  PASS = 2
  DELTAY=PI2
C EACH NEW CELL STARTS HERE.
59 INDEX = 1
  Y=0
  DO 58 I2=1, PARNUM
    IF (Y.EQ.0) GOTO 54
    COSY = COS(Y)
    SINY = INV*SIN(Y)
54 CONTINUE
    DO 57 L = 1, CELNUM
      I = CELDIS * 2 * (L-1) + INDEX
      J = I + CELDIS
      IPN2 = I + N2
      JPN2 = J + N2
      IF (Y.NE.0) GOTO 55
      K1 = X(I) + X(J)
      K2 = X(IPN2) + X(JPN2)
      X(J) = X(I) - X(J)
      X(JPN2) = X(IPN2) - X(JPN2)
      GOTO 56
55 CONTINUE
      R2COSY = X(J)*COSY

```

```
I2COSY = X(JPN2)*COSY
I2SINY = X(JPN2)*SINY
K1 = X(I) + R2COSY + I2SINY
K2 = X(IPN2) - R2SINY + I2COSY
X(J) = X(I) - R2COSY - I2SINY
X(JPN2) = X(IPN2) + R2SINY - I2COSY
56  CONTINUE
    X(I) = K1
    X(IPN2) = K2
57  CONTINUE
    Y = Y + DELTAY
    INDEX = INDEX + 1
58  CONTINUE
    CELNUM=CELCUM/2
    PARNUM=PARNUM*2
    CELDIS=CELCUM*2
    DELTAY=DELTAY/2
    PASS =PASS+1
    IF (CELCUM.NE.0) GO TO 59
    RETURN
    END
    END$
C   THAT'S ALL FOLKS!!!!!!!!!!!!!!!!!!!!!!!!!!!!!!!!!!!!!!!!!!!!!!!!!!!!
```


C*****

PROGRAM NMPLT

C
C SOURCE FILE: GPLT
C BINARY FILE: RPLT
C
C THIS PROGRAM READS A DISC FILE (6 CHARACTERS)
C AND PLOTS THE FILE ON THE ZETA PLOTTER.
C THE COMMAND RU,NMPLT BRINGS THE PROGRAM UP.
C THE TRANSFER FILE TR,TPLT LOADS THE PROGRAM.
C THIS PROG. RUNS ON THE AXISM CALL FROM RZETA4.
C
C LOADER REQUIRES BINARY ZETA PLOTTER FILES 'PLOTS', 'SYMB0',
C 'NUMBE', 'AXISM', 'PLOT', 'PON', AND 'ZZZZ'.
C
C
C THIS PROGRAM ALSO HAS THE CAPABILITY OF PLOTTING
C ABSORPTION AXIS WHEN LOOKING AT TIME DOMAIN SPECTRA
C
C
C

COMMON IZETA(1500)
COMMON IDATA(2048), NN
COMMON SW,AQ
REAL IDATA
1 CONTINUE
IERR=0
LEN=0
70 FREQL=0.0
FREQH=10.0
TIKI=100.0
XL=20.0
YL=15.0
FINCX=1.0
FENCY=1.0
C
101 WRITE(6,102)
102 FORMAT("READ, PLOT, PAKPLT, OR STOP??")
READ(6,103)IRES
103 FORMAT(A2)
IF (IRES.EQ.2HRE) GO TO 400
IF (IRES.EQ.2HPL) GO TO 300
IF (IRES.EQ.2HPA) GO TO 250
IF (IRES.EQ.2HST) STOP
GO TO 101
400 CONTINUE
CALL RDSPC
GO TO 101
250 CONTINUE
NN=NN/2
300 CONTINUE
WRITE(6,500)XL
500 FORMAT("LENGTH OF PLOT (CM) = ",F7.2)
READ(1,*)XL

```

WRITE(6,510)YL
510  FORMAT("PLOT HEIGHT (CM) = ",F7.2)
      READ(1,*)YL
      YLI=YL/2.54
C    CALCULATE THE MAGNITUDE OF THE SCALING FACTOR
C
      YYMAX=IDATA(1)
      DO 301 I=1,NN
      IF(YYMAX.GT.IDATA(I)) GO TO 301
      YYMAX=IDATA(I)
301  CONTINUE
      WRITE(6,888)YYMAX
888  FORMAT("MAX. Y VALUE = ",F7.2)
C
C    CALCULATE THE INCREMENT ON THE X AXIS
C
      FINCX=(XLI)/FLOAT(NN)
C
C    CALCULATE THE INCREMENT ON THE Y AXIS
C
      FINCY=YLI/(YYMAX*2)
      WRITE(6,889)FINCY
889  FORMAT("Y INC. = ",F10.3," IN/PT")
C
C    PLOT THE AXIS
C
      X=0.0
      Y=0.0
      CALL PLOTS(53,0,-1)
      CALL AXISM(0.0,0.0,XLI,1.0,0.0,1.0,0.2)
C    Y=-(YLI/2)
C    CALL AXISM(0.0,Y,YLI,1.0,1.0,1.0,0.2)
C    THE Y AXIS HAS BEEN REMOVED
      CALL PLOT(0.0,0.5,3)
C
345  CONTINUE
      WRITE(6,890)
890  FORMAT("TRANSFERRING DATA TO ZETA PLOTTER")
C
C    PLOT SPECTRUM
      DO 28 I=1,NN
      SUM=FINCY*IDATA(I)
      YY=SUM
      XX=X
      CALL PLOT(XX,YY,2)
      X=X+FINCX
28  CONTINUE
      X=XLI/2.0-3.0
      Y=YLI+0.8
      X=XLI+1.0
      CALL PLOT(X,0.0,999)
      GO TO 101
      END
C

```

```

C      SUBROUTINE RDSPC
        DIMENSION IDCB(144), IBUF(1), NAME(3)
        COMMON IZETA(1500)
        COMMON IDATA(2048), NPTS
        COMMON SW,AQ
        REAL IDATA
C
C      WRITE(6,405)
405     FORMAT("ENTER NAME OF FILE YOU WISH READ")
        READ(6,410)NAME
410     FORMAT(3A2)
C
        CALL OPEN(IDCB, IERR, NAME, .O, 0, 0)
        IF (IERR.LT.0) GO TO 440
C
        CALL READF(IDCB, IERR, IBUF, 1)
        IF (IERR.LT.0) GO TO 440
C
        NPTS=IBUF(1)
        NPT=2*NPTS
C
        CALL READF(IDCB, IERR, IDATA, NPT)
        IF (IERR.LT.0) GO TO 440
C
        MN=2
        CALL READF(IDCB, IERR, AQ, MN)
        IF (IERR.LT.0) GO TO 440
        CALL READF(IDCB, IERR, SW, MN)
        IF (IERR.LT.0) GO TO 440
C
        CALL CLOSE(IDCB, IERR)
        IF (IERR.GE.0) GO TO 445
C
440     WRITE(6,441)
441     FORMAT("ERROR RETURNED WHILE HANDLING FILE (IERR)")
C
445     WRITE(6,446)
446     FORMAT("DISC FILE READ COMPLETED!!")
C
        RETURN
        END
C
C
C
C*****
END$

```

NAM SWEEP,7

* 17/ 6/83

* FORTRAN CALLABLE DATA ACQUISITION ROUTINE:

* THE ROUTINE PROVIDES A SWEEP RAMP (UP TO 2048 STEPS), WITH DATA
 * ACQUISITION AT EACH STEP.
 * DATA ARE STORED IN INTEGER FORM IN THE VECTOR "STOR". THE DIMENS
 * OF "STOR" IS SET BY THE CALLING PROGRAM (<= 2048).

* FORTRAN CALLS:

* CALL RMIN

* CALL RMAX

* CALL SWEEP(ISTRT,NPTS,KLOK,IRATE,NSCAN)

* ISTRT = RELATIVE START ADDRESS ON RAMP

* NPTS = NUMBER OF POINTS ON RAMP

(ISTRT + NPTS <= 2048)

* KLOK = CLOCK (TIME BASE GENERATOR) PERIOD

(0 = 100 MICROSEC, 1 = 1 MSEC, 2 = 10 MSEC, ETC)

* IRATE = CLOCK TICK COUNTER

(I.E. MULTIPLES OF CLOCK PERIOD)

* NSCAN = NUMBER OF SCANS (SWEEPS)

* HP 21MX-E OPERATING UNDER RTE-II

* MEMORY PROTECT IS DISABLED AT THE FIRST INTERRUPT
 * (FROM THE TBG OR THE ADC), & IS RESTORED
 * WHEN SWEEP EXITS, I.E. SWEEP OPERATES WITH
 * MEMORY PROTECT DISABLED.

* THE SYSTEM CLOCK IS DISABLED DURING ACQUISITION OF DATA.
 * IT IS RESTORED WHEN PRIVILEGED INTERRUPTS ARE
 * NO LONGER PENDING.

* USES THE DUAL 12-BIT DAC.

* THE SCAN COUNT IS WRITTEN ON THE TERMINAL DISPLAY.

* THIS ROUTINE DOES NO ERROR CHECKING.

ENT RMIN,RMAX,SWEEP

EXT \$CVT3,\$LIBR,\$LIBX,EXEC,#OPEN,#CLOS,#PRTK,#RINT

EXT .ENTR,MESSS

COM IZETA(1500)

COM STOR(1)

TBG EQU 11B

ADC EQU 13B

TTY EQU 21B

SKLOK EQU 15B

*
* RAMP MINIMUM FOR CALIBRATION

```
RMIN  NOP
      LDA RMIN,I
      STA RETRN
      JSB #OPEN
      LDA =B10000
      OTA DAC      X-AXIS ZERO
      CLA
      OTA DAC      Y-AXIS ZERO
      JSB #CLOS
      JMP RETRN,I
```

*
* RAMP MAXIMUM FOR CALIBRATION

```
RMAX  NOP
      LDA RMAX,I
      STA RETRN
      JSB #OPEN
      LDA =B7777
      OTA DAC      Y-AXIS FULL SCALE
      LDA =B13777
      OTA DAC      X-AXIS FULL SCALE
      JSB #CLOS
      JMP RETRN,I
```

*
* SWEEP AND DIGITIZATION ROUTINE

```
ISTR  BSS 1      RELATIVE START ADDRESS
NPTS  BSS 1      NUMBER OF POINTS ON RAMP
IKLOK BSS 1      CLOCK PERIOD
IRATE BSS 1      CLOCK TICK COUNTER
NSCAN BSS 1      NUMBER OF SCANS
```

*
SWEEP NOP ENTRY POINT

```
JSB .ENTR  TRANSFER FORTRAN DUMMY ARGUMENTS
DEF ISTR
JSB UNBUF  UNBUFFER TERMINAL
LDA ISTR,I START INITIALIZATION
ALS      -**DOUBLE TO ALLOW FOR BLANK ENTRIES
ADA ASTOR
STA ASTRT ABSOLUTE START ADDRESS
LDA IRATE,I
CMA,INA
STA DCNTR  CLOCK TICK COUNTER
LDX =D-10
CLA
STA NOVER
STA SCNT
STA MIN1
STA MAX1
STA SHFTS
STA SHFTS+1
STA SHFTS+2
JSB #OPEN  LOWER MEMORY PROTECT FENCE & DISABLE INTERRUPT
```

LDA =B40000	ADC MODE
OTA ADC	
LDA INTBG	SET INTERRUPT CELL CONTENTS
STA TBG	CLOCK INTERRUPT
LDA INTTY	
STA TTY	TTY INTERRUPT
LDA INADC	
STA ADC	ADC INTERRUPT
CLA	
STA SCNT	ZERO SCAN COUNTER
OTA 1,C	CLEAR SWITCH REGISTER.
* START SCAN	
START LDA SCNT	CHECK NO. OF SCANS
CPA NSCAN,I	
JMP FINIS	EXIT IF FINISHED
ISZ SCNT	
JSB INIT	INITIALIZE ADDRESS INDEX & POINT COUNTER
LDA =B160000	PREPARE TO READ TTY
OTA TTY	
STC TTY,C	ENABLE TTY INTERRUPT
LDA =B10000	
ADA ISTRT,I	
STA XVAL	SET DAC X-AXIS TO START VALUE
OTA DAC	AND OUTPUT TO DAC
CLA	
OTA DAC	SET DAC Y-AXIS TO ZERO
LDA =B3	
OTA TBG	SET 0.1 SEC. DELAY
STC TBG,C	AND TURN ON TBG
SFS TBG	TO ALLOW FOR SETTLING TIME
JMP *-1	
CLC TBG,C	DISABLE TBG
LDA IKLOK,I	SET TBG PERIOD FOR SWEEP
OTA TBG	
LDY DCNTR	INITIALIZE TBG DELAY COUNTER
LIA 1,C	LOAD SWITCH REGISTER INTO "A"
SSA	CHECK SWITCH REGISTER
JMP OUT	EXIT IF S15 SET
CLC SKLOK,C	DISABLE SYSTEM CLOCK
STF 0	ENABLE INTERRUPT SYSTEM
STC TBG,C	START TBG
STC ADC,C	SWITCH ON ADC
LDB SCNT	
OTB 1,C	DISPLAY SCAN NO. IN SWITCH REGISTER
JMP WAIT	
* PROC CMA,INA	
SHFTS NOP	PROCEED AFTER TBG INTERRUPT
NOP	LOCATIONS FOR "ARS"
NOP	
CLO	
ADA ADDR,I	
SOC C	IS THERE AN OVERFLOW ?

```

STA ADDR,I      NO, THEN STORE NEW SUM
ARS,ARS          DIVIDE INTENSITY TO FIT DAC
ARS,ARS
ADA =B1777      ADD 1/4 OF DAC RANGE
OTA DAC         DISPLAY INTENSITY (Y-AXIS)
ISZ ADDR        INCREMENT ADDRESS INDEX
ISZ ADDR        **SKIP ONE ADDRESS
ISZ XVAL        INCREMENT DAC INDEX
LDA XVAL
OTA DAC         STEP X-AXIS SWEEP
ISZ PCNT        IS SCAN COMPLETE ?

*
WAIT JMP *      NO, WAIT FOR TBG INTERRUPT
*
* PROCEED IF SCAN COMPLETED
CLF 0           YES, DISABLE INTERRUPT SYSTEM
CLC TBG,C       DISABLE TBG
CLC ADC,C       DISABLE ADC
JSB #PRTK       RESTORE MEMORY PROTECT
LDA =B10000
OTA DAC         X-AXIS TO ZERO
CLA
OTA DAC         Y-AXIS TO ZERO

*
* OUTPUT SCAN NO. TO VIDEO TERMINAL
ISX             SHOULD SCAN NO. BE OUTPUT ?
JMP SKIP        NO, SKIP
LDX =D-10       YES, PREPARE TO OUTPUT EVERY 10TH SCAN COUNT
JSB #CLOS
JSB DECOD       SCNT TO ASCII
JSB #OPEN
LDA =B120000    PREPARE TO WRITE ON TERMINAL
OTA TTY
LDA =B15        CARRIAGE RETURN
OTA TTY
STC TTY,C
SFS TTY
JMP *-1
LDA =D-3
STA CPCNT
NUMB LDA CADDR,I
ALF,ALF         ROTATE BYTES
AND =B377       MASK
OTA TTY         OUTPUT NUMERAL
STC TTY,C
SFS TTY
JMP *-1
CLC TTY,C
LDA CADDR,I
AND =B377       MASK
OTA TTY         OUTPUT NUMERAL
STC TTY,C
SFS TTY
JMP *-1

```

```

      ISZ CADDR
      ISZ CPCNT
      JMP NUMB
*
SKIP  NOP
      STF 0          ENABLE INTERRUPT SYSTEM
* CHECK FOR POSSIBILITY OF OVER FLOW ON NEXT SCAN
      JSB INIT        CHECK FOR OVERFLOW
      CLA
      STA MIN2
      STA MAX2
LM    LDA ADDR,I      FIND MAXIMUM
      SSA             IS NO. NEGATIVE ?
      JMP NEG         YES
      ADA MAX2        NO, ADD CURRENT +VE MAXIMUM
      SSA
      JMP NEXT
      LDA ADDR,I
      CMA,INA
      STA MAX2
      JMP NEXT
NEG,  CMA,INA
      ADA MIN2
      SSA
      JMP NEXT
      LDA ADDR,I
      STA MIN2
NEXT  ISZ ADDR
      ISZ ADDR        **SKIP ONE ADDRESS
      ISZ PCNT
      JMP LM
      LDA MAX1
      CMA,INA
      ADA MAX2
      CLO
      ALS,ALS
      ADA MAX2
      SOS C           IS AN OVERFLOW LIKELY ?
      JMP #+2         NO, PROCEED
      JMP OVER        YES, GO TO DIVIDE ROUTINE
      LDA MIN1
      CMA,INA
      ADA MIN2
      CLO
      ALS,ALS
      ADA MIN2
      SOS C
      JMP 02
OVER  ISZ NOVER       START DIVIDE ROUTINE
      CCA
      ADA NOVER
      LDB ARSE
      SLA             SKIP IF "A" EVEN
      LDB ARSES

```



```

ADA SHFTA
STB OB,I-
JSB INIT
01 LDA ADDR,I
ARS
STA ADDR,I
ISZ ADDR
ISZ ADDR
ISZ PCNT
JMP 01
LDA MAX2
LDB MIN2
ARS
BRS
JMP *+3
02 LDA MAX2
LDB MIN2
STB MIN1
STA MAX1
LDB NOVER
ADB EXOV
SSB

*
* START NEW SCAN
JMP START
*
* OVERFLOW LIMIT
CLO
STC SKLOK,C
LDA =B120000
OTA TTY
JSB #RINT
JSB REBUF
JSB EXEC
DEF *+5
DEF .2
DEF .7
DEF LIM
DEF .8
JMP TERM

*
* INTERRUPT ROUTINES
*
TTYR NOP
CLC TTY,C
JSB #PRTK
STA SAVE
LDA =B100000
OTA 1,C
LDA SAVE
JMP TTYR,I

TBGR CLF TBG
ISY

```

STORE INSTRUCTION IN ADDRESS IN "A").

**SKIP ONE ADDRESS

OLD MAXIMUM

OVERFLOW LIMIT REACHED ?

NO, START NEW SCAN

YES, STOP SCANNING
ENABLE SYSTEM CLOCK

PREPARE TO WRITE ON TTY
RESTORE INTERRUPT CELL CONTENTS
RE-BUFFER TERMINAL
MESSAGE TO TERMINAL

(OVERFLOW LIMIT)

TTY INTERRUPT

TBG INTERRUPT

```

        LIA ADC
        STC ADC,C      RE-START ADC
        LDY DCNTR
        JMP PROC
*
ADCR   NOP              ADC INTERRUPT
        CLC ADC,C
        JMP ADCR,I
*
*   BINARY TO DECIMAL CONVERSION ROUTINE
*
DECOD  NOP
        JSB $LIBR
        NOP
        LDA SCNT
        CCE
        JSB $CVT3
        STA CADDR
        JSB $LIBX
        DEF DECOD
*
*   NORMAL EXIT
*
FINIS  CLC TTY,C
        CLC ADC,C
        CLC TBG,C
        STC SKLOK,C    ENABLE SYSTEM CLOCK
        LDA =120000    PREPARE TO WRITE ON TERMINAL
        OTA TTY
        JSB #RINT      RESTORE RTE INTERRUPTS
        JSB REBUF      RE-BUFFER TERMINALS
        JSB EXEC        MESSAGE TO TERMINAL
        DEF #+5
        DEF .2
        DEF .7
        DEF FIN        (FINISHED)
        DEF .5
        JMP TERM
*
*   OVERFLOW EXIT
*
OVERF  CLF 0
        CLC TTY,C
        CLC ADC,C
        CLC TBG,C
        STC SKLOK,C    ENABLE SYSTEM CLOCK
        LDA =B120000   PREPARE TO WRITE ON TERMINAL
        OTA TTY
        JSB #RINT
        JSB REBUF      RE-BUFFER TERMINAL
        JSB EXEC        MESSAGE TO TERMINAL
        DEF #+5
        DEF .2
        DEF .7

```

```

DEF .4
JMP SWEEP,I      EXIT

*
*
* ABORT EXIT
*
OUT   JSB #OPEN
      CLC TBG,C
      CLC ADC,C
      CLC TTY,C
      STC SKLOK,C
      LDA =B120000    PREPARE TO WRITE ON TERMINAL
      OTA TTY
      JSB #RINT        RESTORE RTE INTERRUPTS
      CCA
      ADA SCNT
      STA SCNT
      OTA 1,C
      JSB REBUF        REBUFFER TERMINAL
      JSB EXEC
      DEF #+5
      DEF .2
      DEF .7
      DEF ABORT        (ABORTED)
      DEF .5
      JMP TEND         EXIT

*
*
* MAXIMIZE ARRAY BEFORE EXITING
*
TERM  NOP
NLP1  JSB INIT
      LDA PCNT
      ALS
      STA PCNT        POINT COUNT x 2
      CLO
NLP2  LDA ADDR,I      GET DATUM
      ADA ADDR,I      DOUBLE IT
      SOC             IS THERE AN OVERFLOW ?
      JMP NMAX        YES, JUMP TO PROCESSING ROUTINE
      STA ADDR,I      NO, SO STORE DOUBLED DATUM
      ISZ ADDR        SET NEXT ADDRESS
      ISZ PCNT        END OF THE ARRAY ?
      JMP NLP2        NO, SO PROCESS NEXT NUMBER
      JMP NLP1        YES, START NEXT PASS
NMAX  LDA ADDR        FIND ADDRESS
      CMA,INA        AT WHICH
      ADA ASTRT      OVERFLOW OCCURRED
      SZR,RSS        AT FIRST POINT ?
      JMP TEND        YES, SO EXIT
      STA PCNT        NO, SO STORE POINT NO.
      LDA ASTRT      SET START ADDRESS
      STA ADDR        OF ARRAY
NLP3  LDA ADDR,I      GET DATUM

```

```

STA ADDR,I          AND REPLACE
ISZ ADDR            NEXT ADDRESS
ISZ PCNT            END OF PARTIAL ARRAY ?
JMP NLP3
TEND JSB DECOD       DECODE NO. OF SCANS
LDA CADDR,I
STA ACNT
ISZ CADDR
LDA CADDR,I
STA ACNT+1
ISZ CADDR
LDA CADDR,I
STA ACNT+2
JSB EXEC            MESSAGE TO TERMINAL
DEF *+5
DEF .2
DEF .7
DEF ACNT            (NO. OF SCANS)
DEF .6
JMP SWEEP,I

```

```

*
*
*  INITIALIZATION ROUTINE
*

```

```

INIT  NOP
      LDA NPTS,I
      CMA,INA
      STA PCNT      POINT COUNTER
      LDA ASTRT
      STA ADDR      ADDRESS INDEX
      JMP INIT,I

```

```

*
*
*  UNBUFFER CONSOLE & TERMINAL
UNBUF NOP

```

```

      LDA UBUFR
      STA UBUF1
      LDA UBUFR+1
      STA UBUF1+1
      LDA UBUFR+2
      STA UBUF1+2
      LDA UBUFR+3
      STA UBUF1+3
      JSB MESSS
      DEF *+3
      DEF UBUF1
      DEF .9
      JSB MESSS
      DEF *+3
      DEF UBUF7
      DEF .7
      JMP UNBUF,I

```

```

REBUF NOP
      JSB MESSS
      DEF *+3
      DEF RBUF1.
      DEF .9
      JSB MESSS
      DEF *+3
      DEF RBUF7
      DEF .7
      JMP REBUF,I
*
* INTERRUPT STATEMENTS
*
      ORB
INTBG JMP INT1,I
INT1  DEF TBGR
INADC JSB INT2,I
INT2  DEF ADCR
INTTY JSB INT4,I
INT4  DEF TTYR
      ORR
*
*
* CONSTANTS
*
UBUFR ASC 5,EQ,2,0,UN
UBUF1 BSS 6
UBUF7 ASC 4,EQ,3,UN
RBUF1 ASC 5,EQ,2,0,BU
RBUF7 ASC 4,EQ,3,BU
FIN    OCT 6412
      ASC 4,FINISHED
XOVER  ASC 4,OVERFLOW
LIM    OCT 6412
      ASC 7,OVERFLOW LIMIT
ABORT  OCT 6412
      ASC 4,ABORTED
ACNT   BSS 3
      ASC 3,SCANS
ASTOR  DEF STOR
SHFTA  DEF SHFTS
ARSE   ARS
ARSES  ARS,ARS
EXOV   DEC -6
.1     DEC 1
.2     DEC 2
.3     DEC 3
.4     DEC 4
.5     DEC 5
.6     DEC 6
.7     DEC 7
.8     DEC 8
.9     DEC 9

```

* STORAGE

*
NOVER BSS 1
RETRN BSS 1
ASTRT BSS 1
PCNT BSS 1
DCNTR BSS 1
MIN1 BSS 1
MIN2 BSS 1
ADDR BSS 1
XVAL BSS 1
MAX1 BSS 1
MAX2 BSS 1
SAVE BSS 1
SCNT BSS 1
CPCNT BSS 1
CADDR BSS 1
*

END
END\$